AGRICULTURE AND FOOD
www.csiro.au

Comparative performance of CT vs CA under both historical and future climate scenarios (crop production and GHG emissions) – a study using the APSIM model in the Eastern Gangetic Plains

Donald Gaydon, Heidi Horan, Apurbo Chaki, Swaraj Kumar Dutta, Perry Poulton

23 July 2020

Citation

Gaydon DS, Horan H, Chaki AK, Dutta SK, Laing AM and Poulton PL (2020). Comparative performance of CT vs CA under both historical and future climate scenarios (crop production and GHG emissions) – a study using the APSIM model in the Eastern Gangetic Plains. CSIRO, Australia.

Copyright

Important disclaimer

Contents

Abbreviations

APSIM	Agricultural Production Systems sIMulator
CA	Conservation agriculture
CIMMYT	International Maize and Wheat Improvement Centre (CGIAR)
CT	Conventional tillage
DSR	Direct-seeded rice
PTR	Puddled transplanted rice
STM	Strip-tilled maize
STW	Strip-tilled wheat
UPTR	Unpuddled transplanted rice

Acknowledgments

The APSIM modelling in this report is underpinned by field trials conducted with farmers and local partners across Bangladesh, India (West Bengal and Bihar), and in Nepal. We are grateful to them for the data and knowledge they have shared with us. We are also grateful to Ms Emerald Gaydon (CSIRO) who conducted all the statistical analyses and data arrangement for model comparison.

We are also grateful to our collaborating partners, in particular Dr Mahesh Gathala, TP Tiwari, and Saiful Islam (CIMMYT), for their time and expertise.

This work has been undertaken as part of the ACIAR-funded project, *Sustainable and resilient farming systems intensification in the eastern Gangetic Plains ('SRFSI')* (CSE-2011-077).

Executive summary

The parameterisation, calibration and validation of APSIM across the range of selected SRFSI nodes was a major undertaking which consumed the majority of the modelling team's efforts in the SRFSI project (Gaydon et al., 2018). The successful nature of this endeavour now leaves us with a valuable resource – a well-tested APSIM model positioned to contribute to any number of current and future research analyses in the region. In this document, we report on such a subsequent analysis - the effect of historical climate and several future climate changes scenarios on crop production and greenhouse gas emissions under a range of Conventional (CT) and Conservation Agriculture (CA) management interventions. The major findings of this report include:

- Agronomically speaking, the differences in grain yields between CT and CA practice are within the variability window of either, and hence do not appear to be significantly different. This lack of significant difference applies across future climate scenarios and timeframes, and largely reflects what was observed in the on-farm trials. However the general trend was for increased Rabi crop yields (maize and wheat) and slightly reduced kharif rice yields under CA practice compared with CT.
- Yields for Rabi season crops (wheat and maize) tend to decrease with harsher climate scenarios (ie RCP8.5 cf RCP4.5) and with increasing timeframe. This result is expected, but nuanced (Table 5). However, the APSIM modelling has indicated that wet-season rice yields exhibit the opposite trend and are predicted to increase in future years, primarily as a function of increased CO_2 fertilisation, which overshadows any losses due to increased temperatures and shorter seasons. This is under the assumption that irrigation water can meet any rainfall shortages. Purely rainfed crops could be different. In the case of rabi crops, the losses due to increased temperatures (shorter season length and increased grain sterility) outweigh the increased photosynthetic performance from increased CO_2.
- We found no particular protective effect on future grain yields of CA under climate change, compared to CT. The yield gains from implementing CA technologies in wheat under historical, 2050, 2070, and 2090 climates (averaged over all SRFSI sites simulated) were 6%, 5%, 4% and 2% respectively, illustrating a declining value of CA on yield as the climate became harsher. The respective numbers for maize were 1%, 2%, 2% and 4%, illustrating the opposite trend. Kharif rice followed the wheat trend, however the value from CA in any climate was less, negative even. The respective figures for Kharif rice were:- 0%, -1%, -1%,and -1%.
- As other components of SRFSI research have uncovered, however, significant advantages in labour and costs favour CA practice under historical conditions, but this modelling analysis does not take into account any economic system performance and changes in future prices and costs.

- Emissions: Our study found a NET Global Warming Potential (GWP) benefit of around 24% through employing CA technologies in the rice-maize and rice-wheat cropping systems, averaged across the SRFSI sites using historical climate data. This represents emissions due to plant-soil-fertiliser-residue processes in the field only, and does not include emissions related to differentials in machinery, fuel usage, fertiliser production and transport etc., which are beyond the scope of a field-scale model like APSIM. Our simulated in-field values were found to be commensurate with reported values from the literature.
- A changing future climate slightly reduces the GWP benefits from CA, with historical, 2050, 2070, and 2090 climates revealing a 24%, 22%, 21% and 20% benefit, respectively.
- Because our analysis of GHG emissions is only field scale, it does not account for material taken from the field in CT and CA systems, which may be broken down and emit gases in other situations (for example livestock methane, cooking fire smoke etc). To be comprehensive, a whole-of-system approach needs to be taken, accounting for livestock and fuel burning in CT systems, in addition to differences in machinery fuel use/burning between CT and CA. These results must be taken as ‘field scale only’.

1 Introduction

The Sustainable and Resilient Farming Systems Intensification in the Eastern Gangetic Plains (SRFSI; CSE/2011/077) project seeks to increase food production and its sustainability in its target regions. One of the key foundations underpinning SRFSI is a reliable cropping systems model to examine the long term feasibility of a range of farming system adaptations in rice-based cropping systems and to advise and inform on-farm research activities. The Agricultural and Production Systems Simulator (APSIM; Holzworth et al.,2014) is increasingly being used in South Asia for modelling rice-based farming systems and has been successfully parameterised, calibrated and validated for a broad range of locations within South Asia (Gaydon et al., 2017). Within APSIM, the manager module captures farmers' dynamic management practices such as crop selection, deciding when to sow or harvest, when to fertilise or irrigate, and when to conduct field operations including spraying, cultivating, or grazing. The flexibility of the manager module to capture the many, evolving farmer decision options is a critical capability of APSIM that sets it apart from the majority of crop models which have been used in previous studies.

The SRFSI project operates across four regions in northwest Bangladesh, the eastern Nepali Terrai, and the Indian states of West Bengal and Bihar. Within this Eastern Gangetic Plains (EGP) region there is a diversity of soil types, climates, land management practices, cropping systems, irrigation practices, etc, which necessitates detailed parameterisation, calibration and validation of APSIM for each separate location before scenario simulations examining risk, production levels and environmental performance can be evaluated with confidence. Locally parameterising, calibrating, validating, and where necessary improving APSIM formed the major focus of modelling work in SRFSI Phase 1 project, using data collected in both on-station trials and also SRFSI on-farm trials (Gaydon et al., 2018). In this effort, the CSIRO modelling team have taken along four in-country modellers on the journey with them – developing their skills and experience to varying degrees, including the achievement of one ACIAR John Allwright Fellowship for PhD studies (Apurbo Chaki) and one Endeavour Fellowship (Swaraj Kumar Dutta), both now resident with the team in Australia.

In this document, we report on such a subsequent analysis - the effect of historical climate and several future climate changes scenarios on crop production and greenhouse gas emissions under a range of Conventional (CT) and Conservation Agriculture (CA) management interventions.

1.1 Potential role of cropping systems modelling and APSIM

There is a general desire to investigate new practices in cropping systems of Asia with the aim of enhancing water productivity (WP) (Bouman, 2007), and cropping intensity (Dobermann and Witt, 2000) whilst maintaining environmental sustainability (Humphreys et al., 2010). Well-tested and locally-calibrated and validated simulation models are useful tools to explore opportunities within the context of a holistic systems approach − for increasing system productivity, assessing environmental trade-offs, and evaluating the effects of a changing climate. For any simulation model to be a useful tool in rice-based cropping systems research, it must be well tested in a range of possible configurations – different geographical locations, soil types, crop mixes and sequences, agronomic managements (fertilizer, sowing criteria, crop establishment and tillage practices), irrigation practices and variation in incident climatic variables such as temperatures and CO_2. The APSIM model has recently been robustly evaluated in its performance under South Asian conditions (Gaydon et al., 2017).

1.1.1 Overview of the APSIM model

APSIM, the **A**gricultural **P**roduction **S**ystems S**IM**ulator is a modelling platform for simulation of biophysical processes in cropping systems, particularly those relating to the production and ecological outcomes of management practices in the face of climate risk. It resulted from a need for research tools that provided accurate predictions of crop production in relation to climate, genotype, soil and farmer management factors while addressing the long-term natural resource management issues. A particular focus is the simulation of sequences of crops, rotations, and fallow periods, rather than just single crops in their response to daily soil and climate variables. APSIM is a modular framework consisting of numerous individual modules which describe plant, soil, climate and management processes. Detailed descriptions of APSIM are provided by Holzworth et al. (2014) and Keating et al. (2003). Here we merely provide a brief outline. APSIM is a dynamic daily time-step model that combines biophysical and management modules within a central engine to simulate cropping systems. The model is capable of simulating soil water, C, N and P dynamics and their interactions within crop/management systems, driven by daily climate data (solar radiation, maximum and minimum temperatures, rainfall). Daily potential production for a range of crop species is calculated using stage-related radiation-use efficiency (RUE) constrained by climate and available leaf area. The potential production is then limited to actual above-ground biomass production on a daily basis by soil water, nitrogen and (for some crop modules) phosphorus availability (Keating et al., 2003). The soil water balance (SOILWAT) module uses a multi-layer, cascading approach for the soil water balance following CERES (Jones and Kiniry, 1986), however a more process-based soil water-balance module is also available (SWIM3; Huth et al., 2012). The SURFACEOM module simulates the fate of the above-ground crop residues that can be removed from the system, incorporated into the soil or left to decompose on the soil surface. The SOILN module simulates the transformations of C and N in the soil. These include organic matter decomposition, N immobilization, urea hydrolysis, ammonification, nitrification and denitrification. The soil fresh organic matter (FOM) pool constitutes crop residues tilled into the soil together with roots from the previous crop. This pool can decompose to form the BIOM (microbial biomass), HUM (humus), and mineral N ($NO_3$and NH_4) pools. The BIOM pool notionally represents the more labile soil microbial biomass and microbial products, whilst the more stable HUM pool represents the rest of the soil organic matter (SOM) (Probert et al., 1998). APSIM crop modules seek information regarding water and N availability directly from SOILWAT and SOILN modules, for limitation of crop growth on a daily basis. Biological and chemical processes occurring in ponded rice fields are simulated using the POND module within APSIM (APSIM-Pond, Gaydon et al., 2012b). Crop modules specifically relevant to the evaluation presented in this paper are APSIM-Oryza (Gaydon et al., 2012a), APSIM-Wheat (Wang et al., 2003), APSIM-Maize (Carberry and Abrecht, 1991), and APSIM-Mungbean (Robertson et al., 2001; Robertson and Carberry, 1998).

1.2 Aims of this GHG emissions and Climate Change modelling study

The SRFSI on-farm trial data offers a rare geographically-diverse dataset in which to evaluate the value of Conservation Agriculture (CA) technologies across a range of cropping systems and locations in the Eastern Gangetic Plains. The APSIM model was previously calibrated and validated across most sites, using data on water use and crop production. In this study, we extend the model application to compare simulated greenhouse gas (GHG) emissions and crop production under a range of climate change scenarios.

2 Materials and Methods

Before being used to examine different scenarios (i.e. different crop and management options within a system), APSIM must be parameterised and calibrated for a location, and the model's performance must then be validated against an independent data set to ensure it can be used with confidence at that location. This involved and detailed process is detailed in full in the SRFSI-APSIM Modelling Team Final Report (Gaydon et al., 2018). In this current report, we take the calibrated and validated APSIM model and apply it using a range of different climate scenarios, and examine the effect of CA vs CT in each of these on crop production and GHG emissions.

2.1 Field trial locations

This project focuses on the Eastern Gangetic Plains (EGP) of Bangladesh, India and Nepal, home to 300 million people, with the world's highest concentration of rural poverty and a strong dependence on agriculture for food security and livelihoods. The SRFSI project has been established in 40 nodes across four jurisdictions of northwest Bangladesh (Districts of Rajshahi & Rangpur), state of West Bengal, India (Districts of Coochbehar & Malda), state of Bihar, India, (Madhubani & Purnea), and Eastern Terai of Nepal (Dhanusa & Sunsari). Each district has 5 nodes, and each node has between 3-12 participating farmers. Details of the country (jurisdiction), district and nodes which were used for modelling analysis are provided in Table 1.

Table 1: Details of the nodes in which the SRFSI APSIM GHG emissions and CC studies were conducted

Country	District	Node name	Latitude	Longitude	Long term systems trialled and simulated
Bangladesh	Rajshahi	Baduria	24.33784	88.71763	Rice-wheat-mungbean Rice-maize
	Rangpur	Kolkondo	25.87570	89.19976	Rice-wheat (+ jute)* Rice-maize
India (West Bengal)	Coochbehar	Falimari	26.40823	89.77732	Rice-wheat (+ jute)* Rice-maize
	Malda	Bidyanandapur	26.068815	87.979550	Rice-wheat-mungbean Rice-maize
India (Bihar)	Purnea	Dogachi	25.51621	87.33464	Rice-wheat Rice-maize
		Tikapatti	25.31261	87.1241	Rice-wheat Rice-maize
Nepal	Sunsari	NARC Tarahara	27.705	87.256	Rice-wheat

* jute in the actual cropping system at this location, but not simulated in APSIM

2.2 Cropping System Treatments imposed

The treatments imposed at the field trials consisted of a mix of conventional practice plus several versions of CA practice. For the purposes of modelling analysis we have limited our focus to the long-term trials. For the nodes chosen, these were applied in rice-wheat systems (sometimes with rice-wheat alone, but also with mungbean or jute as Kharif 1 crops), rice-maize systems, and rice-

rice systems. Table 1 provided details of the long-term treatments trialled at each node. For example:

T1: CTTPR-CTW (conventionally-tilled puddled transplanted rice, followed by conventionally-tilled wheat) (CONTROL)

T2: CTTPR-STW (same at T1 for T.Aman rice phase, but with strip-tilled wheat)

T3: DSR-STW (Direct-seeded T.Aman rice, followed by strip-tilled wheat)

T4: UPTPR-STW (Unpuddled transplanted T.Aman rice, followed by strip-tilled wheat)

* - Baduria in Bangladesh also included a Kharif 1 mungbean crop in the R-W sequence

The comparative treatments in a rice-maize system would be:

T1: CTTPR-CTM (conventionally-tilled puddled transplanted rice, followed by conventionally-tilled maize) (CONTROL)

T2: CTTPR-STM (same at T1 for T.Aman rice phase, but with strip-tilled maize

T3: DSR-STM (Direct-seeded T.Aman rice, followed by strip-tilled maize

T4: UPTPR-STW (Unpuddled transplanted T.Aman rice, followed by strip-tilled maize)

- In some regions, for example Rangpur Bangladesh, T3 proved problematic due to rapid onset of flooding which would regularly swamp and submerge young direct-seeded rice seedlings. In this case the T3 treatments were dropped and only T1, T2 and T4 conducted.
- Note also that the total amount of residues (from the previous crop) retained in the field was assumed to be the same between CA and CT management systems, although during actual SRFSI field trials these varied somewhat between sites. CT incorporated the residues while CA management retained them on the surface. For the purposes of this GHG and CC simulation study:
    - 75% taken from field in CT; 75% taken from field in CA

2.3 Baseline historical climate data used

Different durations of observed historical climate data were available at each of the sites. Details are as follows:

Table 2. Details of historical climate data employed in APSIM simulations

Location	Met Station name	Duration (years)	
Rajshahi, Bangladesh	Rajshahi (41895)	1982-2017	Bangladesh Meteorological Department (BMD)
Rangpur, Bangladesh	Rangpur (41859)	1954-2017	BMD
Dogachi, Bihar, India	Dogachi	1969-2017	Indian Meteorological Department (IMD)
Tikapatti, Bihar, India	Tikapatti	1969-2017	IMD
Malda, West Bengal, India	Bidyanandapur	1995-2017	IMD
Coochbehar, West Bengal, India	Falimari	1995-2016	IMD
Sunsari, Nepal	Biratnagar airport	1991-2016	Nepal Department of Hydrology and Meteorology

2.4 Climate Change Scenarios Imposed

Fig 1 and Table 3-4 detail the data used for climate change scenarios. The CO2 projections were obtained from the RCP Database of the International Institute for Applied Systems Analysis (https://tntcat.iiasa.ac.at/RcpDb/dsd?Action=htmlpage&page=about)

Information about the RCPs and the scenario development process for the IPCC AR5 can be found in the *IPCC Expert Meeting Report on New Scenarios* (https://www.ipcc.ch/site/assets/uploads/2018/05/EMR_Scenarios-1.pdf) and Moss et al. (2010).

The Climate data projections for temperature and rainfall changes based on these RCP's were obtained from the Climate Change Knowledge Portal, World Bank.

(https://climateknowledgeportal.worldbank.org/country/bangladesh/climate-data-projections)

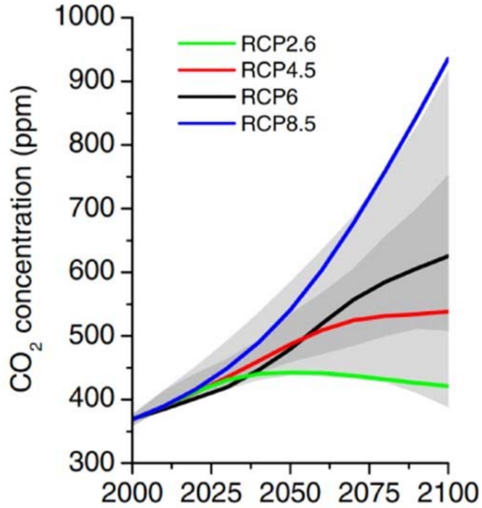

Fig 1. Atmospheric CO2 concentrations associated with each of the Representative Concentration Pathway (RCP) scenarios examined

According to the protocols of the Climate Change Portal, World Bank, we chose to examine time frames of 2050, 2070 and 2090, for each of RCP4.5, RCP6.0, and RCP8.5. The data available from this source could be generated by selecting a specific GCM, or by using the ensemble of 16 GCM's

Two GCM scenarios were investigated:

- CSIRO Mk3.6.0 GCM (https://confluence.csiro.au/public/CSIROMk360) (Table 3)
- Average of the ensemble of 16 GCMs used by the Climate Change Portal (which included CSIRO Mk3.6.0, but also 15 others) (Table 4)

Historical climate files were modified by the relevant factors (Table 3) to provide APSIM input climate files representing each of the time periods under investigation.

Table 3. Changes in average monthly daily maximum temperature, minimum temperature, and rainfall, under the three imposed climate change scenarios (RCP4.5, RCP6.0, RCP8.5) at three time periods (2050, 2070, and 2090) from the CSIRO Mk3.0 GCM.

year	month	MAXT (°C change)			MINT (°C change)			1986-2005 historical RAIN (mm/month)	RAIN (% change)			CO_2 (ppm)		
		RCP4.5	RCP6.0	RCP8.5	RCP4.5	RCP6.0	RCP8.5	n/a	RCP4.5	RCP6.0	RCP8.5	RCP4.5	RCP6.0	RCP8.5
2050	Jan	2.1	1.4	2.6	2.2	1.6	2.7	7.7	62.7	-13.1	-75.9	486.5	477.7	540.5
	Feb	1.4	1.3	1.7	2.0	1.6	2.6	19.3	34.3	21.9	52.3	486.5	477.7	540.5
	Mar	1.3	0.7	1.2	1.9	1.3	2.3	44.1	3.5	24.7	22.8	486.5	477.7	540.5
	Apr	1.4	1.3	1.8	1.8	1.2	1.8	104.4	-5.3	-4.5	-9.2	486.5	477.7	540.5
	May	2.1	2.1	2.6	2.0	1.8	2.3	210.5	-2.6	-0.9	-3.7	486.5	477.7	540.5
	Jun	1.9	2.0	1.9	1.9	1.5	2.0	354.3	-4.0	-14.5	1.5	486.5	477.7	540.5
	Jul	1.7	1.5	1.7	1.6	1.2	1.7	426.4	6.8	-2.2	7.5	486.5	477.7	540.5
	Aug	1.6	1.1	1.6	1.5	1.0	1.6	347.5	2.0	-1.6	18.6	486.5	477.7	540.5
	Sep	1.5	1.2	1.5	1.4	0.9	1.6	295.1	-0.7	-8.7	7.4	486.5	477.7	540.5
	Oct	1.5	1.8	2.1	1.9	1.5	2.2	172.8	10.8	-21.2	5.5	486.5	477.7	540.5
	Nov	1.6	1.3	1.9	2.1	1.6	2.2	43.7	16.5	47.9	19.6	486.5	477.7	540.5
	Dec	1.6	0.9	1.8	2.2	1.5	2.3	7.9	7.6	121.7	-3.2	486.5	477.7	540.5

year	month	MAXT (°C change)			MINT (°C change)			1986-2005 historical RAIN (mm/month)	RAIN (% change)			CO_2 (ppm)		
2070		**RCP4.5**	**RCP6.0**	**RCP8.5**	**RCP4.5**	**RCP6.0**	**RCP8.5**	**n/a**	**RCP4.5**	**RCP6.0**	**RCP8.5**	**RCP4.5**	**RCP6.0**	**RCP8.5**
	Jan	2.9	1.9	3.0	3.2	2.4	4.1	7.7	173.4	30.9	54.1	524.3	549.8	677.1
	Feb	1.9	1.3	3.2	2.8	2.1	3.7	19.3	104.3	10.8	19.4	524.3	549.8	677.1
	Mar	1.5	1.8	2.2	2.5	2.1	3.6	44.1	33.0	4.7	8.1	524.3	549.8	677.1
	Apr	2.1	1.8	2.2	2.6	1.9	3.1	104.4	-1.5	1.8	3.0	524.3	549.8	677.1
	May	3.6	2.2	3.4	3.0	2.2	3.4	210.5	-5.3	1.1	1.6	524.3	549.8	677.1
	Jun	2.8	2.5	2.9	2.7	2.1	3.2	354.3	2.5	0.6	0.9	524.3	549.8	677.1
	Jul	2.3	2.0	3.1	2.1	1.8	2.8	426.4	10.7	0.4	0.7	524.3	549.8	677.1
	Aug	2.0	1.8	2.7	1.9	1.6	2.7	347.5	14.1	0.5	0.8	524.3	549.8	677.1
	Sep	2.0	1.6	2.5	1.9	1.4	2.7	295.1	18.0	0.5	0.9	524.3	549.8	677.1
	Oct	2.5	2.3	2.7	2.3	2.1	3.1	172.8	-21.9	1.2	1.8	524.3	549.8	677.1
	Nov	2.8	1.9	2.9	3.4	2.2	3.9	43.7	71.2	5.0	8.9	524.3	549.8	677.1
	Dec	2.4	1.8	2.7	3.4	2.1	4.2	7.9	88.3	27.0	53.6	524.3	549.8	677.1

year	month	MAXT (°C change)			MINT (°C change)			1986-2005 historical RAIN (mm/month)	RAIN (% change)			CO_2 (ppm)		
2090		RCP4.5	RCP6.0	RCP8.5	RCP4.5	RCP6.0	RCP8.5	n/a	RCP4.5	RCP6.0	RCP8.5	RCP4.5	RCP6.0	RCP8.5
	Jan	3.2	2.4	4.5	3.9	3.4	5.9	7.7	137.1	254.6	102.8	533.7	635.6	844.8
	Feb	3.1	1.7	4.5	3.8	3.1	5.6	19.3	50.8	137.7	47.0	533.7	635.6	844.8
	Mar	2.3	1.1	3.2	3.0	3.0	5.1	44.1	21.7	61.8	53.0	533.7	635.6	844.8
	Apr	2.5	2.3	3.8	2.7	2.7	4.7	104.4	-5.5	3.2	-0.9	533.7	635.6	844.8
	May	3.8	3.0	4.5	3.1	3.0	4.8	210.5	-5.0	-2.6	-1.9	533.7	635.6	844.8
	Jun	3.9	3.7	5.5	3.1	3.1	4.8	354.3	-10.1	-15.1	-20.2	533.7	635.6	844.8
	Jul	3.4	3.1	4.7	2.6	2.5	4.0	426.4	-1.4	10.7	7.8	533.7	635.6	844.8
	Aug	2.5	2.4	3.7	2.3	2.3	3.7	347.5	3.0	1.0	14.7	533.7	635.6	844.8
	Sep	2.2	2.3	3.5	2.2	2.2	3.7	295.1	10.3	14.1	33.0	533.7	635.6	844.8
	Oct	2.5	2.4	3.8	2.5	2.8	4.3	172.8	-8.2	9.2	7.2	533.7	635.6	844.8
	Nov	3.4	2.8	4.3	3.4	3.6	5.1	43.7	20.0	43.9	35.9	533.7	635.6	844.8
	Dec	3.5	2.6	4.5	4.1	3.8	5.7	7.9	63.6	289.6	50.6	533.7	635.6	844.8

Table 4. Changes in average monthly daily maximum temperature, minimum temperature, and rainfall, under the three imposed climate change scenarios (RCP4.5, RCP6.0, RCP8.5) at three time periods (20150, 2070, and 2090) from the Ensemble of GCM's.

year	month	MAXT (°C change)			MINT (°C change)			1986-2005 historical RAIN (mm/month)	RAIN (% change)			CO_2 (ppm)		
		RCP4.5	RCP6.0	RCP8.5	RCP4.5	RCP6.0	RCP8.5	n/a	RCP4.5	RCP6.0	RCP8.5	RCP4.5	RCP6.0	RCP8.5
2050	Jan	1.6	1.2	2.1	1.6	1.4	2.2	7.7	-6.9	-9.7	-56.3	486.5	477.7	540.5
	Feb	1.3	1.0	1.9	1.6	1.4	2.2	19.3	14.1	14.6	19.1	486.5	477.7	540.5
	Mar	1.5	1.0	1.9	1.6	1.2	2.0	44.1	-1.8	0.8	-1.0	486.5	477.7	540.5
	Apr	1.7	1.2	2.1	1.5	1.2	2.1	104.4	-3.2	-2.2	-2.4	486.5	477.7	540.5
	May	1.3	1.1	1.6	1.5	1.2	1.9	210.5	5.3	1.6	4.5	486.5	477.7	540.5
	Jun	1.1	1.0	1.6	1.2	1.1	1.6	354.3	1.9	-4.2	-0.7	486.5	477.7	540.5
	Jul	1.0	0.9	1.5	1.1	1.0	1.5	426.4	6.1	1.4	5.1	486.5	477.7	540.5
	Aug	1.0	0.8	1.5	1.1	0.9	1.5	347.5	6.7	4.1	7.8	486.5	477.7	540.5
	Sep	1.1	0.9	1.5	1.2	1.0	1.6	295.1	4.0	3.3	8.8	486.5	477.7	540.5
	Oct	1.1	0.9	1.5	1.3	1.1	1.7	172.8	5.8	2.8	7.4	486.5	477.7	540.5
	Nov	1.3	1.0	1.9	1.5	1.2	1.9	43.7	-8.8	-3.9	-15.7	486.5	477.7	540.5
	Dec	1.5	1.1	2.0	1.5	1.3	2.0	7.9	-77.1	-22.6	-39.0	486.5	477.7	540.5

year	month	MAXT (^{o}C change)			MINT (^{o}C change)			1986-2005 historical RAIN (mm/month)	RAIN (% change)			CO_2 (ppm)		
2070		RCP4.5	RCP6.0	RCP8.5	RCP4.5	RCP6.0	RCP8.5	n/a	RCP4.5	RCP6.0	RCP8.5	RCP4.5	RCP6.0	RCP8.5
	Jan	2.3	2.0	3.2	2.2	2.1	3.4	7.7	-28.0	27.6	44.8	524.3	549.8	677.1
	Feb	2.0	1.6	2.9	2.1	1.9	3.3	19.3	21.7	10.1	17.2	524.3	549.8	677.1
	Mar	1.9	1.7	2.9	2.0	1.9	3.2	44.1	7.0	4.3	7.2	524.3	549.8	677.1
	Apr	2.0	1.7	3.0	1.9	1.8	3.1	104.4	-0.1	1.7	2.9	524.3	549.8	677.1
	May	1.7	1.6	2.6	1.8	1.7	2.8	210.5	6.1	0.8	1.3	524.3	549.8	677.1
	Jun	1.6	1.7	2.6	1.6	1.7	2.6	354.3	-0.1	0.5	0.7	524.3	549.8	677.1
	Jul	1.5	1.3	2.3	1.5	1.5	2.4	426.4	4.4	0.3	0.6	524.3	549.8	677.1
	Aug	1.5	1.3	2.3	1.4	1.5	2.3	347.5	5.6	0.4	0.7	524.3	549.8	677.1
	Sep	1.5	1.4	2.5	1.5	1.5	2.5	295.1	8.4	0.5	0.9	524.3	549.8	677.1
	Oct	1.5	1.4	2.6	1.6	1.6	2.7	172.8	7.0	0.9	1.5	524.3	549.8	677.1
	Nov	1.8	1.7	2.8	1.9	1.9	3.0	43.7	-1.4	4.2	6.8	524.3	549.8	677.1
	Dec	2.1	1.9	3.0	2.1	1.9	3.1	7.9	-23.1	24.4	39.2	524.3	549.8	677.1

year	month	MAXT (°C change)			MINT (°C change)			1986-2005 historical RAIN (mm/month)	RAIN (% change)			CO_2 (ppm)		
2090		RCP4.5	RCP6.0	RCP8.5	RCP4.5	RCP6.0	RCP8.5	n/a	RCP4.5	RCP6.0	RCP8.5	RCP4.5	RCP6.0	RCP8.5
	Jan	2.4	2.6	4.5	2.4	2.8	4.7	7.7	-5.1	-24.7	-62.9	533.7	635.6	844.8
	Feb	2.2	2.2	4.2	2.4	2.6	4.6	19.3	28.0	23.7	22.4	533.7	635.6	844.8
	Mar	2.2	2.2	4.0	2.2	2.5	4.4	44.1	2.4	6.8	6.6	533.7	635.6	844.8
	Apr	2.3	2.3	4.0	2.1	2.4	4.2	104.4	0.9	1.0	0.5	533.7	635.6	844.8
	May	2.1	2.3	3.5	2.1	2.3	3.8	210.5	4.7	6.5	10.2	533.7	635.6	844.8
	Jun	1.9	2.1	3.6	1.8	2.1	3.5	354.3	4.0	-0.8	3.7	533.7	635.6	844.8
	Jul	1.7	2.0	3.3	1.6	2.0	3.1	426.4	6.3	5.8	12.5	533.7	635.6	844.8
	Aug	1.6	1.9	3.1	1.6	2.0	3.2	347.5	9.9	11.2	17.6	533.7	635.6	844.8
	Sep	1.8	2.0	3.4	1.7	2.1	3.4	295.1	6.8	7.6	10.4	533.7	635.6	844.8
	Oct	1.7	2.2	3.6	1.8	2.3	3.6	172.8	7.7	3.3	8.0	533.7	635.6	844.8
	Nov	2.1	2.3	3.8	2.2	2.5	4.0	43.7	-6.1	5.0	-5.4	533.7	635.6	844.8
	Dec	2.2	2.5	4.3	2.3	2.6	4.4	7.9	-19.4	-5.8	-36.5	533.7	635.6	844.8

2.5 GHG Emissions Variables Considered

The following emissions variables were simulated by APSIM on a daily basis for all cropping and climate scenario combinations. The CO2-equivalents calculations were from top 15cms soil only, as per international protocols.:

Variable name	Units	Description
All_CO2e	kg CO_2 ha^{-1}	Total GHG emissions (from CO_2, CH_4, N_2O) expressed as carbon dioxide equivalents
CH4_CO2e	kg CO_2 ha^{-1}	GHG emissions from CH_4 expressed as carbon dioxide equivalents
N2O_CO2e	kg CO_2 ha^{-1}	GHG emissions from N_20 expressed as carbon dioxide equivalents
CO2_CO2e	kg CO_2 ha^{-1}	GHG emissions from CO_2 expressed as carbon dioxide equivalents
N2O_atm1	kg N ha^{-1}	N loss to the atmosphere from soil layer 1 (0-15cm) as N_20 from denitrification
N2O_atm2	kg N ha^{-1}	N loss to the atmosphere from soil layer 2 (15-30cm) as N_20 from denitrification
dlt_res_c_atm	kg C ha^{-1}	C loss* to the atmosphere from residue decomposition
dlt_hum_c_atm1	kg C ha^{-1}	C loss* to the atmosphere from soil humic material decomposition in soil layer 1 (0-15cm)
dlt_hum_c_atm2	kg C ha^{-1}	C loss* to the atmosphere from soil humic material decomposition in soil layer 2 (15-30cm)
dlt_fom_c_atm1	kg C ha^{-1}	C loss* to the atmosphere from soil fresh organic material decomposition (incorporated crop residues, old crop roots) in soil layer 1 (0-15cm)
dlt_fom_c_atm2	kg C ha^{-1}	C loss* to the atmosphere from soil fresh organic material decomposition (incorporated crop residues, old crop roots) in soil layer 2 (15-30cm)
dlt_biom_c_atm1	kg C ha^{-1}	C loss* to the atmosphere from soil microbial biomass decomposition (layer 1)
dlt_biom_c_atm2	kg C ha^{-1}	C loss* to the atmosphere from soil microbial biomass decomposition (layer 1)

* under aerobic conditions the C is lost as CO_2, but under anaerobic conditions as CH_4

3 Results

Example grain yields and emissions are provided below for Baduria, Bangladesh, comparing Conventional Tillage (CT) with Conservation Agriculture (CA) under the different future climate scenarios (RCP4.5, RCP6.0, and RCP8.5) and timeframes (2050, 2070, and 2090) for the ensemble of 16 GCMs employed by the World Bank Climate Change Portal. Appendix 3 contains results from other sites, which do vary in their magnitudes, breakups, and sources.

3.1 Grain Yields in projected future climate scenarios

3.1.1 Wheat yields

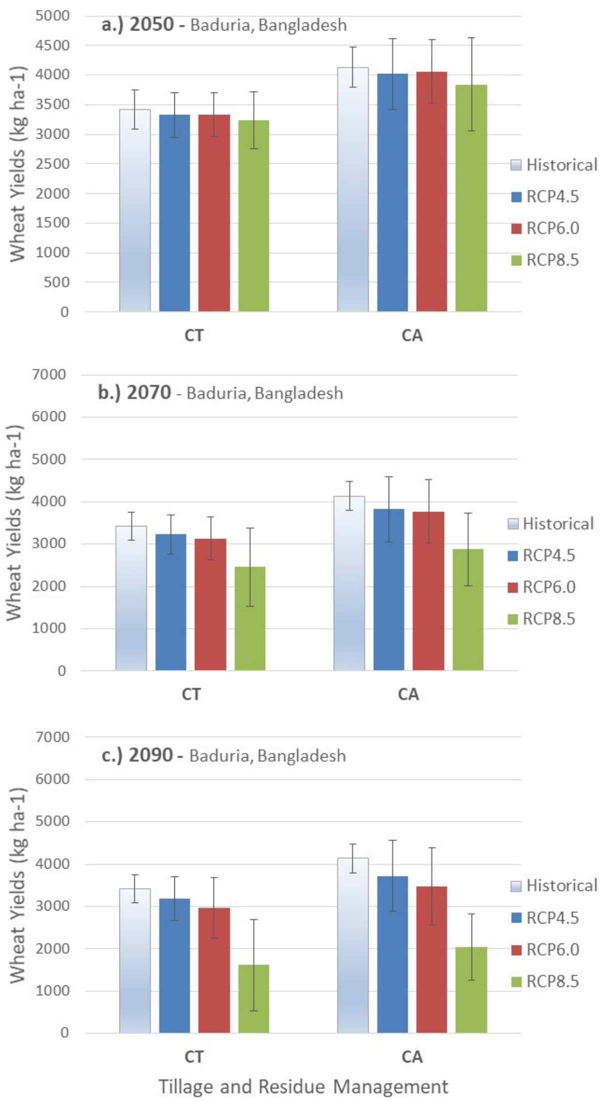

Figure 3.1. Simulated wheat grain yields for Baduria, Rajshahi, Bangladesh, for a.) 2050; b.) 2070; and c.) 2090, comparing performance of CT vs CA under future climate scenarios RCP4.5 (blue), RCP6.0 (red), and RCP8.5 (green)

3.1.2 Maize yields

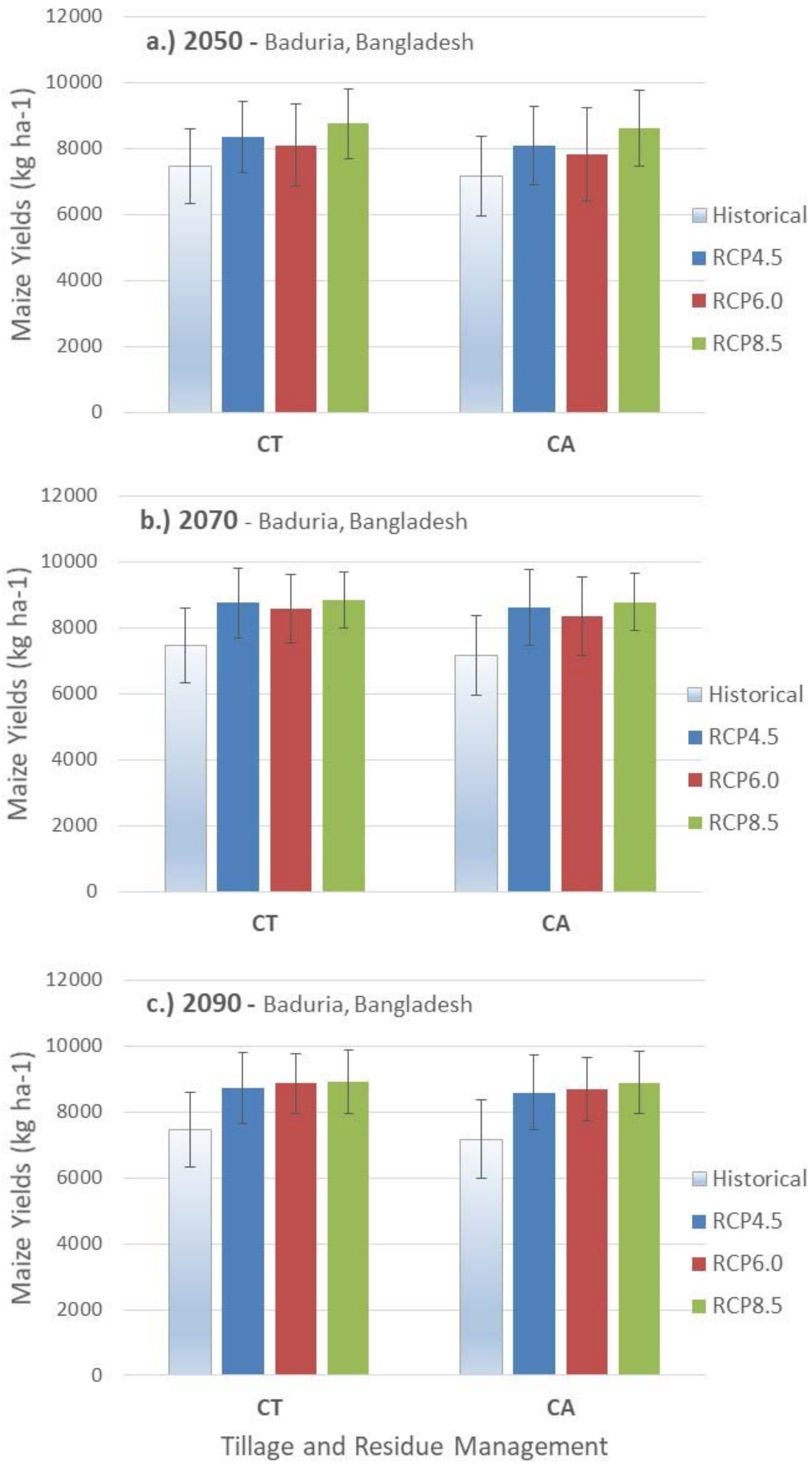

Figure 3.2. Simulated maize grain yields for Baduria, Rajshahi, Bangladesh, for a.) 2050; b.) 2070; and c.) 2090, comparing performance of CT vs CA under future climate scenarios RCP4.5 (blue), RCP6.0 (red), and RCP8.5 (green).

3.1.3 Rice yields

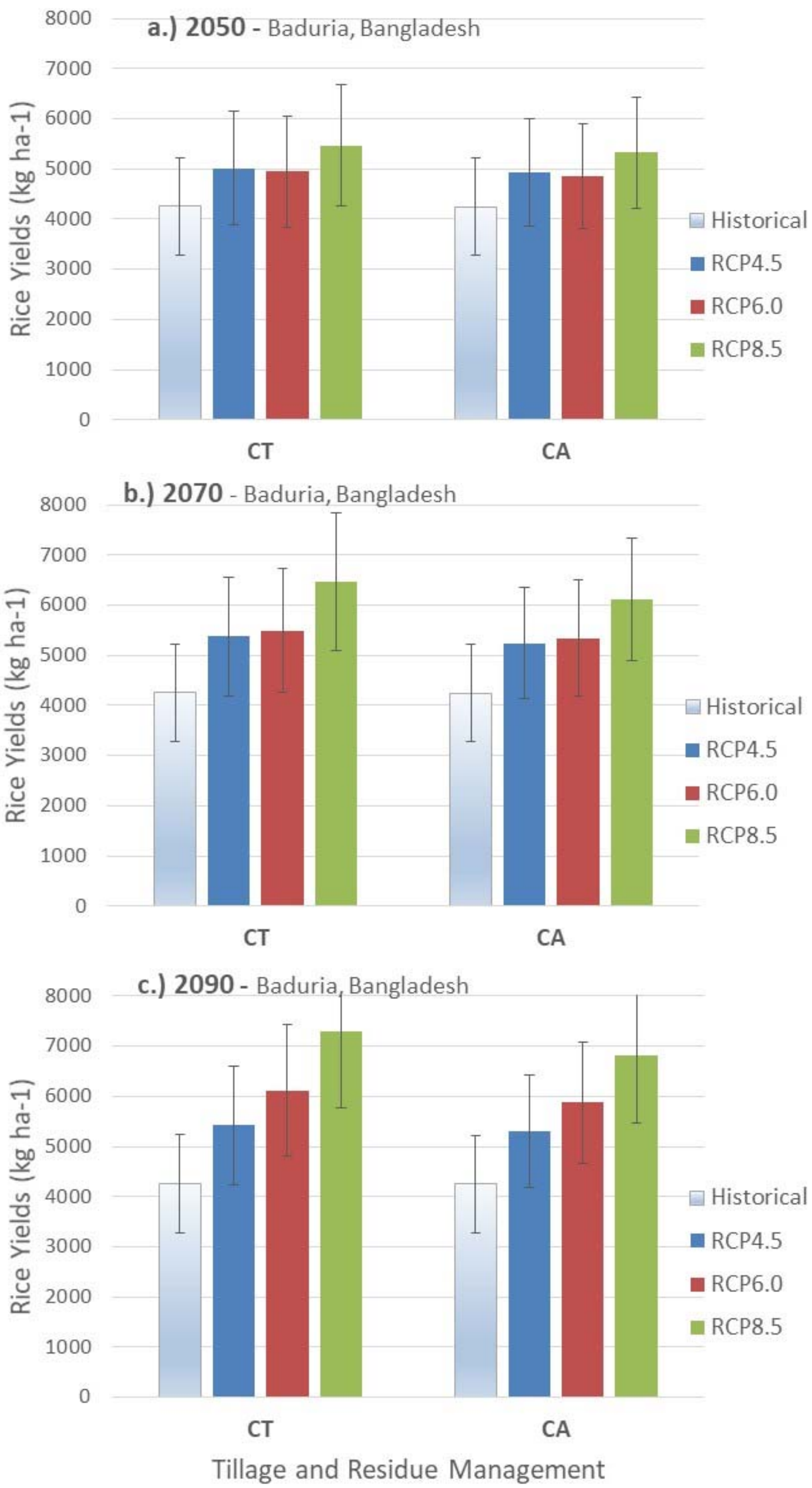

Figure 3.3. Simulated Kharif (wet-season) rice grain yields for Baduria, Rajshahi, Bangladesh, for a.) 2050; b.) 2070; and c.) 2090, comparing performance of CT vs CA under future climate scenarios RCP4.5 (blue), RCP6.0 (red), and RCP8.5 (green).

3.1.4 All crops

Table 5. Percent changes in crop yields under the RCP6.0 climate change scenario

Site	Crop	Tillage	Historical Yields	2050	2070	2090
Baduria, Rajshahi, Bangladesh	Wheat	CT	3488	-3	-8	-13
		CA	4264	-2	-8	-15
	Maize	CT	7503	8	15	18
		CA	7214	9	16	21
	Rice	CT	4377	15	26	37
		CA	4328	13	22	32
Kolkondo, Rangpur, Bangladesh	Wheat	CT	4629	-2	-4	-6
		CA	4553	-2	-5	-11
	Maize	CT	10467	-5	-7	-9
		CA	11874	-4	-7	-9
	Rice	CT	4816	9	16	23
		CA	4610	8	15	20
Malda, WB, India	Wheat	CT	3308	4	6	6
		CA	3982	-1	-5	-10
	Maize	CT	7434	-7	-18	-32
		CA	7840	-1	-4	-11
	Rice	CT	5452	3	6	9
		CA	5463	4	7	9
Coochbehar, WB, India	Wheat	CT	4095	-4	-8	-11
		CA	4568	-4	-7	-11
	Maize	CT	9016	-7	-9	-13

		CA	9021	-8	-11	-15
	Rice	CT	5657	3	5	4
		CA	5559	2	4	3
Tikapatti, Bihar, India	Wheat	CT	3790	2	2	2
		CA	3639	2	-1	-2
	Maize	CT	10036	-8	-13	-20
		CA	9594	-8	-14	-19
	Rice	CT	4859	4	7	8
		CA	5185	0	4	6
Dogachi, Bihar, India	Wheat	CT	4031	3	5	6
		CA	3971	2	3	3
	Maize	CT	10743	-5	-9	-13
		CA	10934	-5	-10	-16
	Rice	CT	4418	4	8	9
		CA	4687	5	9	11
Tarahara, Sunsari, Nepal	Wheat	CT	3274	0	-2	-4
		CA	3324	2	1	0
	Maize	CT	8849	1	0	-1
		CA	8532	0	-1	-3
	Rice	CT	4504	8	11	12
		CA	4236	9	12	12

3.2 Greenhouse Gas Emissions

3.2.1 Overall annual emissions – CO2 Equivalents

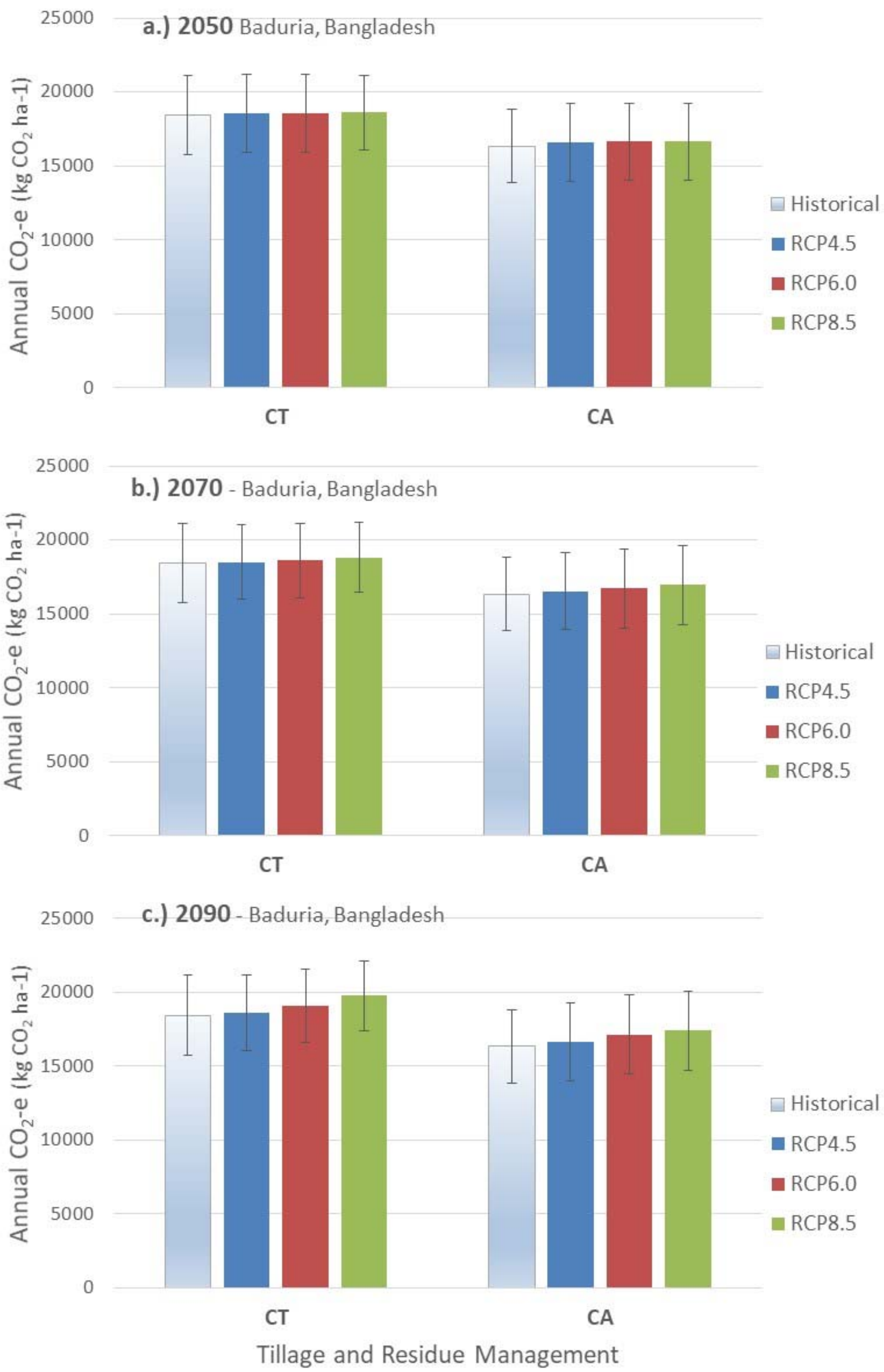

Figure 3.4. Simulated annual GROSS greenhouse gas (GHG) emissions (in CO_2-equivalents) in the rice-maize cropping system at Baduria, Rajshahi, Bangladesh, for a.) 2050; b.) 2070; and c.) 2090, comparing performance of CT vs CA under future climate scenarios RCP4.5 (blue), RCP6.0 (red), and RCP8.5 (green). Emissions are calculated from top 15cms soil.

3.2.2 Overall emissions – relative contributions from CO_2, N_20 and CH_4

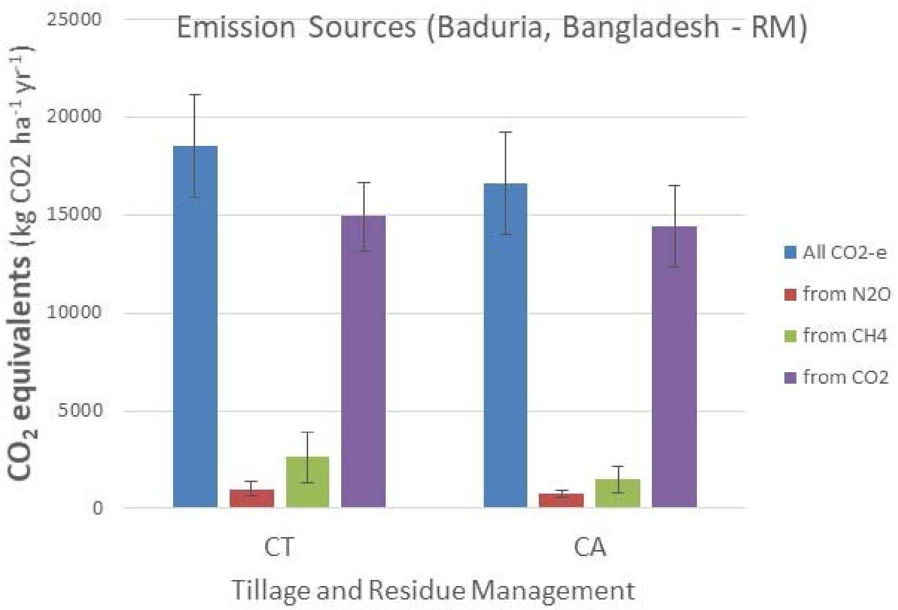

Figure 3.5. Simulated annual greenhouse gas (GHG) emissions (in CO_2-equivalents) in the rice-maize cropping system at Baduria, Rajshahi, Bangladesh, for 2050, RCP6.0, illustrating the relative contributions from CO_2, CH_4 and N_20.

3.2.3 NET Global Warming Potential (GWP) – as defined by Lindquist et al., 2012 (N_20 + CH_4)

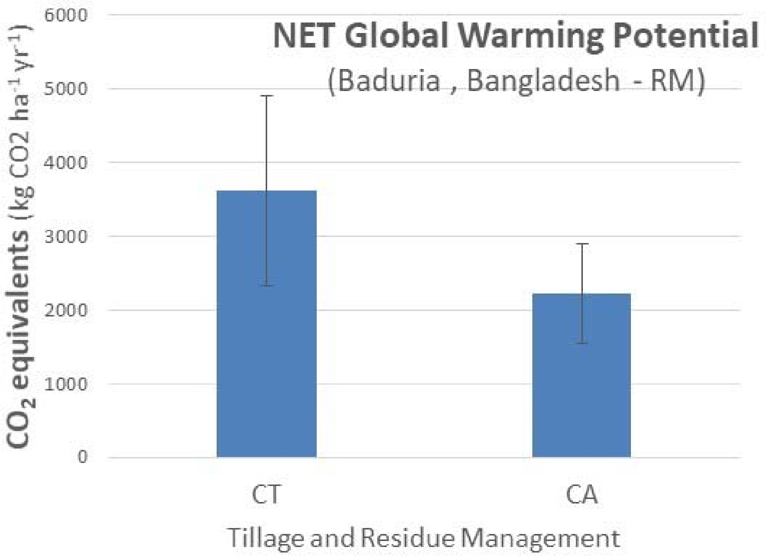

Figure 3.6. Simulated NET Global Warming Potential (GWP) (in CO_2-equivalents) in the rice-maize cropping system at Baduria, Rajshahi, Bangladesh, for 2050, RCP6.0, as defined by Lindquist et al., (2012) which considers only contributions from CH_4 + N_20. For net GWP calculations, it is considered that net CO_2 emissions from crop/soil processes represent < 1% of total GWP and can be ignored, as gross CO_2 emissions are closely matched by atmospheric CO_2 which the growing crops have fixed/assimilated.

Table 6. Percent changes in net Global Warming Potential (GWP) (as defined by Linquist et al., 2012) from 'Historical' for the Rice-Maize system under the RCP6.0 climate change scenario, and either Conventional Tillage (CT) or Conservation Agriculture (CA)

Site	Tillage	Historical Net GWP	2050	2070	2090
Baduria	CT	4111	-10	-17	-16
	CA	2330	1	-2	3
Kolkondo	CT	3979	-1	-1	-1
	CA	3585	0	1	1
Malda	CT	6982	3	5	10
	CA	5220	1	3	6
Coochbehar	CT	5311	-3	-3	-4
	CA	4934	-2	-2	-3
Tikapatti	CT	3662	-1	-1	1
	CA	2361	2	2	9
Dogachi	CT	3920	-2	-2	-3
	CA	3494	0	1	5
Tarahara	CT	4685	-3	-5	-6
	CA	3037	0	0	-2

3.2.4 CO2 emissions – breakup between sources

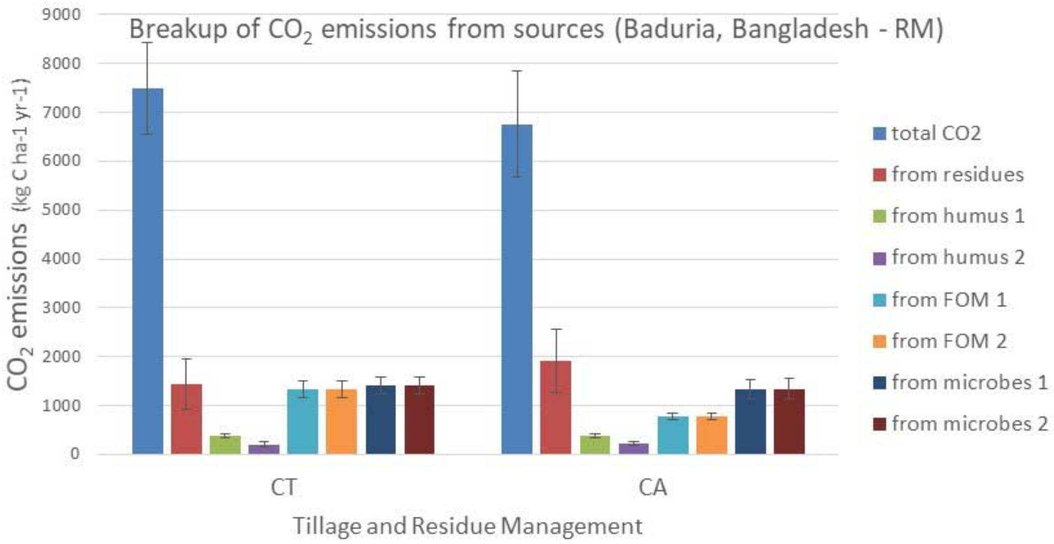

Figure 3.7. Simulated CO2 emissions (in kg C ha^{-1} yr^{-1}) between CT and CA managements in the rice-maize cropping system at Baduria, Rajshahi, Bangladesh, for 2050, RCP6.0, illustrating the relative contributions from breakdown/cycling of crop residues on the surface, soil fresh organic matter (FOM), soil humic materials (Humus) and soil microbiota (microbes). The "1" and "2" refer to soil layers 1 and 2 (0-15 and 15-30cms, respectively)

4 Discussion

4.1 Crop production under climate change – CA vs CT

4.1.1 General effect of future climate conditions on crop production

APSIM modelling of crop production under climate changes takes into account the effects of increased daily temperatures, changes in rainfall, and the effects of CO_2 fertilisation. Increasing temperatures generally decrease crop duration and subsequently production in South Asia (Jalota et al., 2013; Mishra et al., 2013), but if production is limited by historically cold temperatures or frosts (as in some locations globally), future temperature increases may actually have positive effects on production. Locations in which crops already experience heat stresses are likely to experience the negative effects of climate change to a greater degree than non-stressed regions, or low-temperature stressed regions. Mishra et al. (2013) simulated variations in future crop yields in the IGP (both increases or decreases) depending on both the location under consideration, the crop species, and the GCM model used for future climate projections. Whereas most literature reports suggest that projected temperature increases are more likely to exert negative effects on crop yields in the IGP, increasing atmospheric CO2 concentrations tend to offset this by increasing crop growth and the efficiency of photosynthesis. Not all studies consider the effects of CO2 fertilisation as well as temperature effects (Zhao et al., 2016). How these two aspects play out in determining future crop yields varies between location and also crop species/variety. For example, as a C4 crop maize will respond more positively to CO_2 fertilisation than a C3 crop like wheat, due to different chemical sequences which are enacted during photosynthesis (Challinor et al., 2014).

The on-farm trials in SRFSI illustrated limited yield differences between sites over a range of crop species and practices, with CA methods exhibiting yield improvements in some and decreases in others (Islam et al., 2019). Generally however, CA had a more positive effect on crop yields (overall, a significant 5% increase for maize and wheat crops; no significant effect on wet-season rice (Islam et al., 2019)) and the modelling has reflected these same trends as can be seen in Figures 3.1 to 3.3, plus the other site figures in Appendix 3. For example, a poorer showing of CA in Purnea, but positive yield responses in Malda, and Rajshahi, etc.. from the field trials were also reflected in the APSIM modelling. Differential responses between crops were noted in both field trials and modelling, which gives confidence in the modelled outputs. For example, wheat yields were more significantly enhanced than maize yields by CA in Rajshahi, Bangladesh, whereas maize yield gains overshadowed wheat yield gains in Rangpur, Bangladesh. Across all simulated SRFSI sites, the gains in wheat, maize and rice yields through implementation of CA technologies were 6%, 2% and 0% respectively, over CT yields in historical climates.

Yields for Rabi season crops (wheat and maize) tend to decrease with harsher future climate scenarios (ie RCP8.5 cf RCP4.5) and with increasing timeframe across sites. This result is expected. However the APSIM modelling has indicated that wet-season rice yields exhibit the opposite trend and are predicted to increase in future years, primarily as a function of increased CO_2 fertilisation, which overshadows any losses due to increased temperatures and shorter seasons. This finding was also alluded to by Challinor et al (2014) who found that rice was less impacted by climate change than crops like wheat and maize. In this current APSIM study, the effects of rainfall changes on rice crop yields were effectively negated, as we assumed irrigation was available and would meet any shortfall in Kharif rice water demands. Several studies which predict future rice crop yield declines do so heavily on the basis of water shortages in rainfed rice (Erda et al., 2005), whereas some studies indicate that water productivity of rice may increase under increased CO2, if water is available (Kumar et al., 2017). The findings of Erda et al., (2005) indicated that irrigated rice crops in China are likely to experience yield increases into the 2080's, whereas rainfed crops will suffer negative yields. Looking specifically at NW India, Lal et al (1998) indicated benefits to rice growth from increased CO2 would be negatively balanced by increases in temperature and decreases in rainfall. For our APSIM simulations in the SRFSI sites of the EGP, we found that a general balance between positive and negative impacts was the most common, with some sites increasing kharif rice yields into the future (Kolkondo, Bangladesh;) with some slightly decreasing (eg Tikapatti, Bihar; Coochbehar, WB) and others staying roughly the same (Nepal). These would all be driven by local idiosyncrasies in climate but for rice any increases or decreases in future yields were generally small.

In the case of wheat crops, the losses due to increased temperatures (shorter season length and increased grain sterility) outweighed the increased photosynthetic performance from increased CO_2, with future yield declines at the majority of sites. Unsurprisingly, declines were larger with harsher scenarios (ie RCP8.5) and longer timeframes (2090). Some sites are more likely to be negatively affected than others – for example, Rajshahi, Kolkondo (Bangladesh), Tarahara (Nepal), showed greater wheat yield declines than (Dogachi, Tikapatti (Bihar) and Malda, Coochbehar (West Bengal). Once again, these different responses have been driven by local climate differences, particularly how much current wheat growing temperatures are to heat-stress levels.

For maize crops, future yield decreases were simulated at Malda, Coochbehar (West Bengal); Tikapatti, Dogachi (Bihar), with lesser yield declines at Tarahara (Nepal); Kolkondo and Baduria (Bangladesh).

Differential future climate performance of different crops was noted at certain sites, with wheat crops more negatively affected than maize at Baduria, Kolkondo (Bangladesh); Tarahara (Nepal), and Malda (WB), with maize crops more affected that wheat at the two Bihar sites, and Coochbehar (WB).

4.1.2 Is there a protective effect of CA against climate changes?

Comparing percentage changes in crop yields into the future (between current and future CT and CA treatments), did not reveal any particular 'protective' advantage from CA over CT in the face of climate change. The average yield decline in CT wheat (across sites) by 2070 was -1.29%, whereas the figure for CA wheat was -3.29%. For maize, it was reversed, CA was -4.51% and CT was -5.94% (Calculations from Table 5). The was no significant difference between CT and CA at any site or for any cropping system, hence we found no evidence that CA provides enhanced protection against a changing climate than CT. This analysis could be different if the cropping systems are entirely rainfed, where the surface residue retention in CA systems may provide significant soil moisture advantages.

There were differentials between crops:- the yield gains from implementing CA technologies in wheat under historical, 2050, 2070, and 2090 climates (averaged over all SRFSI sites simulated) were 6%, 5%, 4% and 2% respectively, illustrating a declining value of CA on yield as the climate became harsher. The respective numbers for maize were 1%, 2%, 2% and 4%, illustrating the opposite trend. Kharif rice followed the wheat trend, however the value from CA in any climate was less, negative even. The respective figures for Kharif rice were:- 0%, -1%, -1%,and -1%.

4.2 Global Warming Potential (GWP) – CA vs CT

4.2.1 Comparing GWP of CA vs CT under historical climate

The greenhouse gas (GHG) emissions and global warming potential (GWP) analysis presented here includes only aspects related to plant-soil-fertiliser-residue interactions, and does not include any emissions due to machinery, transport, fuel, and fertiliser production. This is because APSIM is a purely biophysical model, and can only contribute biophysical data to more comprehensive, all-of-system analyses. This is important to note when comparing our results with those reported in literature, as many such reports include all these aspects. Some however are like ours. Lindquist et al., 2012, present the global warming potential of several important cereal crops, compiled as a meta-analysis of measured (not simulated) data across 22 sites in Africa, the Americas, Asia and Australia. In their analysis they focus on GWP (presented as kg CO2-equivalents ha^{-1} yr^{-1}) from emissions of methane (CH_4) and nitrous oxide (N_20) from plant-soil-residue processes only. Their analysis is considered as a NET warming potential analysis, as a GROSS analysis would also include emissions of CO_2 – however Lindquist et al., 2012 argue that NET CO_2 emissions in agricultural systems represent <1% of NET GWP, since emissions of gaseous CO_2 are matched with (and hence cancel out) inputs of CO_2 from atmospheric sources, fixed by growing crops and algae. For this reason, they regard CO_2 emissions from plant-soil-fertiliser-residue processes as negligible in a NET GWP analysis, although significant in a GROSS sense. The average NET GWP from major cereal crops according to Lindquist et al., 2012, and the range of each, are:

- Rice – 3757 kg CO2-equivalents ha^{-1} yr^{-1} (range 174 – 22,237)
- Wheat – 662 kg CO2-equivalents ha^{-1} yr^{-1} (range 147 – 4349)
- Maize – 1399 kg CO2-equivalents ha^{-1} yr^{-1} (range 136 – 5389)

In our analysis, we have presented GWP in both GROSS terms (including CO2; Figures 3.4 and 3.5 for Baduria, Rajshahi, Bangladesh; plus all remaining sites in Appendix 3) and also in NET terms (figure 3.6, in Appendix 3, and Table 6). Comparing out average NET figures with those of Lindquist et al 2012 (above), we found our simulated values are well within the ball-park of these figures. For example, the average APSIM figures across all sites and tillage practices for the Rice-Maize system under a historical climate was 4115 kg CO2-equivalents ha^{-1} yr^{-1}, which compares acceptably well with the Lindquist figure for rice-maize of 5156 kg CO2-equivalents ha^{-1} yr^{-1} (3757 for rice + 1399 for maize) across a diverse spectrum of cropping practices and environments.

From our analysis, when the residue percentage retained is same (25% in the case of these simulations) then CA invariably had less NET GWP than CT for the same location, climate and cropping pattern (Table 6). This likely reflects a number of things:- (i) less soil disturbance in CA as emissions from soil fresh organic matter are less; (ii) reduced methane production under CA as the increased percolation rate results in reduced ponding and less time under anaerobic soil conditions than CT; (iii) more productive crops under CA use more of the applied N fertiliser leaving less available for denitrification; and (iv) less waterlogged conditions likely under CA practices due to better drainage, leading to less denitrification. All these aspects can be seen in the simulated balances between CH4 and N2O emissions in CT and CA systems (Figure 3.5 and 3.7; plus similar ones for other sites in Appendix 3). In our APSIM simulations across all sites for the rice-maize system, the average NET GWP under CT was 4664 kg CO_2-equivalents ha^{-1} yr^{-1}, compared with the NET GWP under CA of 3566 kg CO_2-equivalents ha^{-1} yr^{-1}. This represents a 24% reduction in GWP under CA.

Various other reports in the literature compare GWP of CT systems with CA systems, however most also include emissions from fertiliser production and transport, burning of residues, fuel and machinery emissions. Kakraliya et al., 2018, found a CT GWP figure of 7500 kg CO_2-equivalents ha^{-1} yr^{-1}, compared with around 5000 for a suite of CA practices, in the Western IGP for a rice-wheat system. This represents a 33% reduction in GWP under CA. As expected, it is a greater calculated CA benefit than from our analyses as it also includes the differential in reduced machinery and fuels emissions which favour CA.

Pathak et al (2011) conducted a simulation analysis in the rice-wheat system of the Western IGP using the InfoRCT model. They considered a similar range of emission sources as Kakraliya et al (2018), and found an annual NET GWP under CT of 5853 kg CO_2-equivalents ha^{-1} yr^{-1}, compared with 4408 under CA – representing a CA GWP saving of 25%. Sapkota et al (2015), also focussing on the Western IGP and the rice-wheat system found a NET GWP saving of 10-15% through use of CA practices.

From this we can conclude that our APSIM-simulated NET GWP figures are commensurate in magnitude with similar reports from literature, although it is important to note that ours is the only simulated study focussing on the EGP and both rice-wheat and rice-maize systems. Gathala et al., (2020) captured the field trial results from the SRFSI project and compared CT vs CA systems over a number of variables, including GWP. They found that GWP benefits of CA over CA ranged from 10-20%, with an average around 15%, across all SRFSI sites.

As far as we could determine, ours is the only study to look at the effect of changed future climatic conditions on the comparison between CA and CT GWP (see below).

4.2.2 Comparing GWP of CA vs CT under future projected climates

As an example, we compared the GWP benefits of CA over CT in the RM system under the RCP6.0 scenario as we went from historical climate, to 2050, to 2070, to 2090. We found a slightly decreasing benefit of CA over this time progression, with figures of 24%, 22%, 21% and 20% (for hist, 2050, 2070, 2090, respectively). The trend was similar for each cropping system.

Generally, the overall GWP of simulated farming systems decreased into the future, however it was nuanced (Table 6).

5 Conclusions

5.1 Major points

- Agronomically speaking, the differences in grain yields between CT and CA practice are within the variability window of either, and hence do not appear to be significantly different. This lack of significant difference applies across future climate scenarios and timeframes, and largely reflects what was observed in the on-farm trials. However the general trend was for increased Rabi crop yields (maize and wheat) and slightly reduced kharif rice yields under CA practice compared with CT.
- Yields for Rabi season crops (wheat and maize) tend to decrease with harsher climate scenarios (ie RCP8.5 cf RCP4.5) and with increasing timeframe. This result is expected, but nuanced (Table 5). However, the APSIM modelling has indicated that wet-season rice yields exhibit the opposite trend and are predicted to increase in future years, primarily as a function of increased CO_2 fertilisation, which overshadows any losses due to increased temperatures and shorter seasons. This is under the assumption that irrigation water can meet any rainfall shortages. Purely rainfed crops could be different. In the case of rabi crops, the losses due to increased temperatures (shorter season length and increased grain sterility) outweigh the increased photosynthetic performance from increased CO_2.
- We found no particular protective effect on future grain yields of CA under climate change, compared to CT. The yield gains from implementing CA technologies in wheat under historical, 2050, 2070, and 2090 climates (averaged over all SRFSI sites simulated) were 6%, 5%, 4% and 2% respectively, illustrating a declining value of CA on yield as the climate became harsher. The respective numbers for maize were 1%, 2%, 2% and 4%, illustrating the opposite trend. Kharif rice followed the wheat trend, however the value from CA in any climate was less, negative even. The respective figures for Kharif rice were:- 0%, -1%, -1%,and -1%.
- As other components of SRFSI research have uncovered, however, significant advantages in labour and costs favour CA practice under historical conditions, but this modelling analysis does not take into account any economic system performance and changes in future prices and costs.
- Emissions: Our study found a NET Global Warming Potential (GWP) benefit of around 24% through employing CA technologies in the rice-maize and rice-wheat cropping systems, averaged across the SRFSI sites using historical climate data. This represents emissions due to plant-soil-fertiliser-residue processes in the field only, and does not include emissions related to differentials in machinery, fuel usage, fertiliser production and transport etc., which are beyond the scope of a field-scale model like APSIM. Our simulated in-field values were found to be commensurate with reported values from the literature.
- A changing future climate slightly reduces the GWP benefits from CA, with historical, 2050, 2070, and 2090 climates revealing a 24%, 22%, 21% and 20% benefit, respectively.

- Because our analysis of GHG emissions is only field scale, it does not account for material taken from the field in CT and CA systems, which may be broken down and emit gases in other situations (for example livestock methane, cooking fire smoke etc). To be comprehensive, a whole-of-system approach needs to be taken, accounting for livestock and fuel burning in CT systems, in addition to differences in machinery fuel use/burning between CT and CA. These results must be taken as 'field scale only'.

5.2 Potential future work using the APSIM model in the SRFSI context.

The parameterisation, calibration and validation of APSIM across the range of SRFSI nodes was a major undertaking which has consumed the majority of the modelling team's efforts in the SRFSI project. The successful nature of this endeavour now leaves us with a valuable resource:- a well-tested model which is positioned to contribute to any number of future research analyses in the region. These include:-

- Varietal options. Instead of just comparing different Rabi crop species, the DST could be broadened to also compare the performance of different varieties within species
- Research into the trade-offs of retaining different percentages of residue in the field. Crop residues which are removed from the field by farmers currently serve other important purposes like fuel for heating, cooking and feeding livestock. However we also know that if farmers leave greater percentages of residue in the field which are incorporated back into the soil and cropping system, there are long-term benefits for soil health and crop production levels. Where is the optimum trade-off between retaining residues in the field and removing them for cooking and livestock? Even though farmers would need to source fuel and feed from other sources were they to increase their retained residue percentage in the field, there may be a 'sweet spot' where the overall farmer outcome is maximised. For example, in a preliminary APSIM simulation at Baduria, Rajshahi, Bangladesh, the clear value of retaining increased residue percentages in the field on soil organic carbon levels and long-term maize production was evident (Figure 4.1-4.2)

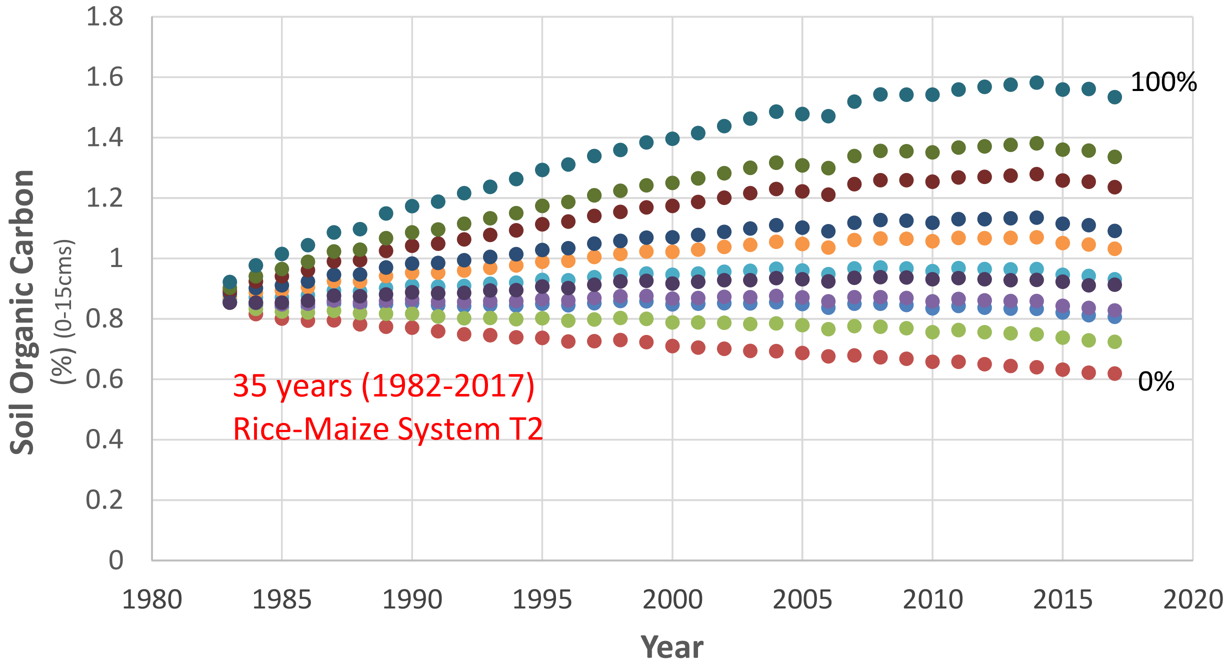

Figure 4.1. The long-term (35 years) effect of different percentage residue retention in a rice-maize rotation on soil organic carbon in the top 15 cms of soil. Simulation from Baduria, Rajshahi, Bangladesh.

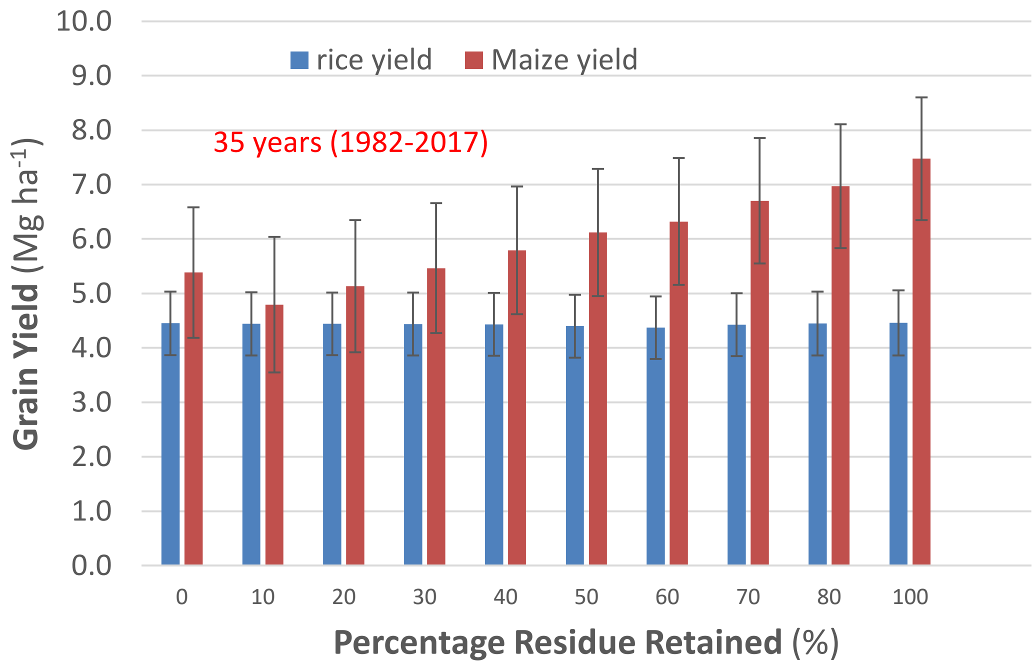

Figure 4.2. The long-term (35 years) effect of different percentage residue retention in a rice-maize rotation on rice and maize productivity. Simulation from Baduria, Rajshahi, Bangladesh.

6 References

Bouman, B.A.M., 2007. A conceptual framework for the improvement of crop waterproductivity at different spatial scales. *Agric. Syst*. 93 (1–3), 43–60.

Carberry, P.S., Abrecht, D.G., 1991. Tailoring crop models to the semi-arid tropics. In: Muchow, R.C., Bellamy, J.A. (Eds.), Climatic Risk in Crop Production: Models and Management for the Semiarid Tropics and Subtropics. CAB International, Wallingford, UK, pp. 157–182.

Challinor, A.J., Watson, J., Lobell, D.B., Howden, S.M., Smith, D.R. and Chhetri, N., 2014. A meta-analysis of crop yield under climate change and adaptation. Nature Climate Change, 4(4), pp.287-291.

Choudhury, AM and Kumar, A *Line Sown Direct Seed Rice (DSR) – A Climate Resilient Strategy for Food Security* Unpublished MS

Dobermann, A., Witt, C., 2000. The potential impact of crop intensification on carbon and nitrogen cycling in intensive rice systems. In: Kirk, G.J.D., Olk, D.C. (Eds.), Carbon and Nitrogen Dynamics in Flooded Rice: Proceedings of the Workshop on Carbon and Nitrogen Dynamics in Flooded Soils. IRRI, Los Banõs, Laguna, Philippines, 19–22 Apr 2000 (188 p.).

Erda, L., Wei, X., Hui, J., Yinlong, X., Yue, L., Liping, B. and Liyong, X., 2005. Climate change impacts on crop yield and quality with CO2 fertilization in China. Philosophical Transactions of the Royal Society B: Biological Sciences, 360(1463), pp.2149-2154.

Gathala, MK, Ladha, JK, Saharawat, YS, Kumar, V, Kumar, V, Sharma, PK, 2011. Effect of tillage and crop establishment methods on physical properties of a medium-textured soil under a seven-year rice-wheat rotation. *Soil Sci Soc Am J* 75, 1851-1862

Gathala, M.K., Laing, A.M., Tiwari, T.P., Timsina, J., Islam, M.S., Chowdhury, A.K., Chattopadhyay, C., Singh, A.K., Bhatt, B.P., Shrestha, R. and Barma, N.C.D., 2020. Enabling smallholder farmers to sustainably improve their food, energy and water nexus while achieving environmental and economic benefits. *Renewable and Sustainable Energy Reviews*, 120, p.109645.

Gaydon, D.S., Probert, M.E., Buresh, R.J., Meinke, H., Suriadi, A., Dobermann, A., Bouman, B.A.M., Timsina, J., 2012a. Rice in cropping systems – modelling transitions between flooded and non-flooded soil environments. *Eur. J. Agron*.39, 9–24.

Gaydon, D.S., Probert, M.E., Buresh, R.J., Meinke, H., Timsina, J., 2012b. Capturing the role of algae in rice crop production and soil organic carbon maintenance. *Eur. J. Agron*. 39, 35–43.

Gaydon, D.S., Balwinder-Singh, Wang, E., Poulton, P.L., Ahmad, B., Ahmed, F., Akhter, S., Ali, I., Amarasingha, R., Chaki, A.K., Chen, C., Choudhury, B.U. , Darai, R., Das, A., Hochman, Z., Horan, H., Hosang, E.Y., Kumar, P.V., Khan, A.S.M.M.R., Laing, A.M., Liu, L., Malaviachichi, M.A.P.W.K., Mohapatra, K.P., Muttaleb, Md. A., Power, B., Radanielson, A.M., Rai, G.S., Rashid, Md. H., Rathanayake, W.M.U.K., Sarker, M.M.R., Sena, D.R., Shamim, M., Subash, N., Suriyagoda, L.D.B., Wang, G., Wang, J., Yadav, R.K., Roth, C.H., 2017. Evaluation of the APSIM model in cropping systems of Asia, *Field Crops Research* 204, pp52-75.

Gaydon, D.S., Chaki, A.K., Dutta, S.K., Laing, A.M. and Poulton, P.L., 2018. APSIM Modelling for on-farm SRFSI trials in the EGP: (i) Calibration and validation using field data (2014-17) and (ii) Scenario Analysis for development of a decision-support tool for rabi crop choice. CSIRO, Australia.

Holzworth, D.P., Huth, N.I., deVoil, P.G., Zurcher, E.J., Herrmann, N.I., McLean, G., Chenu, K., van Oosterom, E., Snow, V., Murphy, C., Moore, A.D., Brown, H., Whish, J.P.M., Verrall, S., Fainges, J., Bell, L.W., Peake, A.S., Poulton, P.L., Hochman, Z., Thorburn, P.J., Gaydon, D.S., Dalgliesh, N.P., Rodriguez, D., Cox, H., Chapman, S., Doherty, A., Teixeira, E., Sharp, J., Cichota, R., Vogeler, I., Li, F.Y., Wang, E., Hammer, G.L., Robertson, M.J., Dimes, J., Carberry, P.S., Hargreaves, J.N.G., MacLeod, N., McDonald, C., Harsdorf, J., Wedgwood, S., Keating, B.A., 2014. APSIM - Evolution towards a new generation of agricultural systems simulation, *Environmental Modelling and Software* 62, 327-350.

Humphreys, E., Kukal, S.S., Christen, E.W., Hira, G.S., Balwinder-Singh, Sudhir-Yadav, Sharma, R.K., 2010. Halting the groundwater decline in North West India − which crop technologies will be winners? *Adv. Agron*. 109,155–217.

Islam, S., Gathala, M.K., Tiwari, T.P., Timsina, J., Laing, A.M., Maharjan, S., Chowdhury, A.K., Bhattacharya, P.M., Dhar, T., Mitra, B. and Kumar, S., 2019. Conservation agriculture based sustainable intensification: increasing yields and water productivity for smallholders of the Eastern Gangetic Plains. *Field Crops Research*, 238, pp.1-17.

Jalota, S.K., Kaur, H., Kaur, S. and Vashisht, B.B., 2013. Impact of climate change scenarios on yield, water and nitrogen-balance and-use efficiency of rice–wheat cropping system. Agricultural water management, 116, pp.29-38.

Kakraliya, S.K., Jat, H.S., Singh, I., Sapkota, T.B., Singh, L.K., Sutaliya, J.M., Sharma, P.C., Jat, R.D., Choudhary, M., Lopez-Ridaura, S. and Jat, M.L., 2018. Performance of portfolios of climate smart agriculture practices in a rice-wheat system of western Indo-Gangetic plains. *Agricultural Water Management*, 202, pp.122-133.

Keating, B.A., Carberry, P.S., Hammer, G.L., Probert, M.E., Robertson, M.J., Holzworth, D., Huth, N.I., Hargreaves, J.N.G., Meinke, H., Hochman, Z., McLean, G., Verburg, K., Snow, V., Dimes, J.P., Silburn, M., Wang, E., Brown, S., Bristow, K.L., Asseng, S., Chapman, S., McCown, R.L., Freebairn, D.M., Smith, C.J., 2003.An Overview of APSIM a model designed for farming systems simulation. *Eur. J. Agron*. 18, 267–288.

Kumar, U., Quick, W.P., Barrios, M., Sta Cruz, P.C. and Dingkuhn, M., 2017. Atmospheric CO2 concentration effects on rice water use and biomass production. PLoS One, 12(2), p.e0169706.

Lal, M., Singh, K.K., Rathore, L.S., Srinivasan, G., Saseendran, S.A., 1998. Vulnerability of rice and wheat yields in NW India to future changes in climate. Agricultural and Forest Meteorology, 89, 101–114.

Linquist, B., Van Groenigen, K.J., Adviento-Borbe, M.A., Pittelkow, C. and Van Kessel, C., 2012. An agronomic assessment of greenhouse gas emissions from major cereal crops. Global Change Biology, 18(1), pp.194-209.

Maclean, J.L., Dawe, D.C., Hardy, B., Hettel, G.P., 2013. Rice Almanac (fourth ed.), International Rice Research Institute (IRRI), Los Baños, Philippines (2013), 283 pp.

Mishra, A., Singh, R., Raghuwanshi, N.S., Chatterjee, C. and Froebrich, J., 2013. Spatial variability of climate change impacts on yield of rice and wheat in the Indian Ganga Basin. Science of the Total Environment, 468, pp.S132-S138.

Mondal, M.K., Saha, N.K., Ritu, S.P., Paul, P.L.C., Sharifullah, A.K.M., Humphreys, E., Tuong, T.P. and Rashid, M.A., 2015. Optimum sowing window for Boro cultivation in the coastal zone of Bangladesh, in "Revitalizing the Ganges Coastal Zone: Turning Science into Policy and Practices Conference Proceedings", Humphreys E, Tuong TP, Buison MC Pukinkis and Phillips M. (Eds.), Colombo, Sri Lanka: CGIAR Challenge Program on Water and Food (CPWF), pp. 389-404.

Moss, R.H., Edmonds, J.A., Hibbard, K.A., Manning, M.R., Rose, S.K., Van Vuuren, D.P., Carter, T.R., Emori, S., Kainuma, M., Kram, T. and Meehl, G.A., 2010. The next generation of scenarios for climate change research and assessment. *Nature,* 463(7282), p.747.

Pathak, H., Saharawat, Y.S., Gathala, M. and Ladha, J.K., 2011. Impact of resource-conserving technologies on productivity and greenhouse gas emissions in the rice-wheat system. *Greenhouse Gases: Science and Technology*, 1(3), pp.261-277.

Poulton, P, 2010. A modelling approach in exploring dry (*rabi*) season cropping options with subsistence farmers in India's West Bengal region. Report to ACIAR. CSIRO, Toowoomba, Australia, 21 pp.

Probert, M.E.P., Dimes, J.P., Keating, B.A., Dalal, R.C., Strong, W.M., 1998. APSIM's water and nitrogen modules and simulation of the dynamics of water and nitrogen in fallow systems. *Agric. Syst*. 56 (1), 1–28.

Robertson, M.J., Carberry, P.S., 1998. Simulating growth and development of soybean in APSIM. In: Proceedings Tenth Australian Soybean Conference, Brisbane, 15–17 September, pp. 130–136.

Robertson, M.J., Holland, J.F., Kirkegaard, J.A., Smith, C.J., 1999. Simulating growth and development of canola in Australia. Proceedings Tenth International Rapeseed Congress. (CD-Rom Proceedings).

Robertson, M.J., Carberry, P.S., Huth, N.I., Turpin, J.E., Probert, M.E., Poulton, P.L., Bell, M., Wright, G.C., Yeates, S.J., Brinsmead, R.B., 2001. Simulation of growth and development of diverse legume species in APSIM. *Aust. J. Agric*. Res. 53,429–446.

Robertson, M.J., Lilley, J.M., 2016. Simulation of growth, development and yield of canola (Brassica napus) in APSIM. *Crop Pasture Sci*. 67 (4), 332–344.

Sapkota, T.B., Jat, M.L., Aryal, J.P., Jat, R.K. and Khatri-Chhetri, A., 2015. (JIA-2015-0558) Climate change adaptation, greenhouse gas mitigation and economic profitability of conservation agriculture: some examples from cereal systems of Indo-Gangetic Plains. Journal of Integrative Agriculture, p.1917.

Saxton, K.E., Rawls, W., Romberger, J.S. and Papendick, R.I., 1986. Estimating generalized soil-water characteristics from texture. *Soil Science Society of America Journal*, 50(4), pp.1031-1036.

Singh, R, Kundu, DK, Kumar, A, 2009. *Characterisation of Dominant Soil Subgroups of Eastern India for Formulating Water Management Strategies: Research Bulletin 44*. Water Technology Centre for Eastern Region (Indian Council of Agricultural Research), Bhubaneswar, India, 55 pp.

Wang, E., van Oosterom, E.J., Meinke, H., Asseng, S., Robertson, M.J., Huth, N.I., Keating, B.A., Probert, M.E., 2003. The new APSIM-Wheat model —performance and future improvements. In 'Solutions for a better environment. In: Proceedings of the 11th Australian Agronomy Conference, Geelong, Victoria, 2003' (Australian Society of Agronomy).

Zhao, C., Piao, S., Wang, X., Huang, Y., Ciais, P., Elliott, J., Huang, M., Janssens, I.A., Li, T., Lian, X. and Liu, Y., 2016. Plausible rice yield losses under future climate warming. Nature plants, 3(1), pp.1-5.

Appendix I: Data required for APSIM

Data on climate, soil, crop and management practices are required to parameterise, calibrate and validate APSIM.

Daily climate data

Rainfall (mm); maximum and minimum temperatures (^{o}C) and solar radiation (MJm^{-2})
Latitude and longitude (in decimal degrees) of the location are also required.

Soil data

Soil parameterisation in APSIM is required on a layered basis, the depth and number of layers being arbitrary. Both soil water and soil chemical parameters are required. Key water-related parameters required for each soil layer are:

- Initial soil moisture content (in volumetric terms, $mm.mm^{-1}$)
- Bulk Density ($g.cm^{-3}$)
- Water-holding moisture contents of each layer (saturation, field capacity, 15 bar lower limit, and air dry) in volumetric terms (mm $water.mm^{-1}$ soil)
- ksat – saturated percolation rate ($mm.day^{-1}$); the rate at which water can pass through a specified soil layer when it is saturated.
- Soil Evaporation parameters
- Soil albedo
- Runoff partitioning parameters
- Maximum ponding height (mm)

Key soil chemical parameters required for each soil layer are:

- Organic carbon (%)
- pH
- Soil organic matter partitioning (% inert, humic, and micro-organism matter)
- Initial fresh organic matter mass and C:N ratio
- Initial NO_3 and NH_4 levels ($kg.ha^{-1}$ or ppm)
- Cation exchange capacity (CEC)

Information on the initial amount and type of crop stubble present in the system is required.

Crop Data

For each variety of each crop type to be simulated detailed phenological information are required:

- Date of sowing
- Date of emergence

- Date of transplanting
- Plant establishment numbers
- Date panicle initiation
- Date of anthesis
- Date of maturity
- Date of harvest
- Biomass (kg.ha^{-1}) at anthesis and maturity
- Grain weight (kg.ha^{-1}) at harvest

Management Data

Detailed information is required on:

- Sowing windows and/or sowing rules for each crop or pasture in the simulation
- Amount, type and rates of fertiliser application
- Irrigation schedules and amounts applied
- Residue management practices
- The presence and depth of ponded water

Wherever possible management data are generated (or validated) through focus group discussions and/or farmer interviews

Scenario data

To conduct scenario analyses at a location for which APSIM has been validated additional data may be required, depending on the scenario under investigation. These additional data are generally either climate or management related (although this is not necessary) and may include:

- Modified weather files for a future climate
- Modified irrigation water supply
- Alterations to crops or varieties in rotation
- Altered stubble management practices
- New fertiliser regimes or types

Wherever possible the relevant scenario characteristics are generated through focus group discussions and/or farmer interviews.

Appendix 2: Parameterisation of APSIM soil at each node

Baduria, Rajshahi, Bangladesh

Table A3-1: Soil data used for Baduria, Rajshahi, Bangladesh

Soil layer (cm)	Bulk density (g/cc)	Air Dry (mm/mm)	LL 15 (mm/mm)	Drained upper limit (mm/mm)	Saturation (mm/mm)	Saturated hydraulic conductivity (Ks, mm/day)	Organic C (%)	pH
0-15	1.400	0.061	0.121	0.230	0.468	40.0	0.53	8.3
15-30	1.550	0.090	0.097	0.192	0.415	2.0	0.58	8.3
30-60	1.510	0.060	0.070	0.157	0.431	35.0	0.30	8.3
60-90	1.540	0.060	0.069	0.162	0.418	30.0	0.10	8.3
90-120	1.540	0.066	0.069	0.162	0.418	25.0	0.1	8.3
120-150	1.540	0.066	0.069	0.162	0.418	25.0	0.1	8.3

Premtoli, Rajshahi, Bangladesh

Table A3-2: Soil data used for Premtoli, Rajshahi, Bangladesh

Soil layer (cm)	Bulk density (g/cc)	Air Dry (mm/mm)	LL 15 (mm/mm)	Drained upper limit (mm/mm)	Saturation (mm/mm)	Saturated hydraulic conductivity (Ks, mm/day)	Organic C (%)	pH
0-15	1.840	0.061	0.135	0.221	0.306	40.0	0.67	7.25
15-30	1.580	0.090	0.147	0.258	0.403	2.0	0.44	7.92
30-60	1.590	0.060	0.159	0.271	0.400	35.0	0.30	7.92
60-90	1.590	0.060	0.159	0.268	0.398	30.0	0.10	7.92
90-120	1.590	0.066	0.159	0.268	0.398	25.0	0.10	7.92
120-150	1.590	0.066	0.159	0.268	0.398	25.0	0.10	7.92

Kondondo, Rangpur, Bangladesh

Table A3-3: Soil data used for Kondondo, Rangpur, Bangladesh

Soil layer (cm)	Bulk density (g/cc)	Air Dry (mm/mm)	LL 15 (mm/mm)	Drained upper limit (mm/mm)	Saturation (mm/mm)	Saturated hydraulic conductivity (Ks, mm/day)	Organic C (%)	pH
0-15	1.37	0.02	0.035	0.100	0.470	40.0	1.48	5.63
15-30	1.41	0.04	0.054	0.129	0.462	2.0	0.80	5.63
30-60	1.57	0.03	0.043	0.111	0.406	35.0	0.40	5.63
60-90	1.50	0.02	0.029	0.089	0.434	30.0	0.10	5.63
90-120	1.50	0.02	0.029	0.089	0.434	25.0	0.10	5.63
120-150	1.50	0.02	0.029	0.089	0.434	25.0	0.10	5.63

Mohonpur, Rangpur, Bangladesh

Table A3-4: Soil data used for Mohonpur, Rangpur, Bangladesh

Soil layer (cm)	Bulk density (g/cc)	Air Dry (mm/mm)	LL 15 (mm/mm)	Drained upper limit (mm/mm)	Saturation (mm/mm)	Saturated hydraulic conductivity (Ks, mm/day)	Organic C (%)	pH
0-15	1.75	0.02	0.073	0.122	0.339	40.0	1.68	5.42
15-30	1.84	0.04	0.085	0.132	0.305	2.0	0.90	5.42
30-60	1.56	0.03	0.073	0.137	0.411	35.0	0.50	5.42
60-90	1.89	0.02	0.060	0.091	0.288	30.0	0.15	5.42
90-120	1.89	0.02	0.060	0.091	0.288	25.0	0.10	5.42
120-150	1.89	0.02	0.060	0.091	0.288	25.0	0.05	5.42

Simariya, Sunsari, Nepal

Table A3-5: Soil data used for Simariya, Sunsari, Nepal

Soil layer (cm)	Bulk density (g/cc)	Air Dry (mm/mm)	LL 15 (mm/mm)	Drained upper limit (mm/mm)	Saturation (mm/mm)	Saturated hydraulic conductivity (Ks, mm/day)	Organic C (%)	pH
0-15	1.390	0.120	0.240	0.420	0.470	60.0	0.983	7.1
15-30	1.390	0.183	0.245	0.435	0.472	40.0	0.580	7.1
30-60	1.400	0.255	0.255	0.450	0.474	2.0	0.090	7.1
60-90	1.410	0.286	0.286	0.445	0.467	10.0	0.060	7.1
90-120	1.410	0.286	0.286	0.445	0.467	10.0	0.050	7.1
120-150	1.410	0.286	0.286	0.445	0.467	10.0	0.050	7.1

Kaptangunj, Sunsari, Nepal

Table A3-6: Soil data used for Kaptangunj, Sunsari, Nepal

Soil layer (cm)	Bulk density (g/cc)	Air Dry (mm/mm)	LL 15 (mm/mm)	Drained upper limit (mm/mm)	Saturation (mm/mm)	Saturated hydraulic conductivity (Ks, mm/day)	Organic C (%)	pH
0-15	1.390	0.120	0.240	0.420	0.470	60.0	0.840	6.5
15-30	1.390	0.183	0.245	0.435	0.472	40.0	0.580	7.1
30-60	1.400	0.255	0.255	0.450	0.474	2.0	0.090	7.1
60-90	1.410	0.286	0.286	0.445	0.467	10.0	0.060	7.1
90-120	1.410	0.286	0.286	0.445	0.467	10.0	0.050	7.1
120-150	1.410	0.286	0.286	0.445	0.467	10.0	0.050	7.1

Bhaluwa, Sunsari, Nepal

Table A3-7: Soil data used for Bhaluwa, Sunsari, Nepal

Soil layer (cm)	Bulk density (g/cc)	Air Dry (mm/mm)	LL 15 (mm/mm)	Drained upper limit (mm/mm)	Saturation (mm/mm)	Saturated hydraulic conductivity (Ks, mm/day)	Organic C (%)	pH
0-15	1.390	0.120	0.240	0.420	0.470	60.0	0.840	6.5
15-30	1.390	0.183	0.245	0.435	0.472	40.0	0.580	7.1
30-60	1.400	0.255	0.255	0.450	0.474	2.0	0.090	7.1
60-90	1.410	0.286	0.286	0.445	0.467	10.0	0.060	7.1
90-120	1.410	0.286	0.286	0.445	0.467	10.0	0.050	7.1
120-150	1.410	0.286	0.286	0.445	0.467	10.0	0.050	7.1

Dogachi, Purnea, Bihar, India

Table A3-7: Soil data used for Dogachi, Purnea, Bihar, India

Soil layer (cm)	Bulk density (g/cc)	Air Dry (mm/mm)	LL 15 (mm/mm)	Drained upper limit (mm/mm)	Saturation (mm/mm)	Saturated hydraulic conductivity (Ks, mm/day)	Organic C (%)	pH
0-15	1.380	0.070	0.150	0.315	0.368	100.000	0.510	7.020
15-30	1.390	0.120	0.160	0.300	0.354	80.000	0.490	7.050
30-60	1.460	0.140	0.140	0.280	0.361	2.000	0.410	7.160
60-90	1.500	0.140	0.140	0.273	0.356	8.000	0.310	7.240
90-120	1.570	0.130	0.130	0.250	0.344	20.000	0.230	7.540
120-150	1.580	0.130	0.130	0.240	0.346	25.000	0.210	7.520

Tikapatti, Purnea, Bihar, India

Table A3-7: Soil data used for Tikapatti, Purnea, Bihar, India

Soil layer (cm)	Bulk density (g/cc)	Air Dry (mm/mm)	LL 15 (mm/mm)	Drained upper limit (mm/mm)	Saturation (mm/mm)	Saturated hydraulic conductivity (Ks, mm/day)	Organic C (%)	pH
0-15	1.410	0.110	0.210	0.385	0.421	100.000	0.510	7.020
15-30	1.430	0.150	0.190	0.330	0.395	80.000	0.490	7.050
30-60	1.470	0.170	0.170	0.310	0.361	4.000	0.410	7.160
60-90	1.490	0.140	0.140	0.290	0.356	8.000	0.310	7.240
90-120	1.520	0.100	0.100	0.230	0.344	20.000	0.230	7.540
120-150	1.540	0.100	0.100	0.210	0.346	25.000	0.210	7.520

Malda, West Bengal, India

Table A3-7: Soil data used for Bidyanandapur, Malda, West Bengal, India

Soil layer (cm)	Bulk density (g/cc)	Air Dry (mm/mm)	LL 15 (mm/mm)	Drained upper limit (mm/mm)	Saturation (mm/mm)	Saturated hydraulic conductivity (Ks, mm/day)	Organic C (%)	pH
0-15	1.400	0.061	0.121	0.230	0.468	40.000	1.500	8.300
15-30	1.550	0.086	0.086	0.192	0.415	2.000	1.000	8.300
30-60	1.510	0.060	0.070	0.157	0.431	35.000	0.310	8.300
60-90	1.540	0.060	0.069	0.162	0.418	30.000	0.190	8.300
90-120	1.540	0.066	0.069	0.162	0.418	25.000	0.140	8.300
120-150	1.540	0.066	0.069	0.162	0.418	25.000	0.140	8.300

Coochbehar, West Bengal, India

Table A3-7: Soil data used for Falimari, Coochbehar, West Bengal, India

Soil layer (cm)	Bulk density (g/cc)	Air Dry (mm/mm)	LL 15 (mm/mm)	Drained upper limit (mm/mm)	Saturation (mm/mm)	Saturated hydraulic conductivity (Ks, mm/day)	Organic C (%)	pH
0-15	1.390	0.075	0.091	0.210	0.468	40.000	0.900	6.2
15-30	1.430	0.060	0.080	0.220	0.465	2.000	1.000	6.2
30-60	1.420	0.050	0.060	0.190	0.443	35.000	0.310	6.2
60-90	1.400	0.030	0.050	0.180	0.420	30.000	0.190	6.2
90-120	1.400	0.030	0.050	0.170	0.420	25.000	0.140	6.2
120-150	1.400	0.030	0.050	0.160	0.420	25.000	0.140	6.2

Appendix 3. Climate change and GHG emission studies across sites and cropping systems

A3.1 Kolkondo, Rangpur, Bangladesh

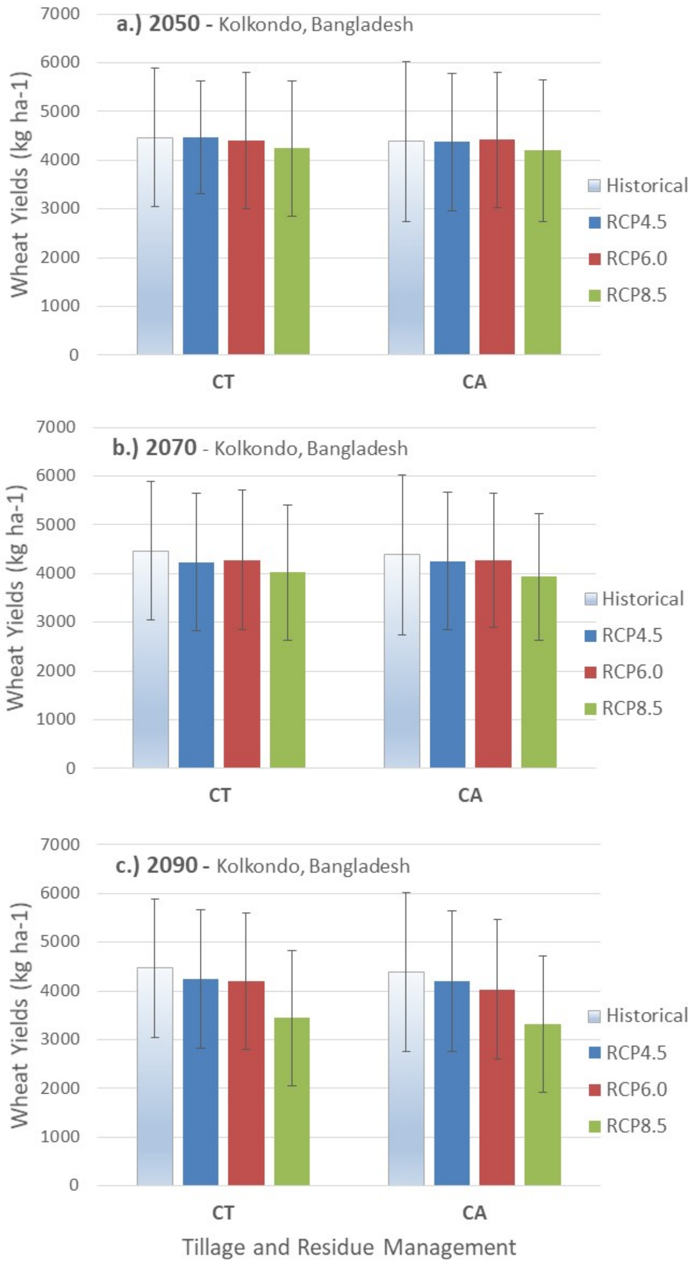

Figure A3.1. Simulated wheat grain yields for Kolkondo, Rangpur, Bangladesh, for a.) 2050; b.) 2070; and c.) 2090, comparing performance of CT vs CA under future climate scenarios RCP4.5 (blue), RCP6.0 (red), and RCP8.5 (green)

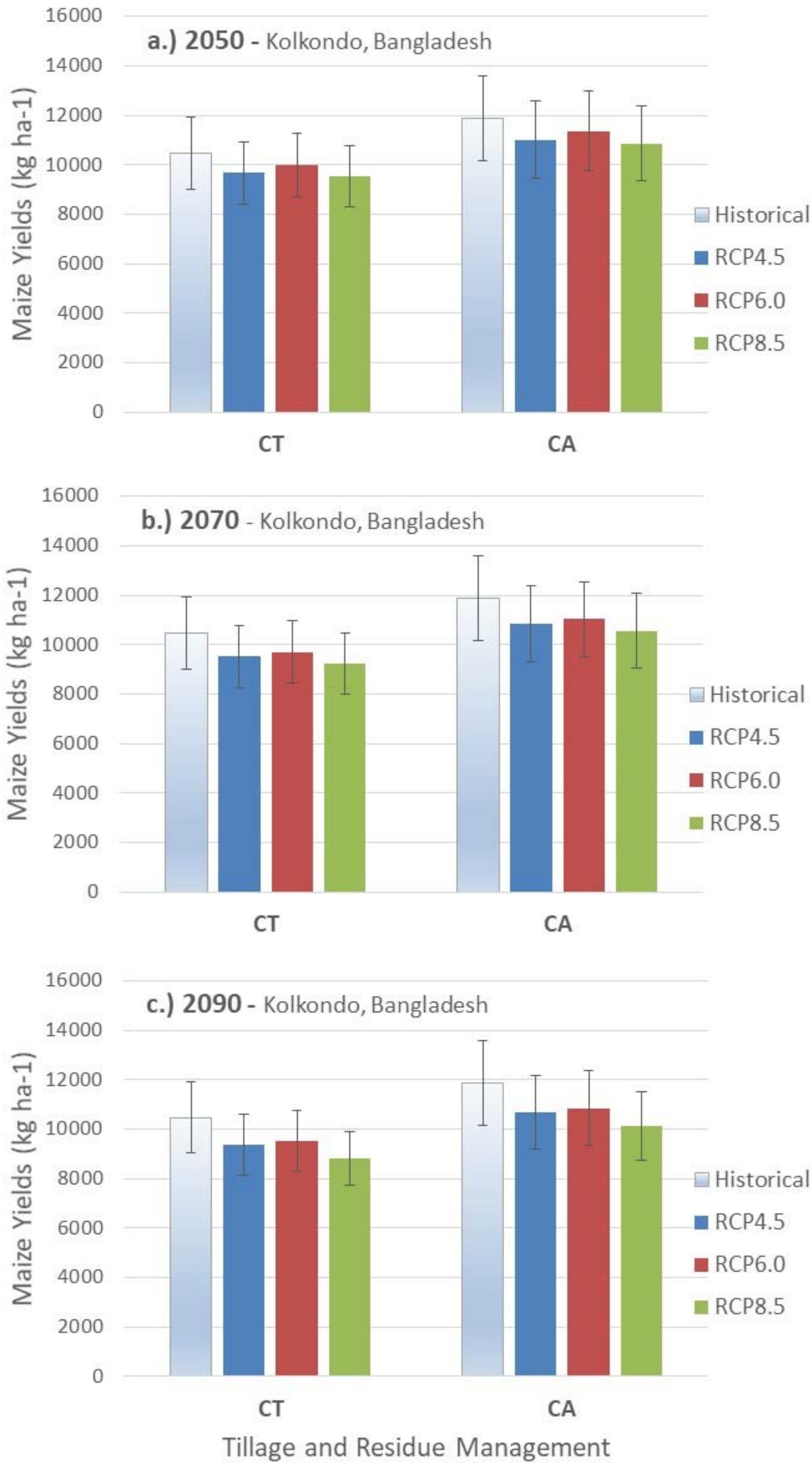

Figure A3.2. Simulated maize grain yields for Kolkondo, Rangpur, Bangladesh, for a.) 2050; b.) 2070; and c.) 2090, comparing performance of CT vs CA under future climate scenarios RCP4.5 (blue), RCP6.0 (red), and RCP8.5 (green)

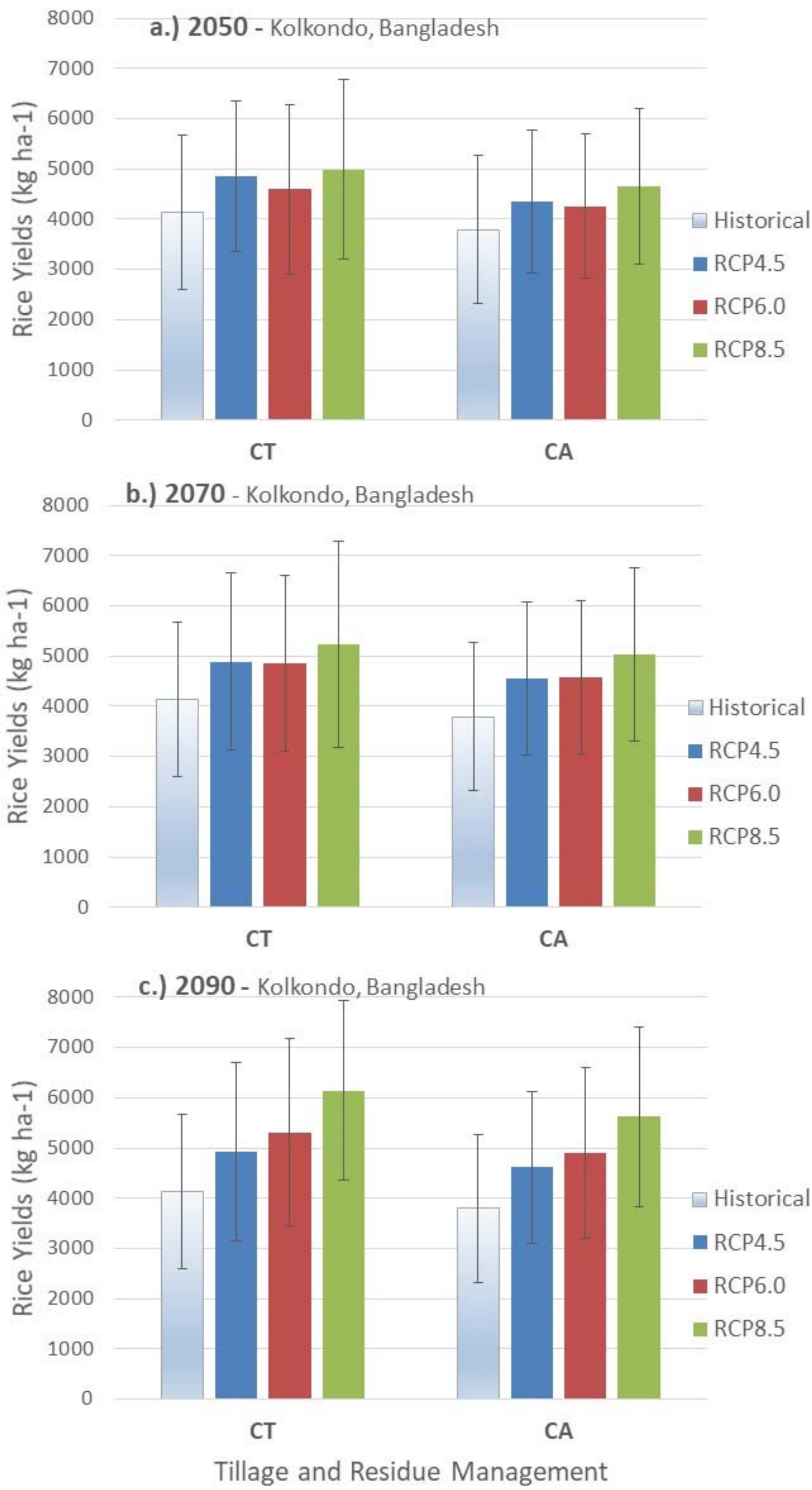

Figure A3.3. Simulated Kharif (wet-season) rice grain yields for Kolkondo, Rangpur, Bangladesh, for a.) 2050; b.) 2070; and c.) 2090, comparing performance of CT vs CA under future climate scenarios RCP4.5 (blue), RCP6.0 (red), and RCP8.5 (green)

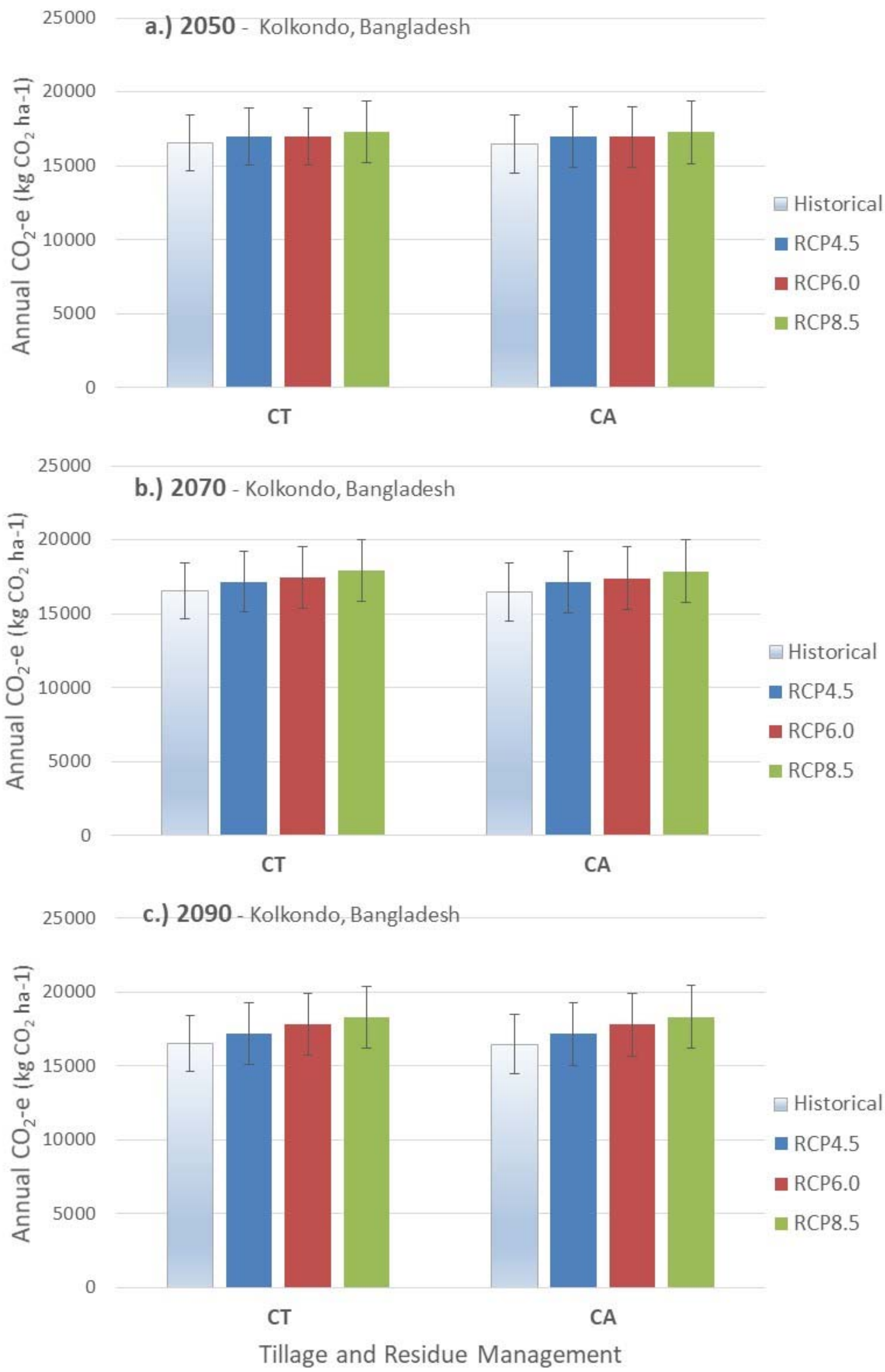

Figure A3.4. Simulated annual GROSS greenhouse gas (GHG) emissions (in CO_2-equivalents) in the rice-maize cropping system at Kolkondo, Rangpur, Bangladesh, for a.) 2050; b.) 2070; and c.) 2090, comparing performance of CT vs CA under future climate scenarios RCP4.5 (blue), RCP6.0 (red), and RCP8.5 (green). Emissions are calculated from top 15cms soil, as per international protocols.

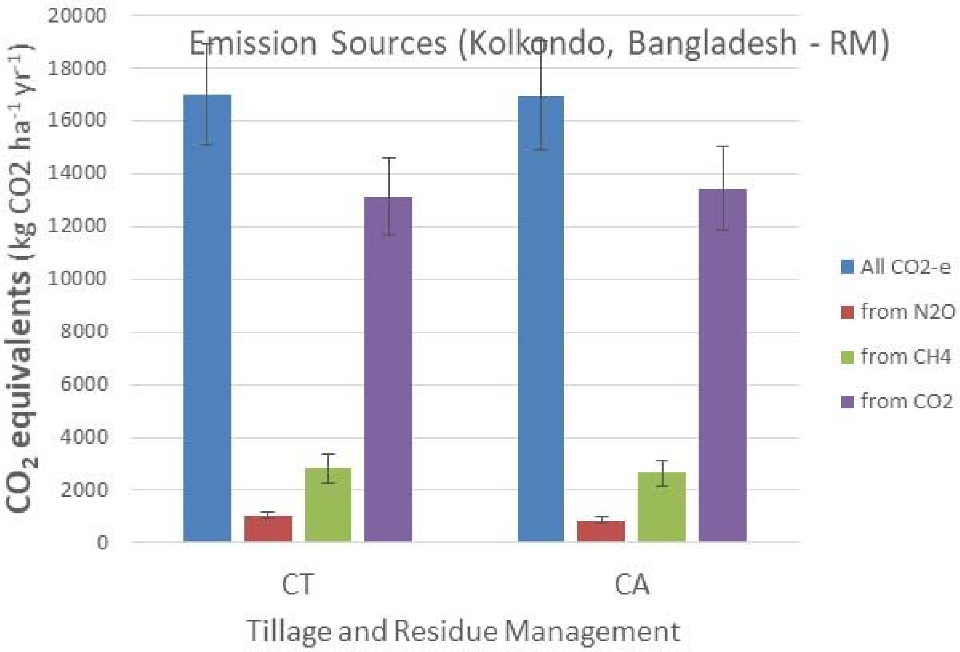

Figure A3.5. Simulated annual greenhouse gas (GHG) emissions (in CO_2-equivalents) in the rice-maize cropping system at Kolkondo, Rangpur, Bangladesh, for 2050, RCP6.0, illustrating the relative contributions from CO_2, CH_4 and N_20.

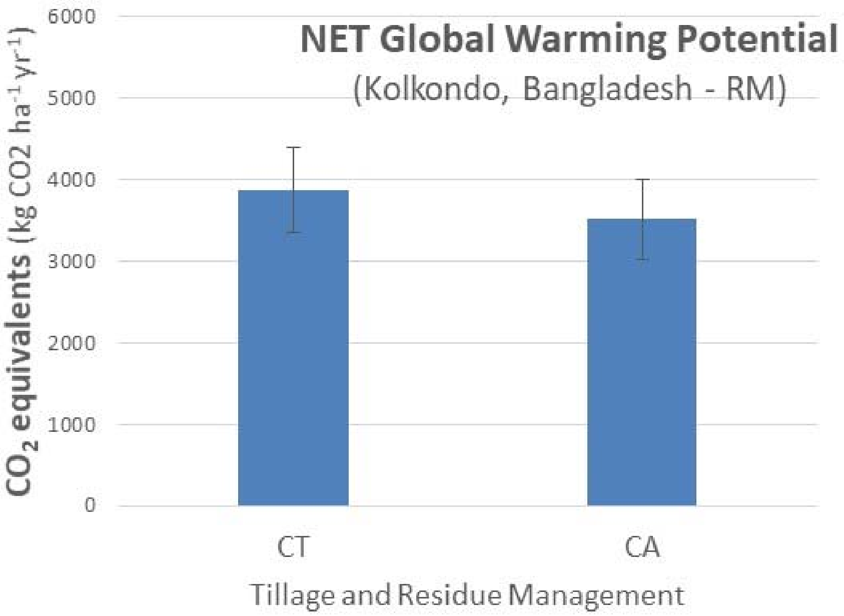

Figure A3. 6. Simulated NET Global Warming Potential (GWP) (in CO_2-equivalents) in the rice-maize cropping system at Kolkondo, Rangpur, Bangladesh, for 2050, RCP6.0, as defined by Lindquist et al., (2012) which considers only contributions from CH_4 + N_20. For net GWP calculations, it is considered that net CO_2 emissions represent < 1% of total GWP, as gross CO_2 emissions are closely matched by atmospheric CO_2 which the growing crops have fixed.

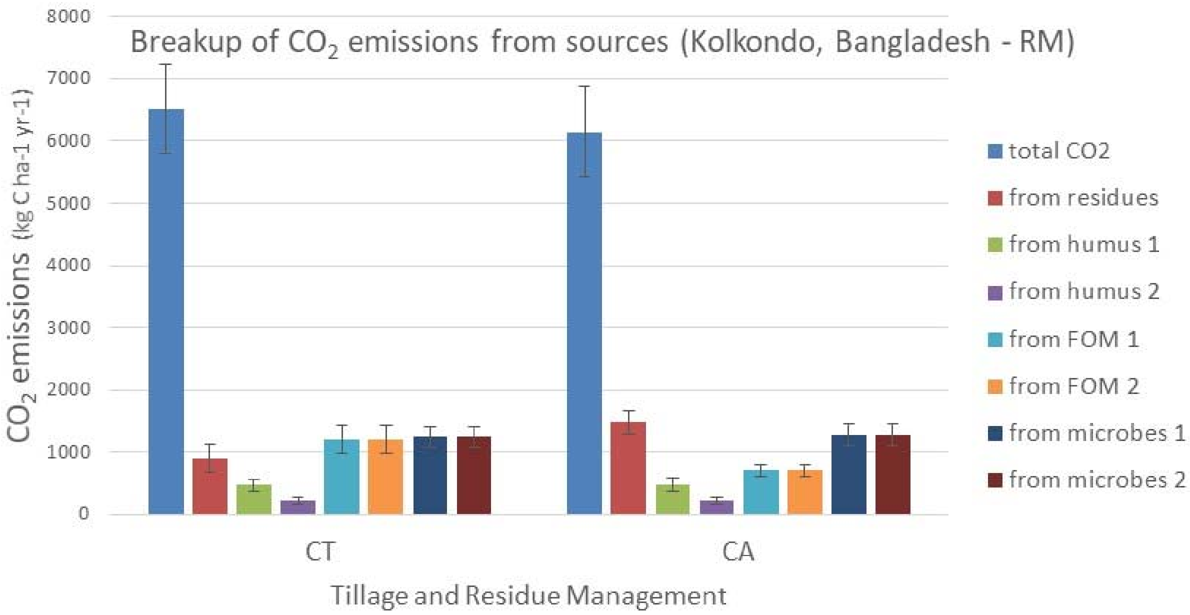

Figure A3.7. Simulated CO2 emissions (in kg C ha^{-1} yr^{-1}) between CT and CA managements in the rice-maize cropping system at Kolkondo, Rangpur, Bangladesh, for 2050, RCP6.0, illustrating the relative contributions from breakdown/cycling of crop residues on the surface, soil fresh organic matter (FOM), soil humic materials (Humus) and soil microbiota (microbes). The “1” and “2” refer to soil layers 1 and 2 (0-15 and 15-30cms, respectively)

A.3.2 Dogachi, Purnea, Bihar, India

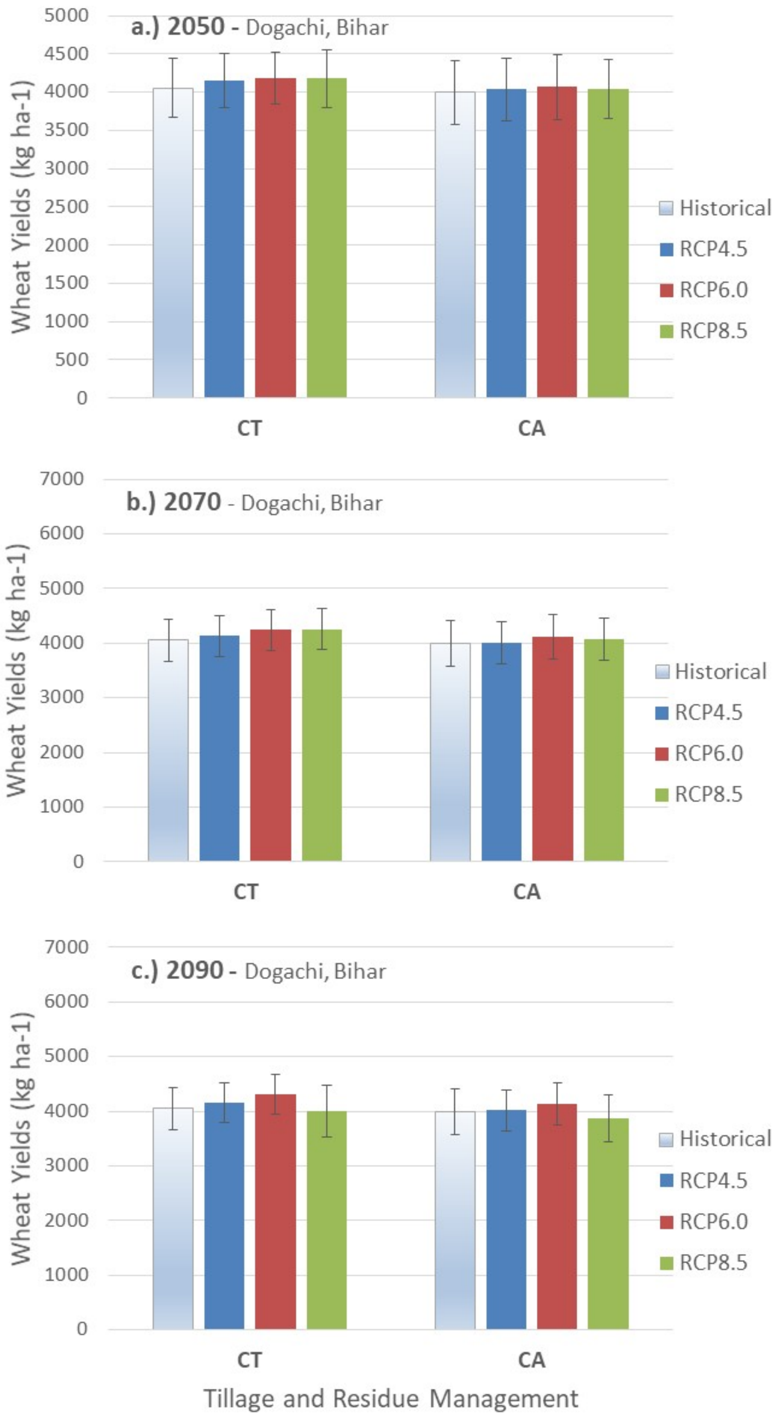

Figure A3.8. Simulated wheat grain yields for Dogachi, Purnea, Bihar, India, for a.) 2050; b.) 2070; and c.) 2090, comparing performance of CT vs CA under future climate scenarios RCP4.5 (blue), RCP6.0 (red), and RCP8.5 (green)

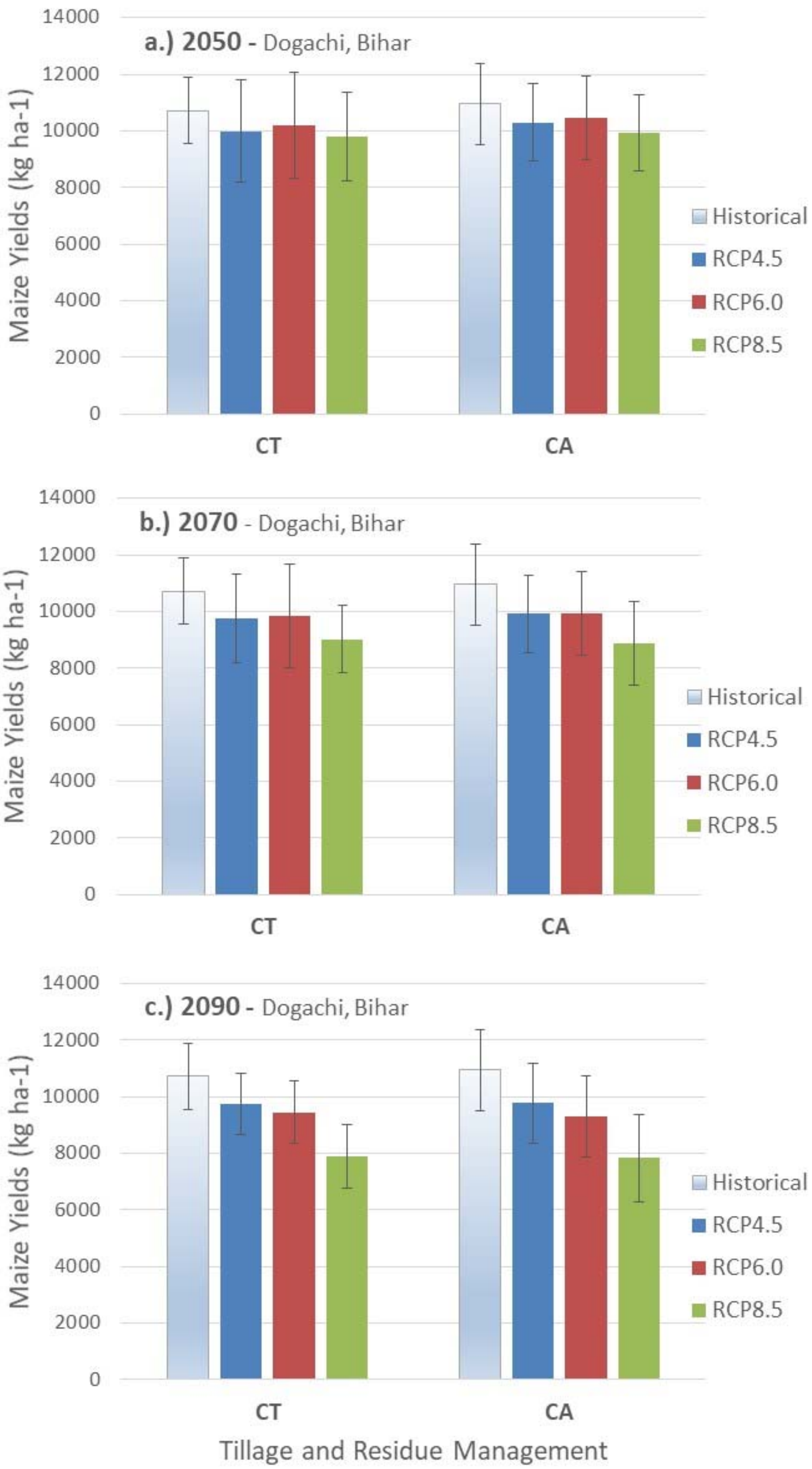

Figure A3.9. Simulated maize grain yields for Dogachi, Purnea, Bihar, India, for a.) 2050; b.) 2070; and c.) 2090, comparing performance of CT vs CA under future climate scenarios RCP4.5 (blue), RCP6.0 (red), and RCP8.5 (green)

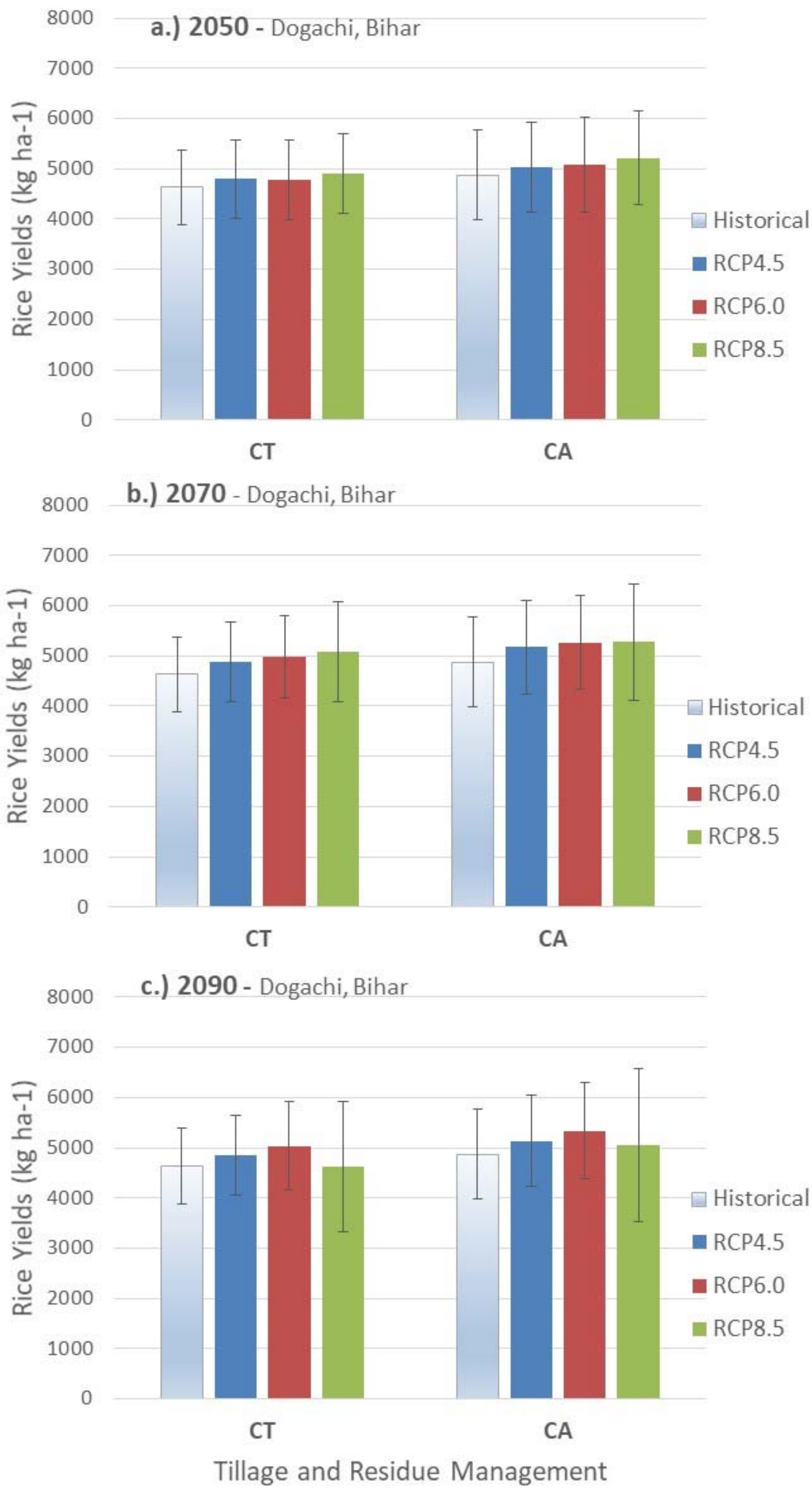

Figure A3.10. Simulated Kharif (wet-season) rice grain yields for Dogachi, Purnea, Bihar, India, for a.) 2050; b.) 2070; and c.) 2090, comparing performance of CT vs CA under future climate scenarios RCP4.5 (blue), RCP6.0 (red), and RCP8.5 (green)

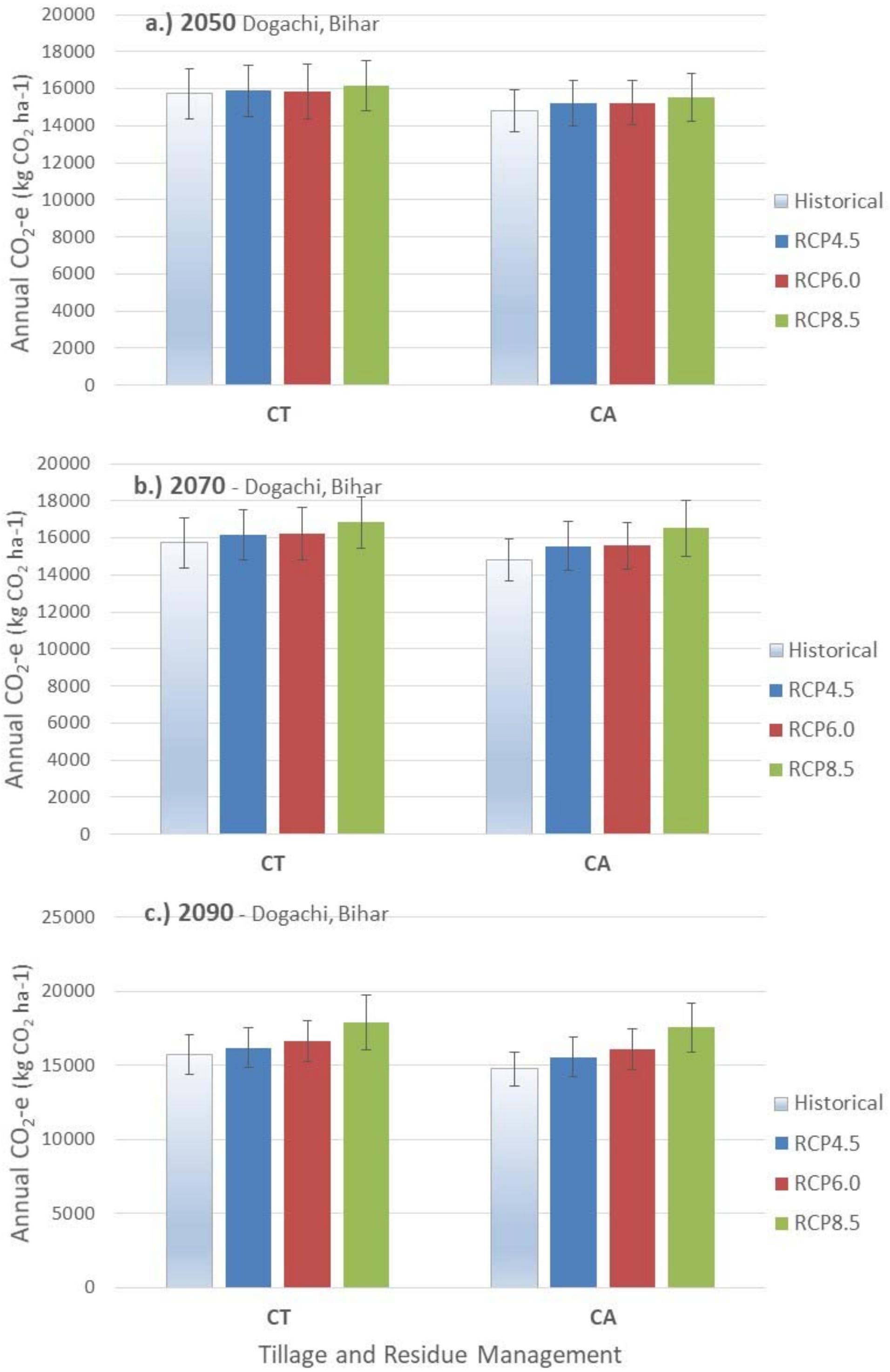

Figure A3.11. Simulated annual GROSS greenhouse gas (GHG) emissions (in CO_2-equivalents) in the rice-maize cropping system at Dogachi, Purnea, Bihar, India, for a.) 2050; b.) 2070; and c.) 2090, comparing performance of CT vs CA under future climate scenarios RCP4.5 (blue), RCP6.0 (red), and RCP8.5 (green). Emissions are calculated from top 15cms soil.

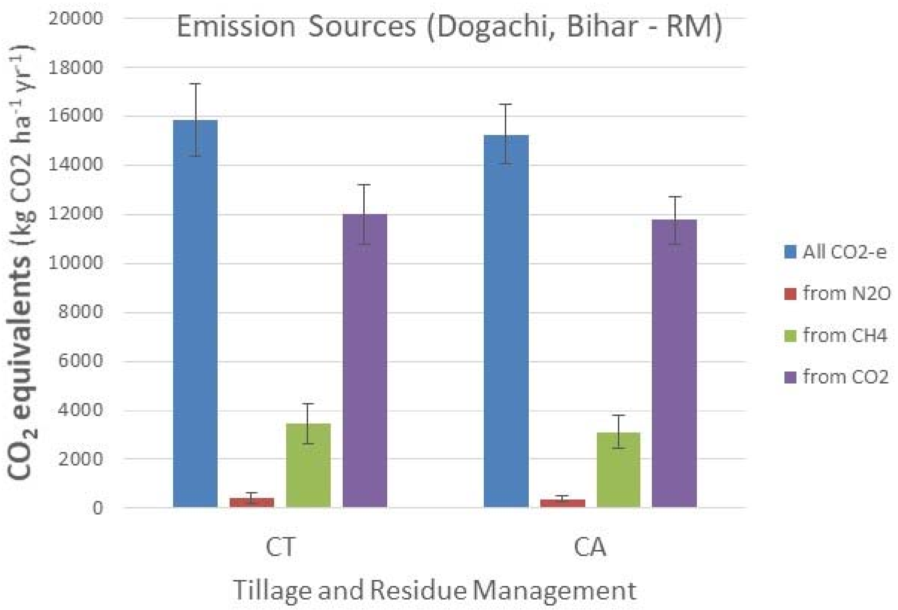

Figure A3.12. Simulated annual greenhouse gas (GHG) emissions (in CO_2-equivalents) in the rice-maize cropping system at Dogachi, Purnea, Bihar, India, for 2050, RCP6.0, illustrating the relative contributions from CO_2, CH_4 and N_20.

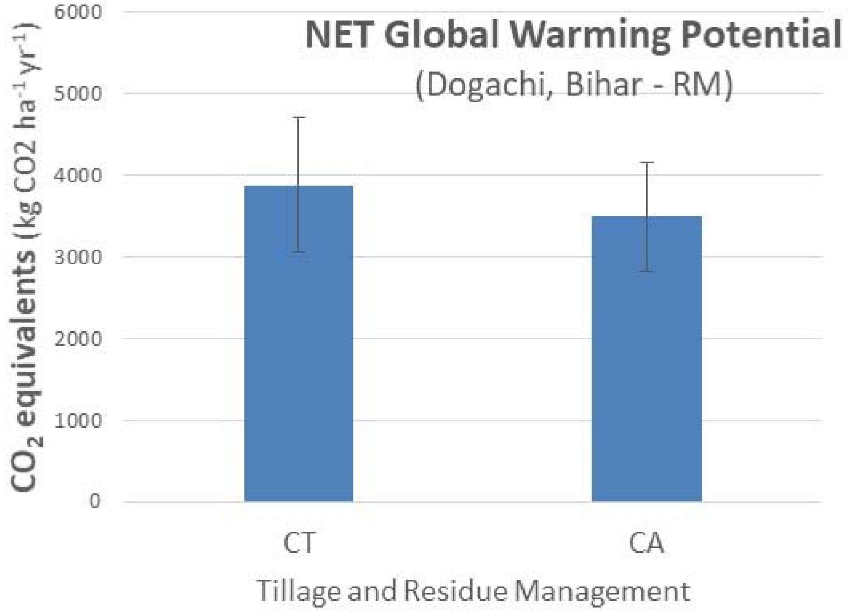

Figure A3.13. Simulated NET Global Warming Potential (GWP) (in CO_2-equivalents) in the rice-maize cropping system at Dogachi, Purnea, Bihar, India, for 2050, RCP6.0, as defined by Lindquist et al., (2012) which considers only contributions from CH_4 + N_20. For net GWP calculations, it is considered that net CO_2 emissions represent < 1% of total GWP, as gross CO_2 emissions are closely matched by atmospheric CO_2 which the growing crops have fixed.

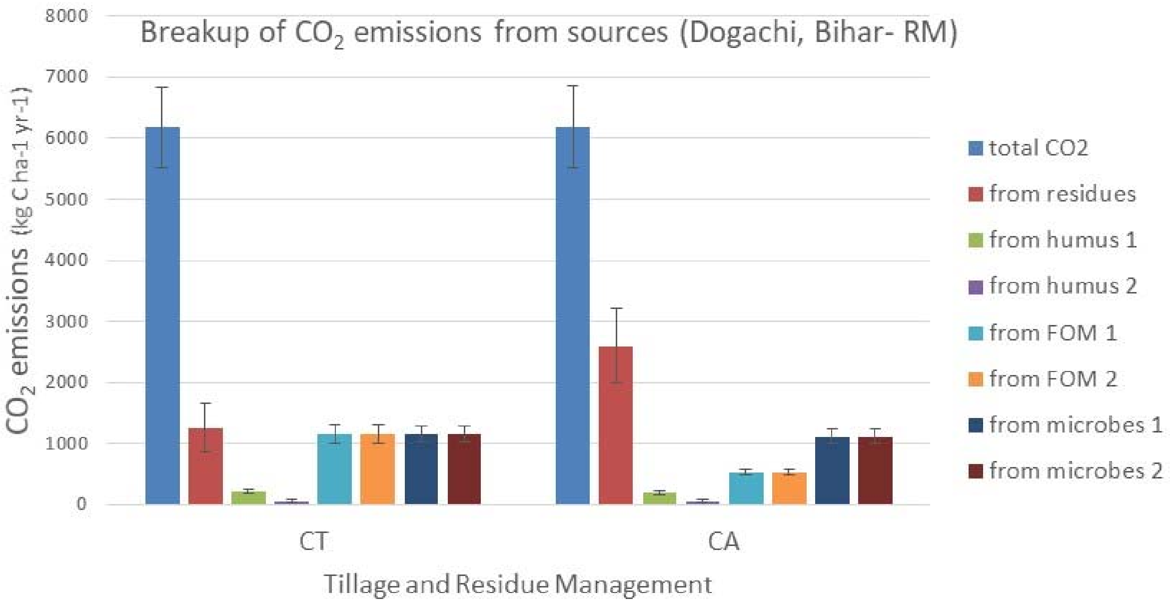

Figure A3.14. Simulated CO2 emissions (in kg C ha^{-1} yr^{-1}) between CT and CA managements in the rice-maize cropping system at Dogachi, Purnea, Bihar, India, for 2050, RCP6.0, illustrating the relative contributions from breakdown/cycling of crop residues on the surface, soil fresh organic matter (FOM), soil humic materials (Humus) and soil microbiota (microbes). The “1” and “2” refer to soil layers 1 and 2 (0-15 and 15-30cms, respectively)

A 3.3 Tikapatti, Bihar, India

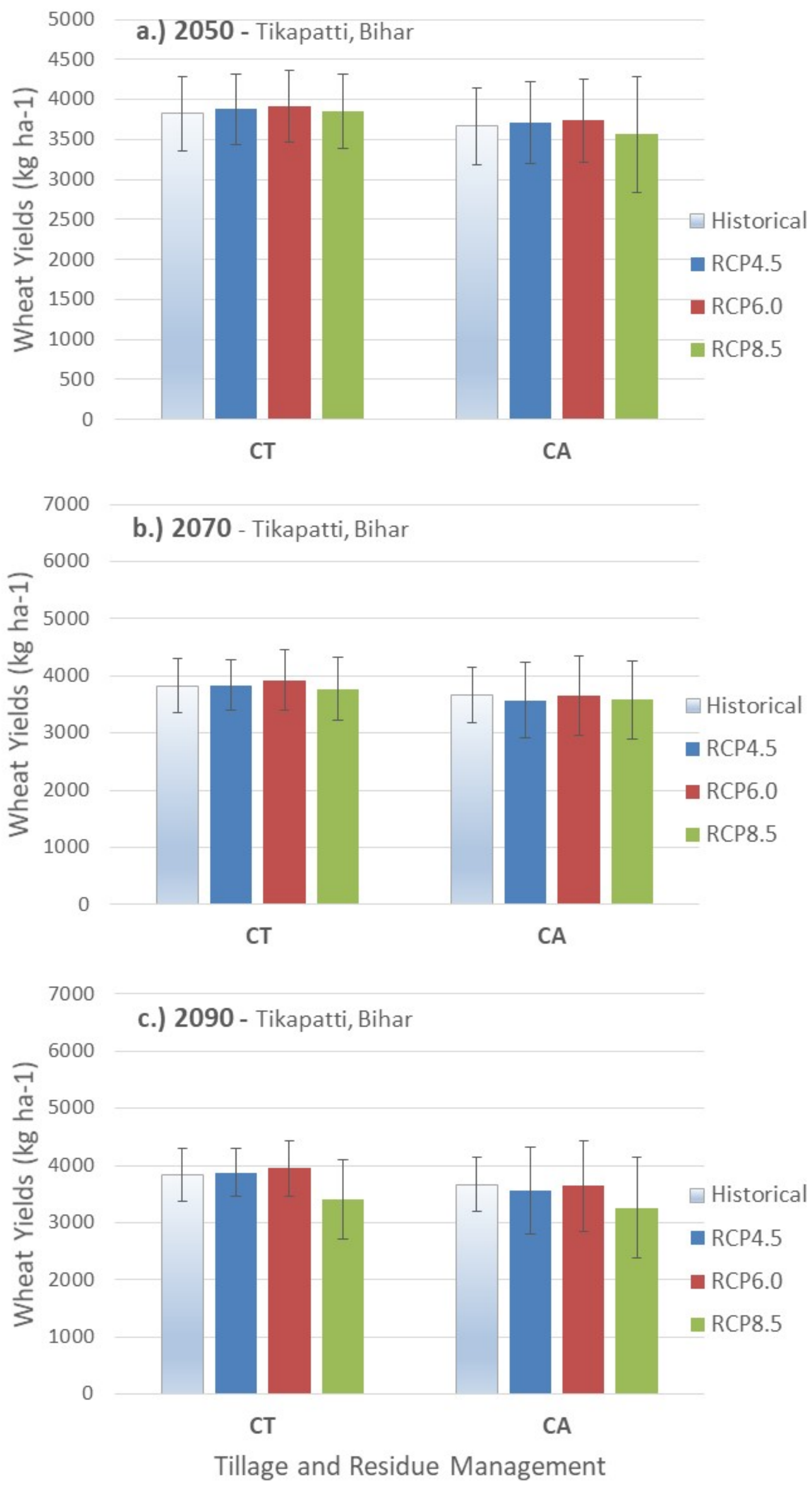

Figure A3.15. Simulated wheat grain yields for Tikapatti, Bihar, India, for a.) 2050; b.) 2070; and c.) 2090, comparing performance of CT vs CA under future climate scenarios RCP4.5 (blue), RCP6.0 (red), and RCP8.5 (green)

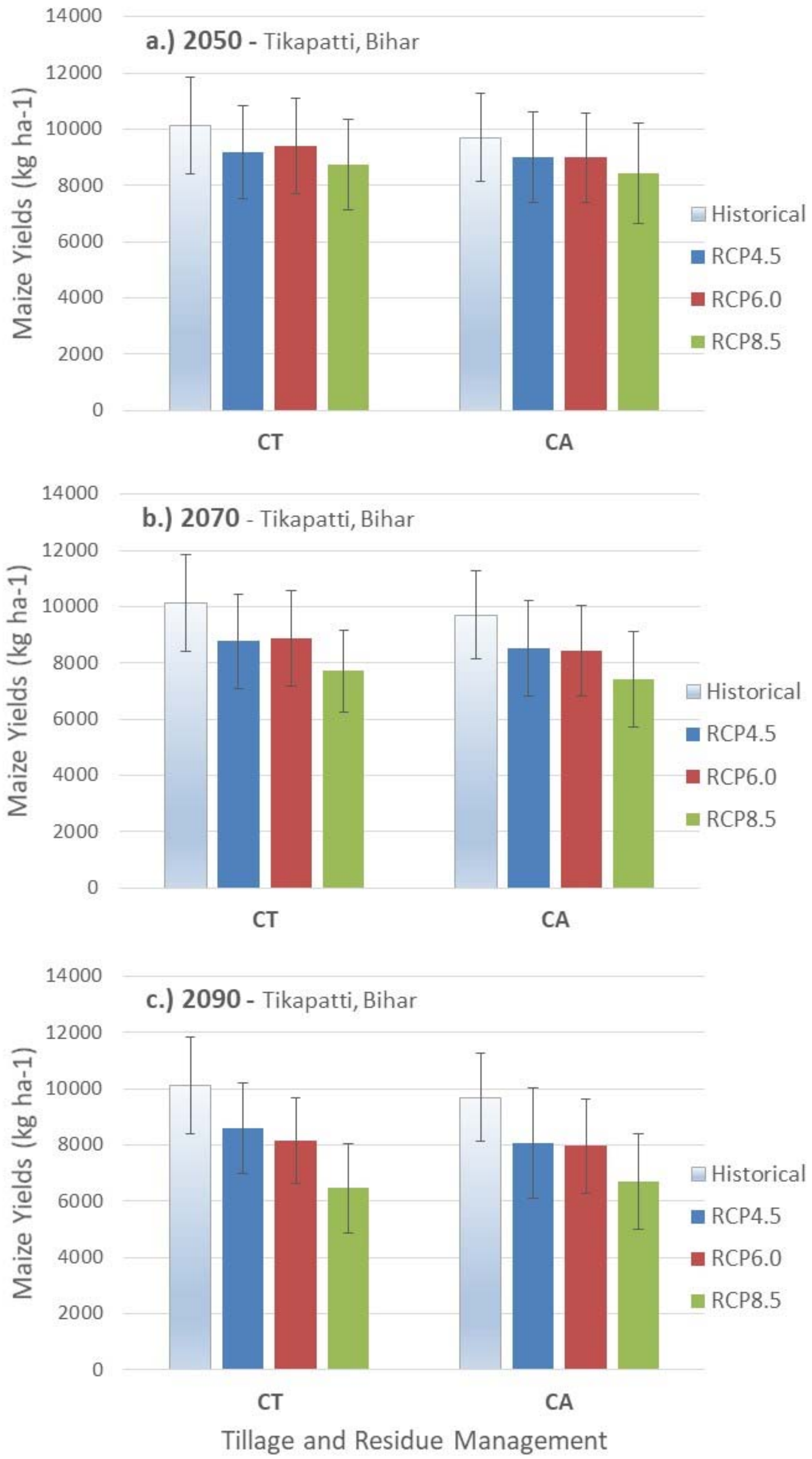

Figure A3.16. Simulated maize grain yields for Tikapatti, Bihar, India, for a.) 2050; b.) 2070; and c.) 2090, comparing performance of CT vs CA under future climate scenarios RCP4.5 (blue), RCP6.0 (red), and RCP8.5 (green)

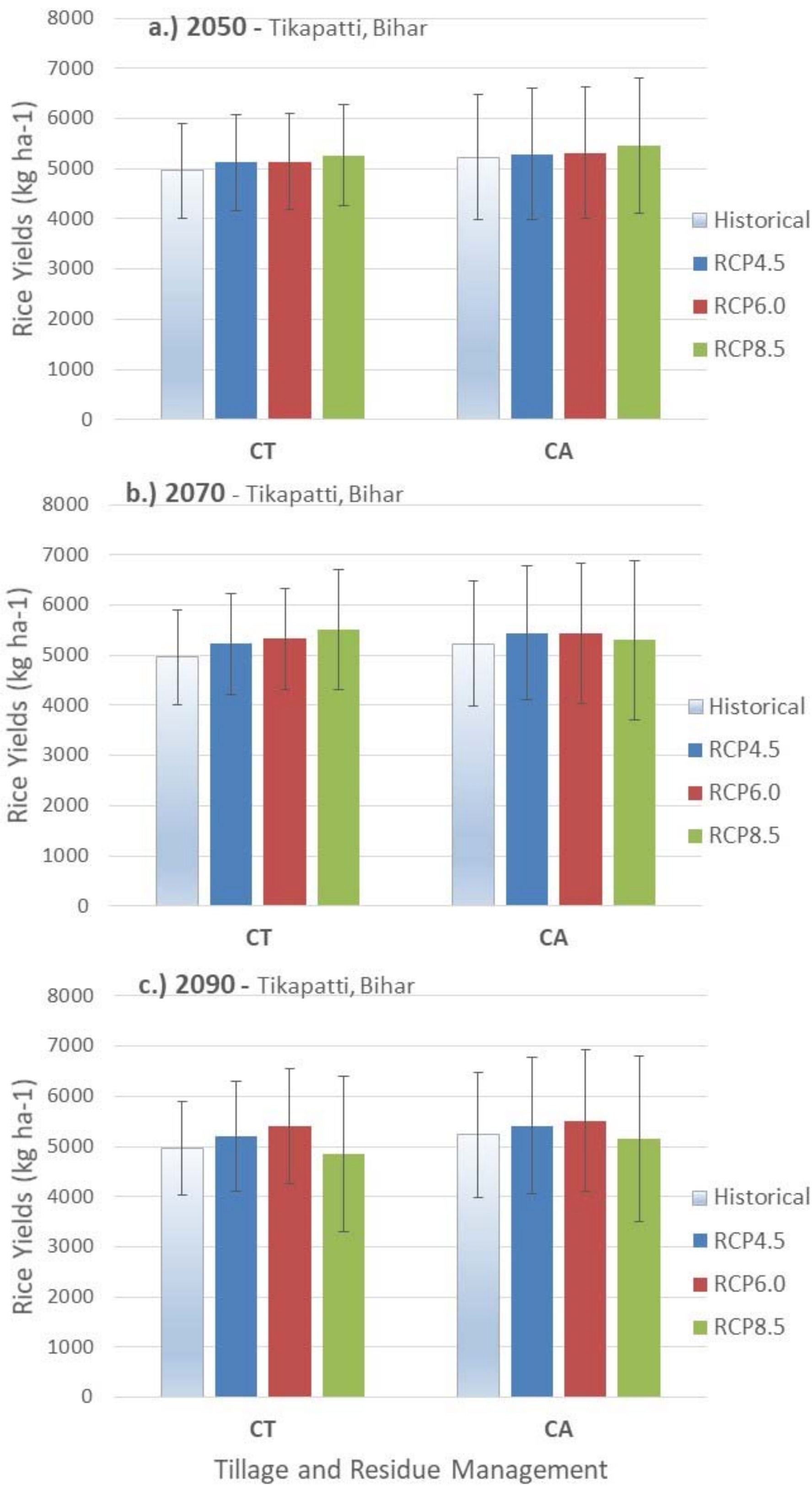

Figure A3.17. Simulated Kharif (wet-season) rice grain yields for Tikapatti, Bihar, India, for a.) 2050; b.) 2070; and c.) 2090, comparing performance of CT vs CA under future climate scenarios RCP4.5 (blue), RCP6.0 (red), and RCP8.5 (green)

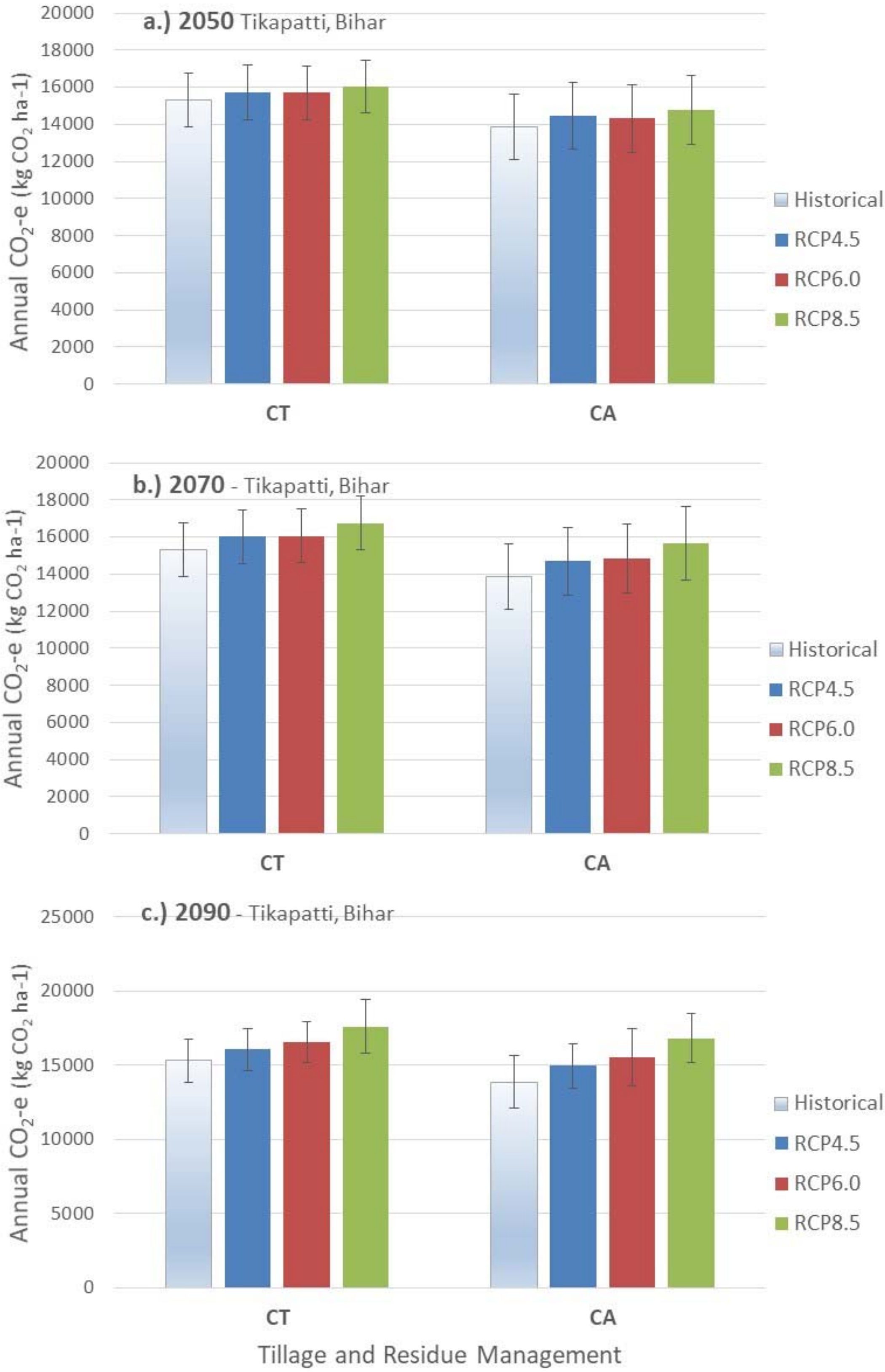

Figure A3.18. Simulated annual GROSS greenhouse gas (GHG) emissions (in CO_2-equivalents) in the rice-maize cropping system at Tikapatti, Bihar, India, for a.) 2050; b.) 2070; and c.) 2090, comparing performance of CT vs CA under future climate scenarios RCP4.5 (blue), RCP6.0 (red), and RCP8.5 (green). Emissions are calculated from top 15cms soil.

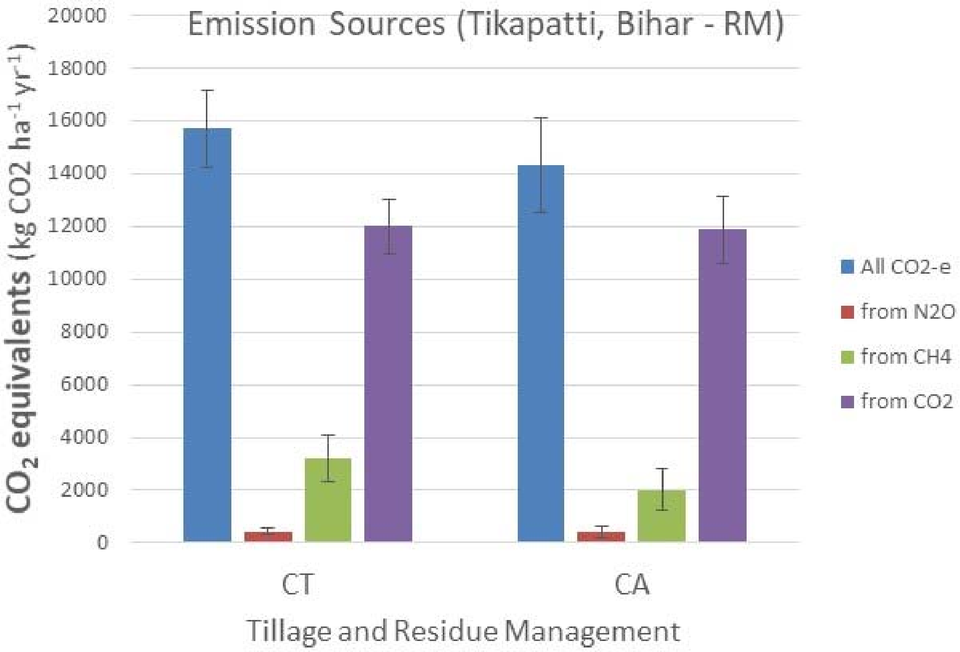

Figure A3.19. Simulated annual greenhouse gas (GHG) emissions (in CO_2-equivalents) in the rice-maize cropping system at Tikapatti, Bihar, India, for 2050, RCP6.0, illustrating the relative contributions from CO_2, CH_4 and N_20.

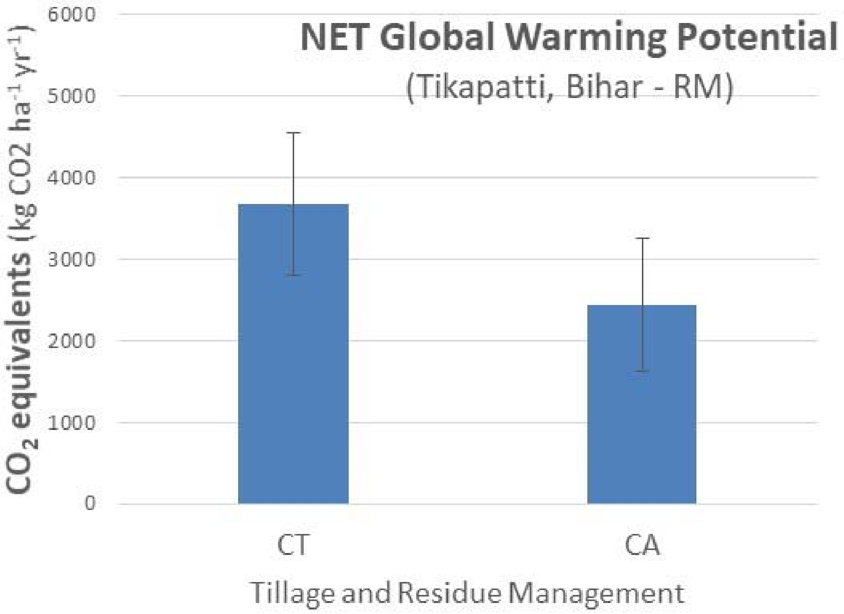

Figure A3.20. Simulated NET Global Warming Potential (GWP) (in CO_2-equivalents) in the rice-maize cropping system at Tikapatti, Bihar, India, for 2050, RCP6.0, as defined by Lindquist et al., (2012) which considers only contributions from CH_4 + N_20. For net GWP calculations, it is considered that net CO_2 emissions represent < 1% of total GWP, as gross CO_2 emissions are closely matched by atmospheric CO_2 which the growing crops have fixed.

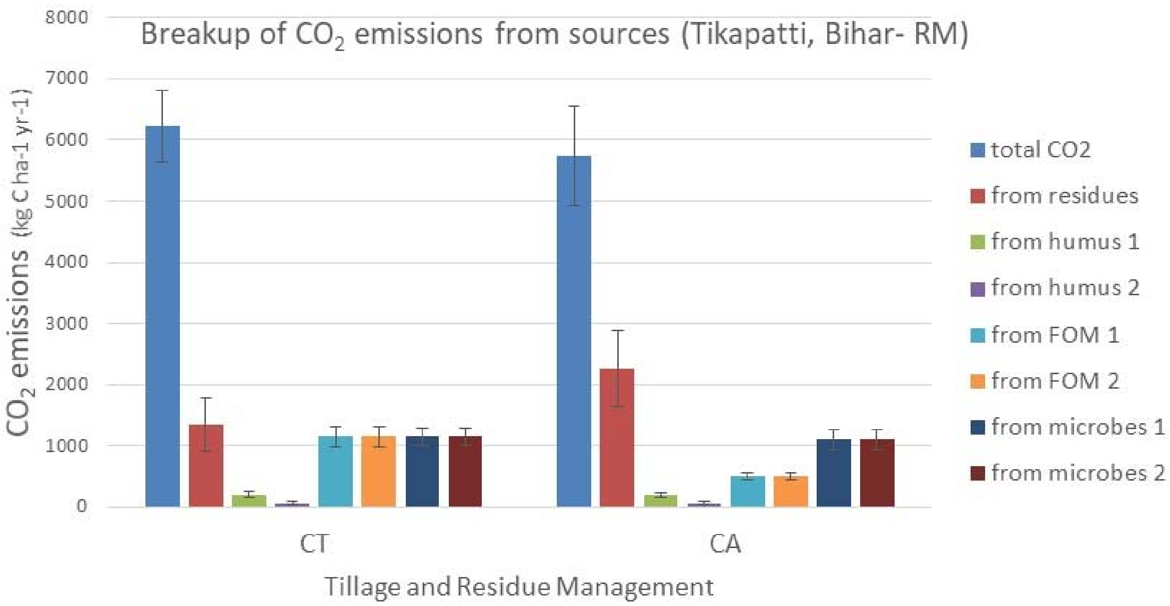

Figure A3.21. Simulated CO2 emissions (in kg C ha^{-1} yr^{-1}) between CT and CA managements in the rice-maize cropping system at Tikapatti, Bihar, India, for 2050, RCP6.0, illustrating the relative contributions from breakdown/cycling of crop residues on the surface, soil fresh organic matter (FOM), soil humic materials (Humus) and soil microbiota (microbes). The “1” and “2” refer to soil layers 1 and 2 (0-15 and 15-30cms, respectively)

A3.4 Tarahara, Sunsari, Nepal

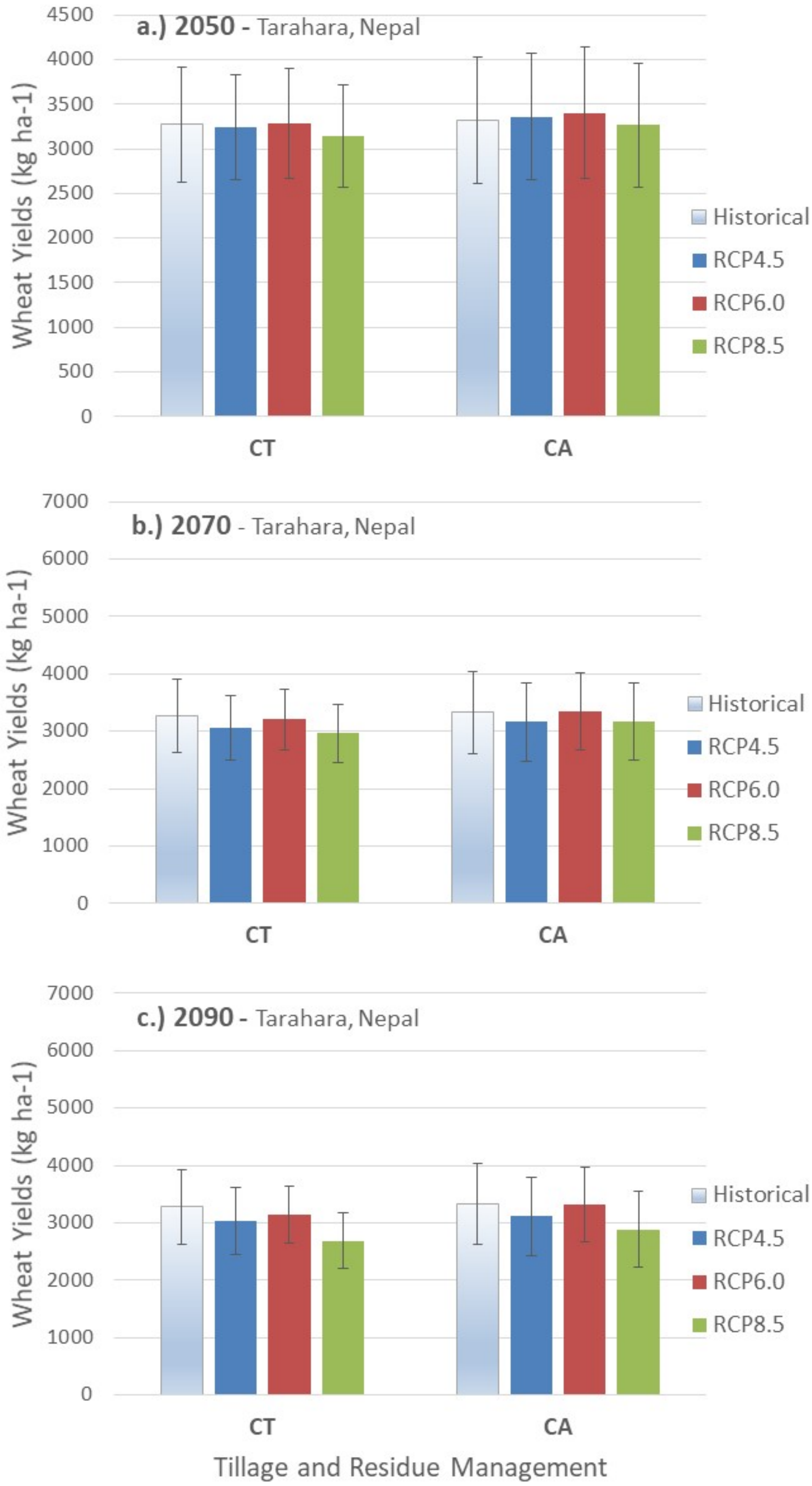

Figure A3.22. Simulated wheat grain yields for Tarahara, Sunsari, Nepal, for a.) 2050; b.) 2070; and c.) 2090, comparing performance of CT vs CA under future climate scenarios RCP4.5 (blue), RCP6.0 (red), and RCP8.5 (green)

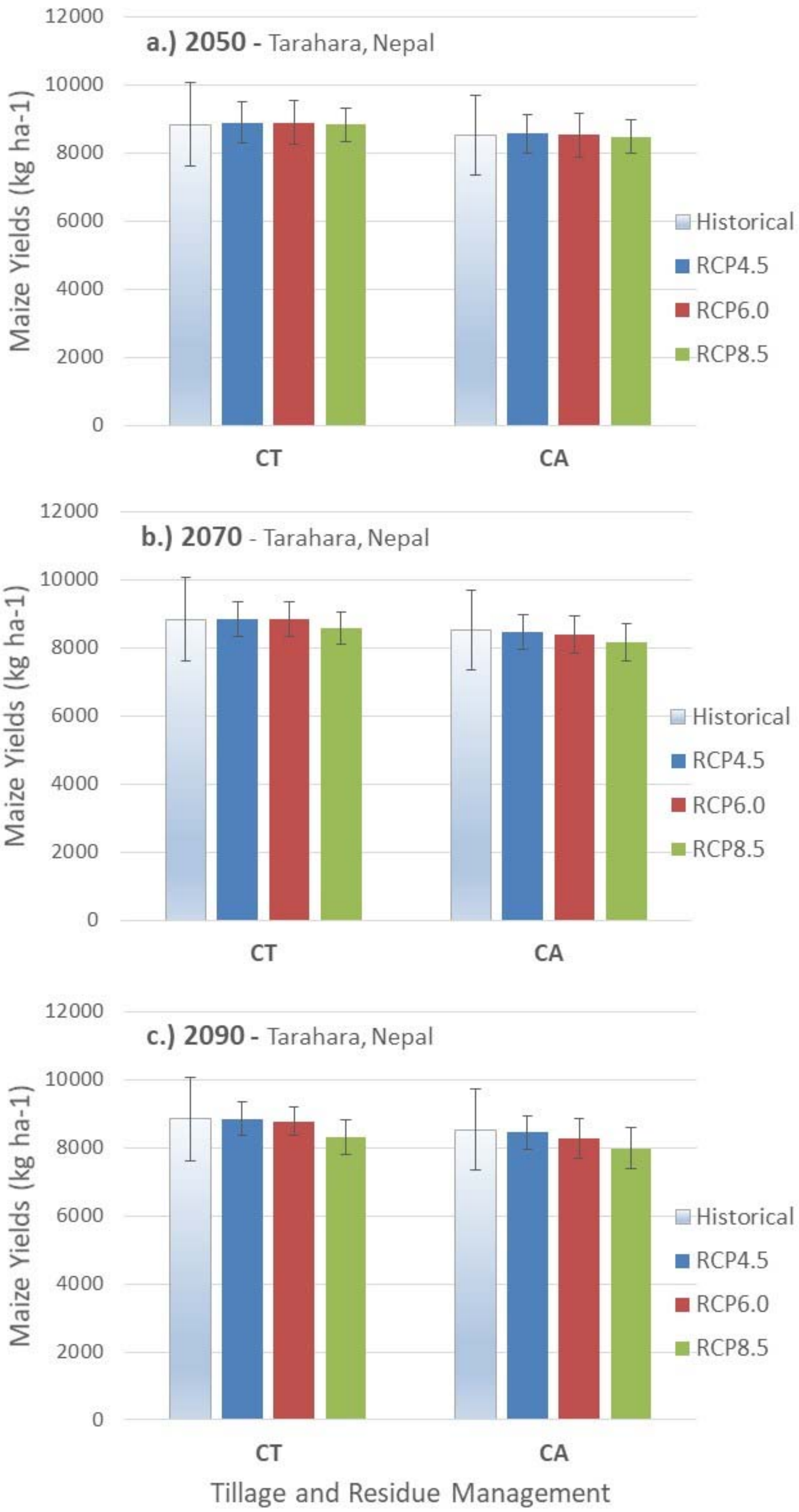

Figure A3.23. Simulated maize grain yields for Tarahara, Sunsari, Nepal, for a.) 2050; b.) 2070; and c.) 2090, comparing performance of CT vs CA under future climate scenarios RCP4.5 (blue), RCP6.0 (red), and RCP8.5 (green)

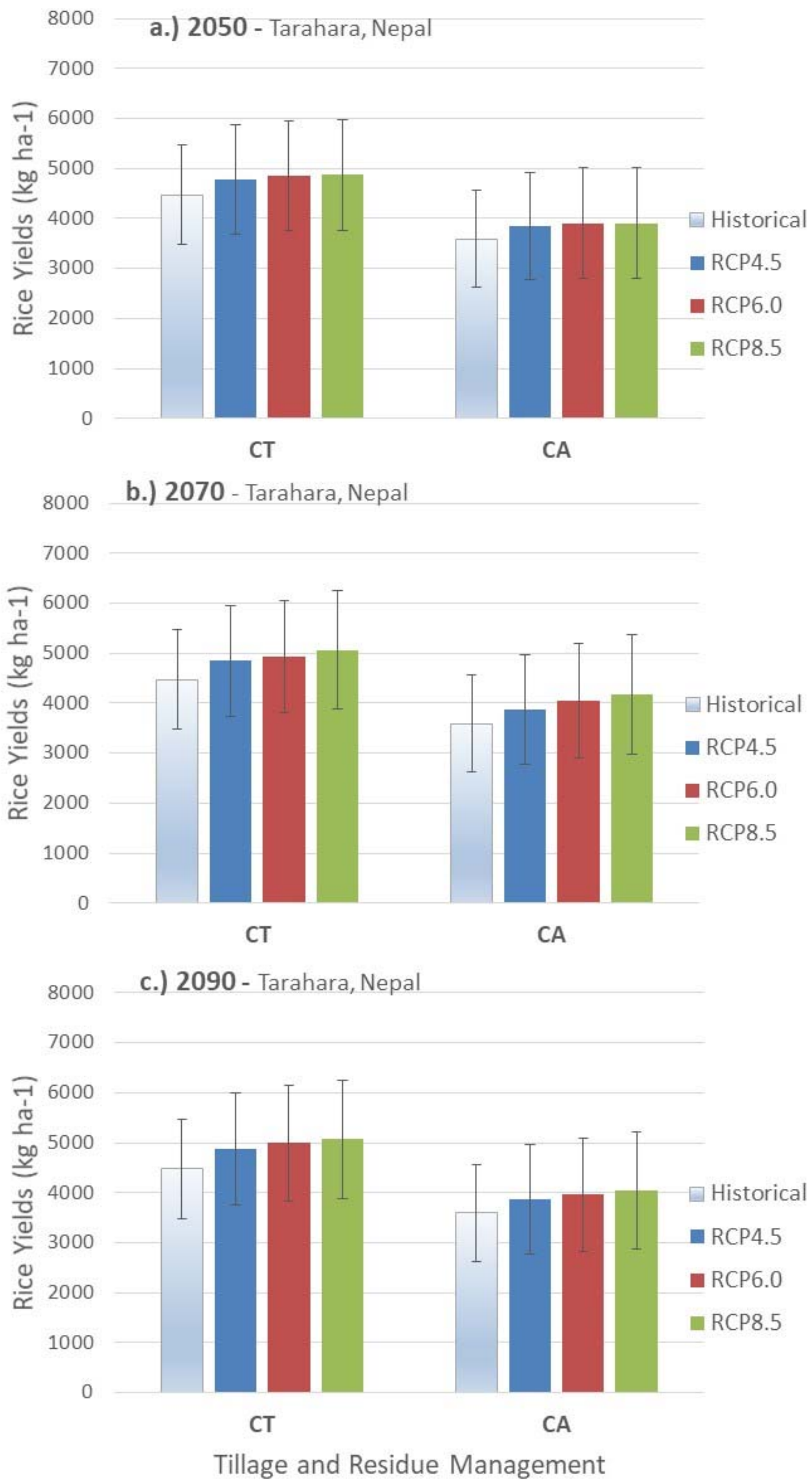

Figure A3.24. Simulated Kharif (wet-season) rice grain yields for Tarahara, Sunsari, Nepal, for a.) 2050; b.) 2070; and c.) 2090, comparing performance of CT vs CA under future climate scenarios RCP4.5 (blue), RCP6.0 (red), and RCP8.5 (green)

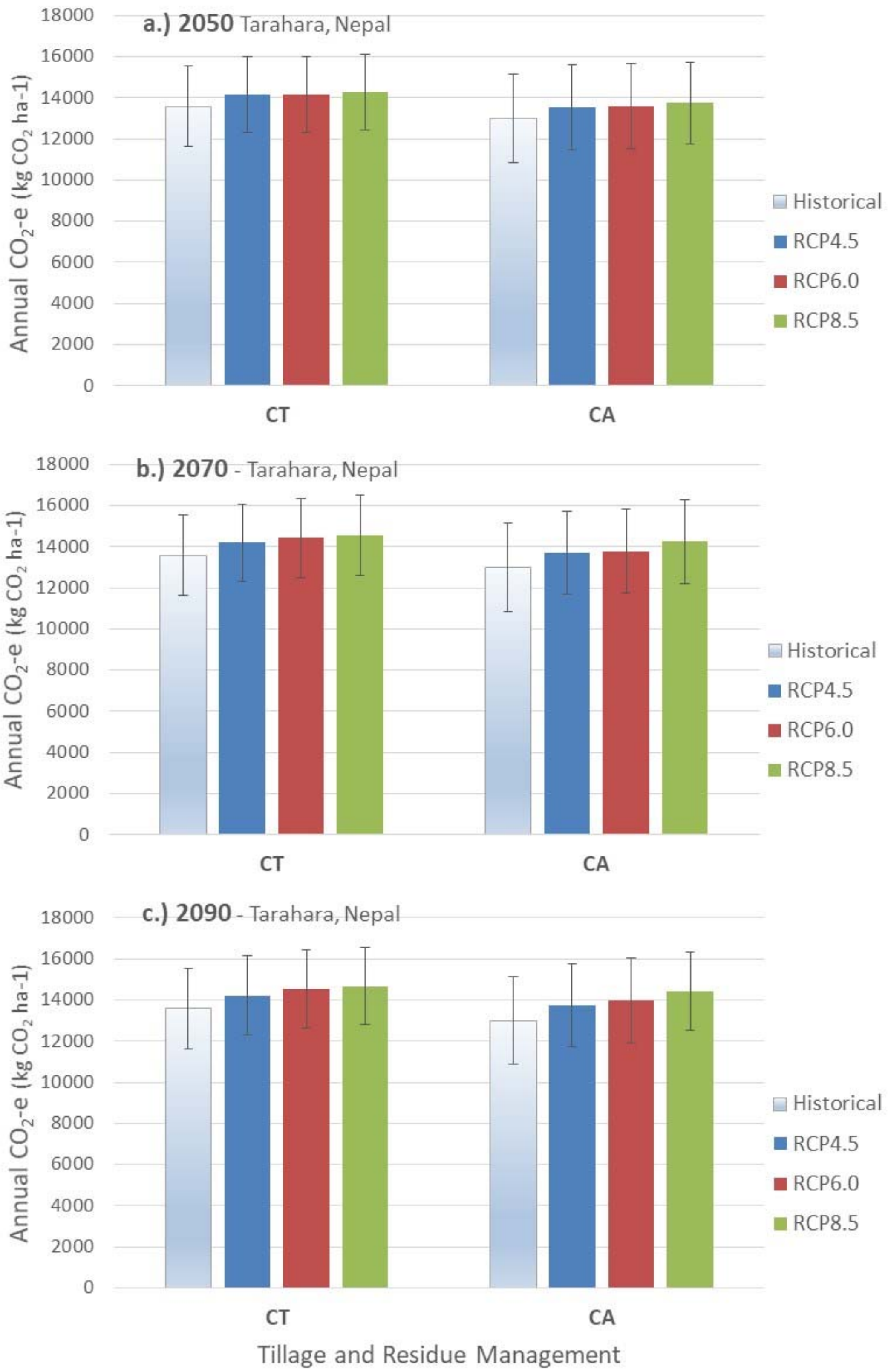

Figure A3.25. Simulated annual GROSS greenhouse gas (GHG) emissions (in CO_2-equivalents) in the rice-maize cropping system at Tarahara, Sunsari, Nepal, for a.) 2050; b.) 2070; and c.) 2090, comparing performance of CT vs CA under future climate scenarios RCP4.5 (blue), RCP6.0 (red), and RCP8.5 (green). Emissions are calculated from top 15cms soil.

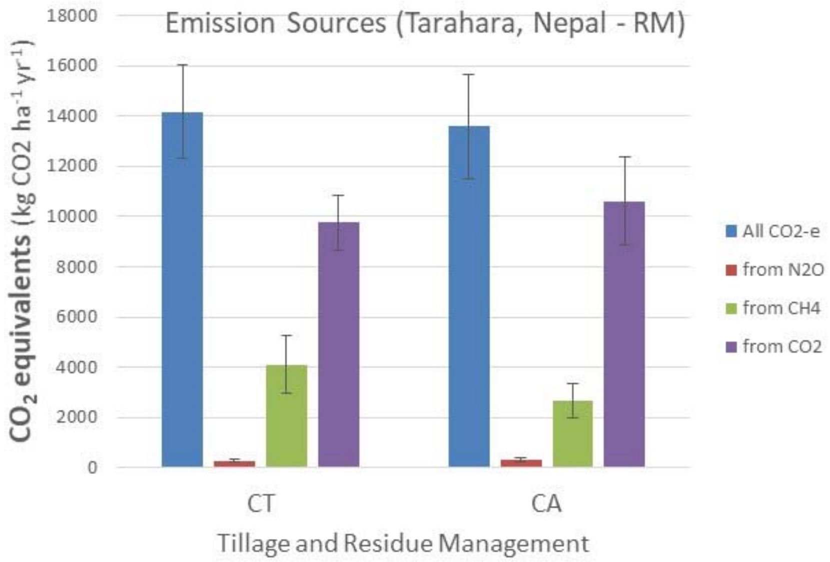

Figure A3.26. Simulated annual greenhouse gas (GHG) emissions (in CO_2-equivalents) in the rice-maize cropping system at Tarahara, Sunsari, Nepal, for 2050, RCP6.0, illustrating the relative contributions from CO_2, CH_4 and N_20.

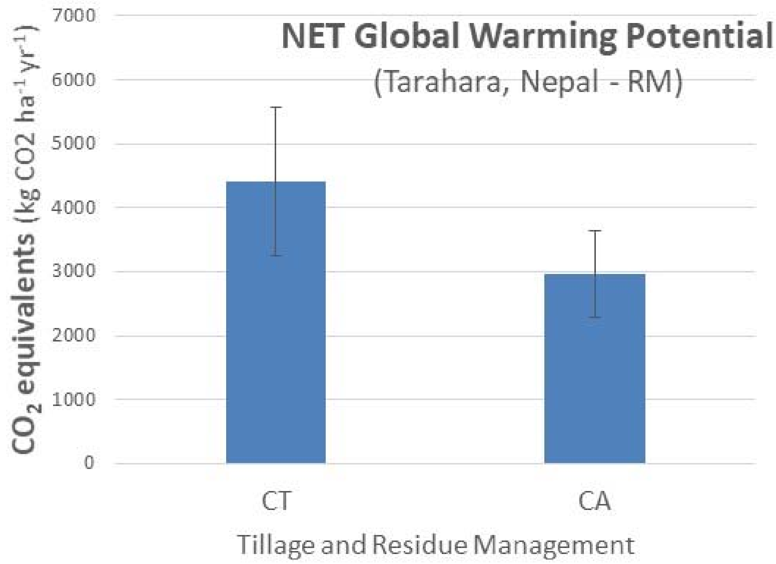

Figure A3.27. Simulated NET Global Warming Potential (GWP) (in CO_2-equivalents) in the rice-maize cropping system at Tarahara, Sunsari, Nepal, for 2050, RCP6.0, as defined by Lindquist et al., (2012) which considers only contributions from CH_4 + N_20. For net GWP calculations, it is considered that net CO_2 emissions represent < 1% of total GWP, as gross CO_2 emissions are closely matched by atmospheric CO_2 which the growing crops have fixed.

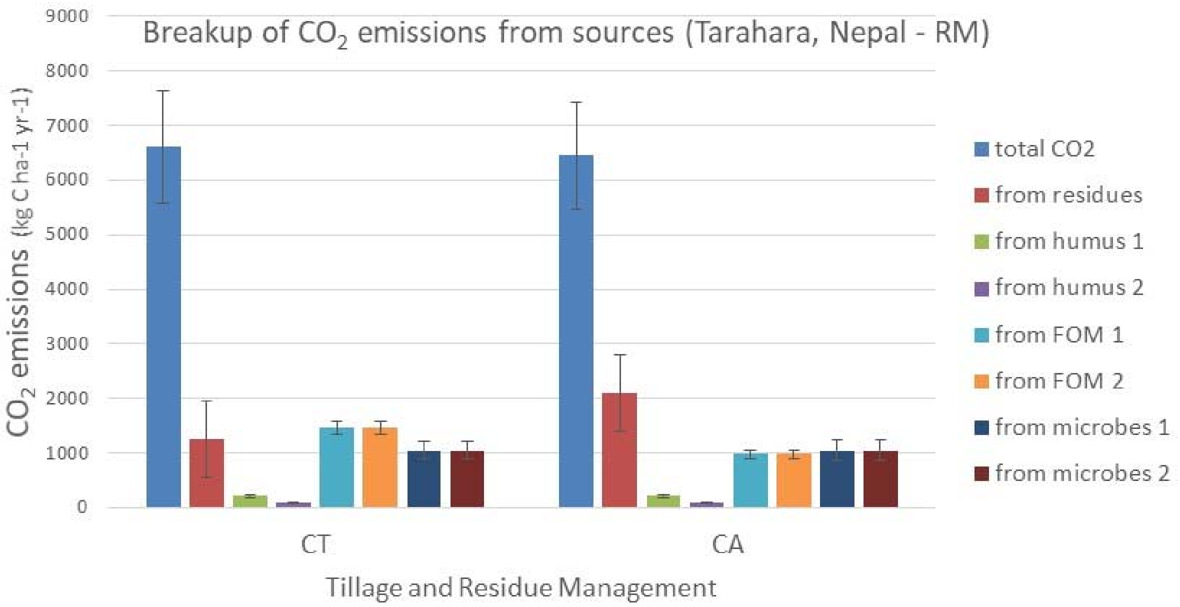

Figure A3.28. Simulated CO2 emissions (in kg C ha^{-1} yr^{-1}) between CT and CA managements in the rice-maize cropping system at Tarahara, Sunsari, Nepal, for 2050, RCP6.0, illustrating the relative contributions from breakdown/cycling of crop residues on the surface, soil fresh organic matter (FOM), soil humic materials (Humus) and soil microbiota (microbes). The “1” and “2” refer to soil layers 1 and 2 (0-15 and 15-30cms, respectively)

A3.5 Malda, West Bengal, India

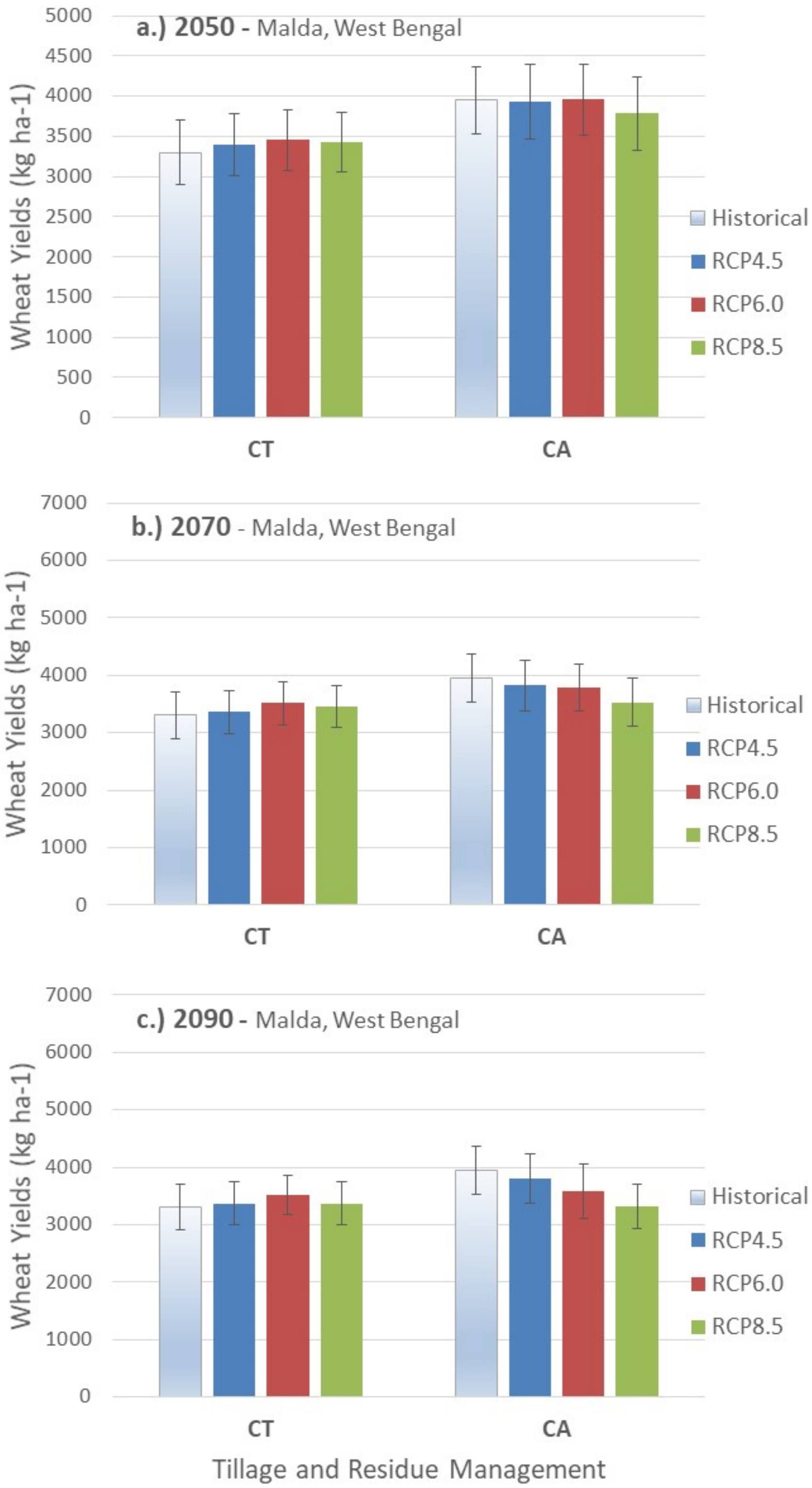

Figure A3.29. Simulated wheat grain yields for Malda, West Bengal, India, for a.) 2050; b.) 2070; and c.) 2090, comparing performance of CT vs CA under future climate scenarios RCP4.5 (blue), RCP6.0 (red), and RCP8.5 (green)

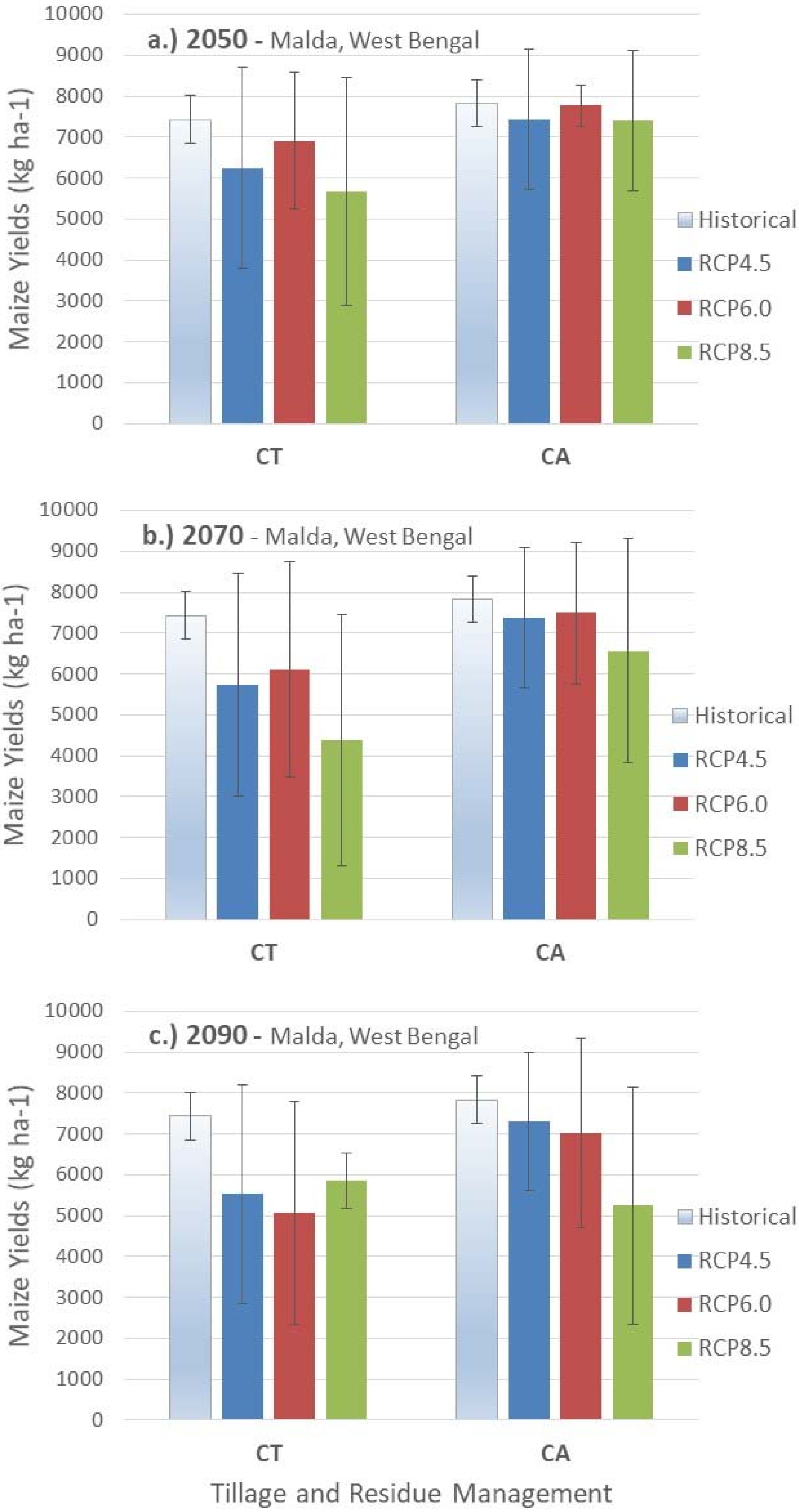

Figure A3.30. Simulated maize grain yields for Malda, West Bengal, India, for a.) 2050; b.) 2070; and c.) 2090, comparing performance of CT vs CA under future climate scenarios RCP4.5 (blue), RCP6.0 (red), and RCP8.5 (green)

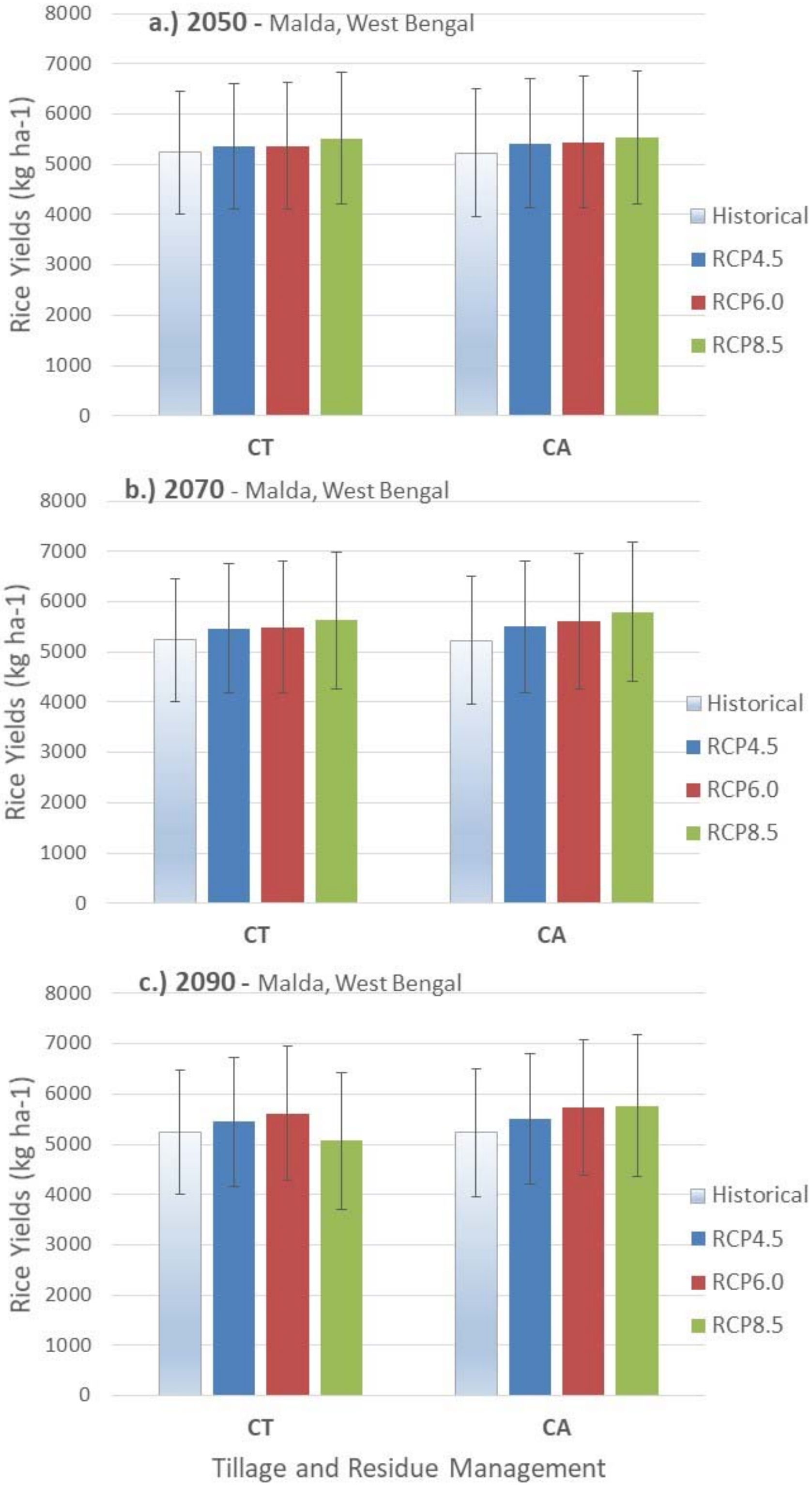

Figure A3.31. Simulated Kharif (wet-season) rice grain yields for Malda, West Bengal, India, for a.) 2050; b.) 2070; and c.) 2090, comparing performance of CT vs CA under future climate scenarios RCP4.5 (blue), RCP6.0 (red), and RCP8.5 (green)

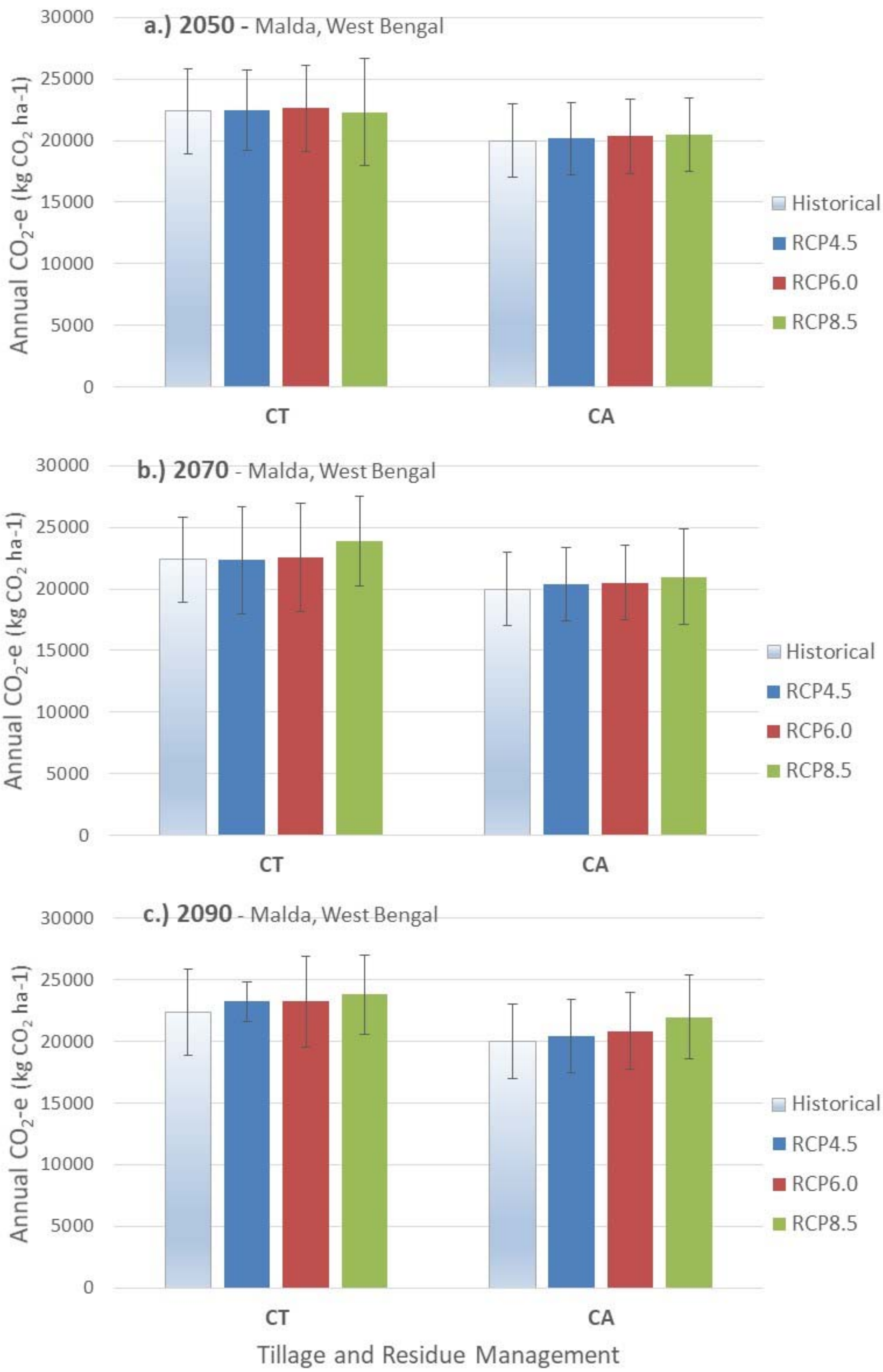

Figure A3.32. Simulated annual GROSS greenhouse gas (GHG) emissions (in CO_2-equivalents) in the rice-maize cropping system at Malda, West Bengal, India, for a.) 2050; b.) 2070; and c.) 2090, comparing performance of CT vs CA under future climate scenarios RCP4.5 (blue), RCP6.0 (red), and RCP8.5 (green). Emissions are calculated from top 15cms soil, as per international protocols.

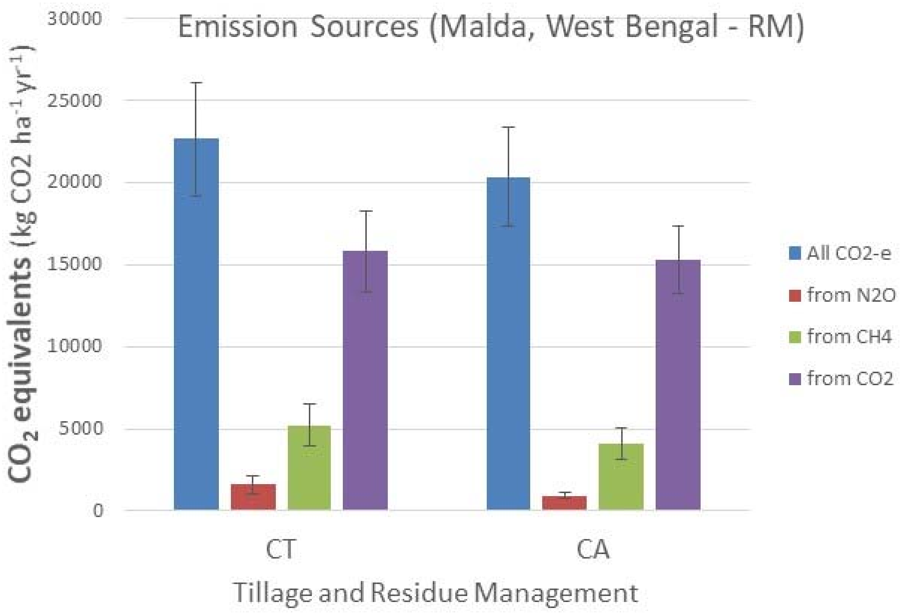

Figure A3.33. Simulated annual greenhouse gas (GHG) emissions (in CO_2-equivalents) in the rice-maize cropping system at Malda, West Bengal, India, for 2050, RCP6.0, illustrating the relative contributions from CO_2, CH_4 and N_20.

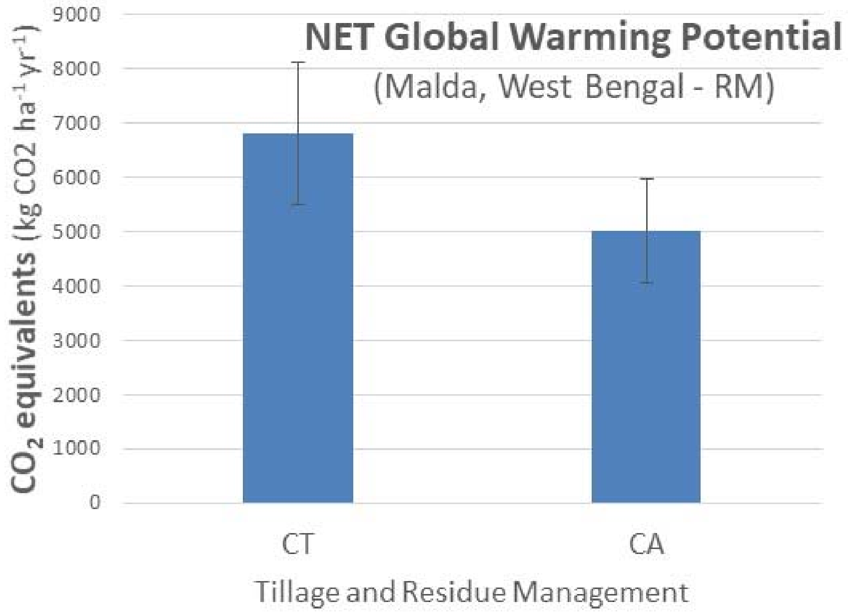

Figure A3.34. Simulated NET Global Warming Potential (GWP) (in CO_2-equivalents) in the rice-maize cropping system at Malda, West Bengal, India, for 2050, RCP6.0, as defined by Lindquist et al., (2012) which considers only contributions from CH_4 + N_20. For net GWP calculations, it is considered that net CO_2 emissions represent < 1% of total GWP, as gross CO_2 emissions are closely matched by atmospheric CO_2 which the growing crops have fixed.

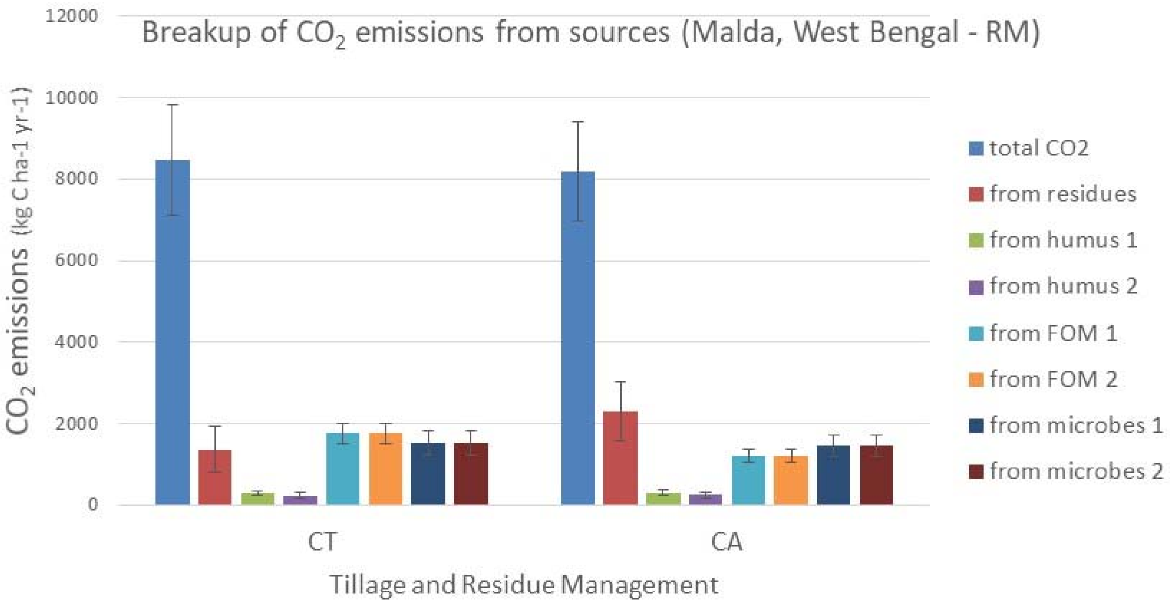

Figure A3.35. Simulated CO2 emissions (in kg C ha^{-1} yr^{-1}) between CT and CA managements in the rice-maize cropping system at Malda, West Bengal, India, for 2050, RCP6.0, illustrating the relative contributions from breakdown/cycling of crop residues on the surface, soil fresh organic matter (FOM), soil humic materials (Humus) and soil microbiota (microbes). The "1" and "2" refer to soil layers 1 and 2 (0-15 and 15-30cms, respectively)

A3.6 Coochbehar, West Bengal, India

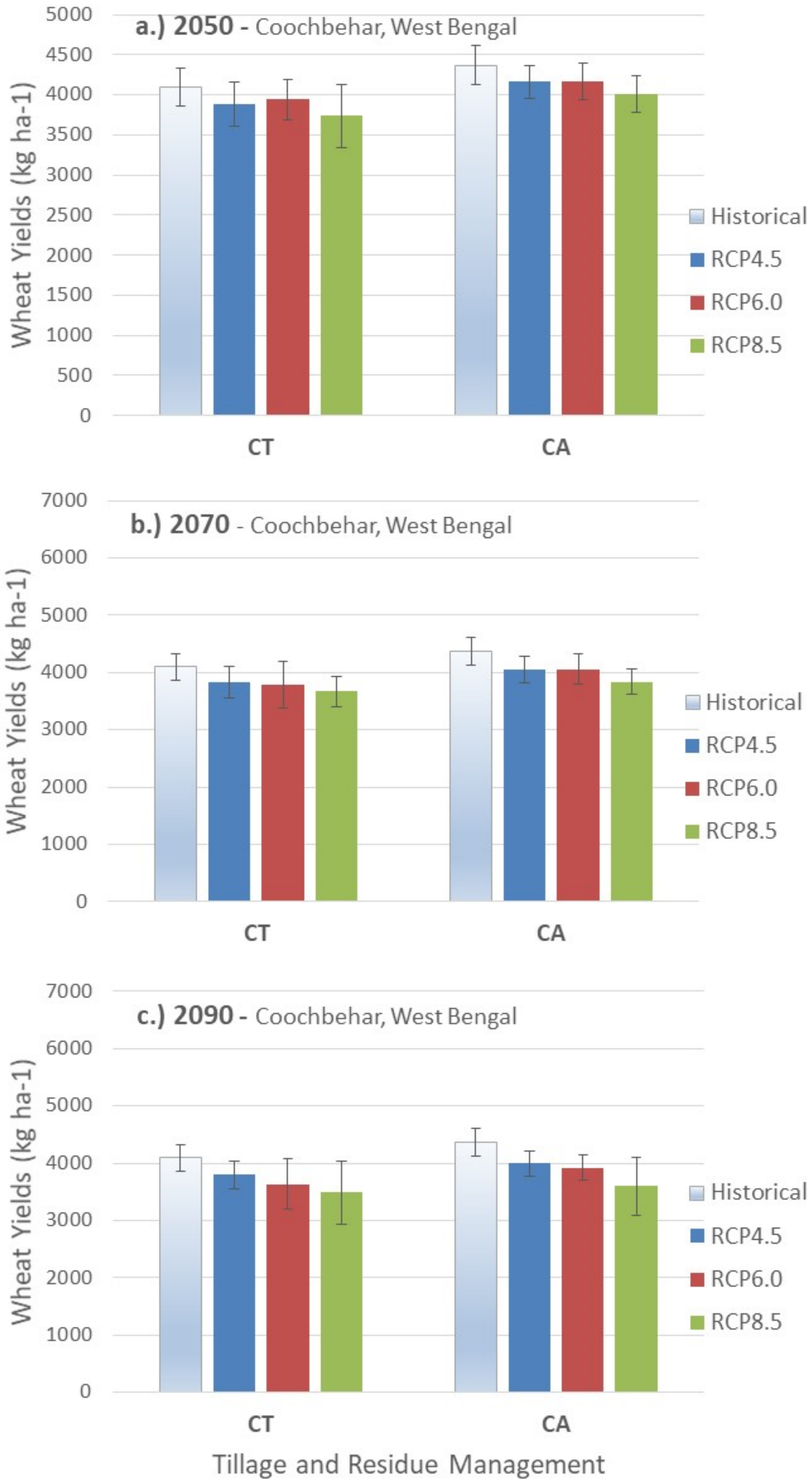

Figure A3.36. Simulated wheat grain yields for Coochbehar, West Bengal, India, for a.) 2050; b.) 2070; and c.) 2090, comparing performance of CT vs CA under future climate scenarios RCP4.5 (blue), RCP6.0 (red), and RCP8.5 (green)

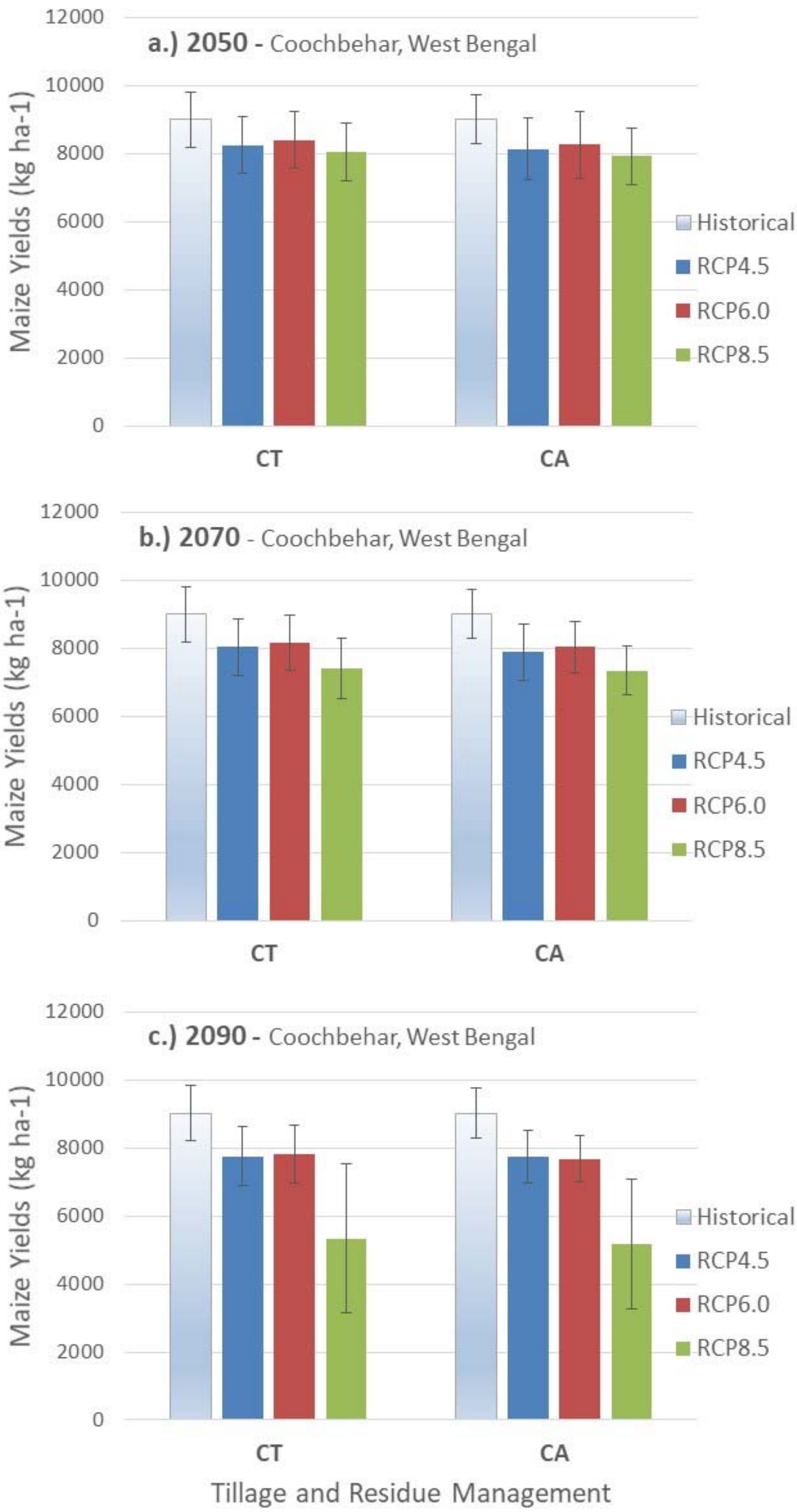

Figure A3.37. Simulated maize grain yields for Coochbehar, West Bengal, India, for a.) 2050; b.) 2070; and c.) 2090, comparing performance of CT vs CA under future climate scenarios RCP4.5 (blue), RCP6.0 (red), and RCP8.5 (green)

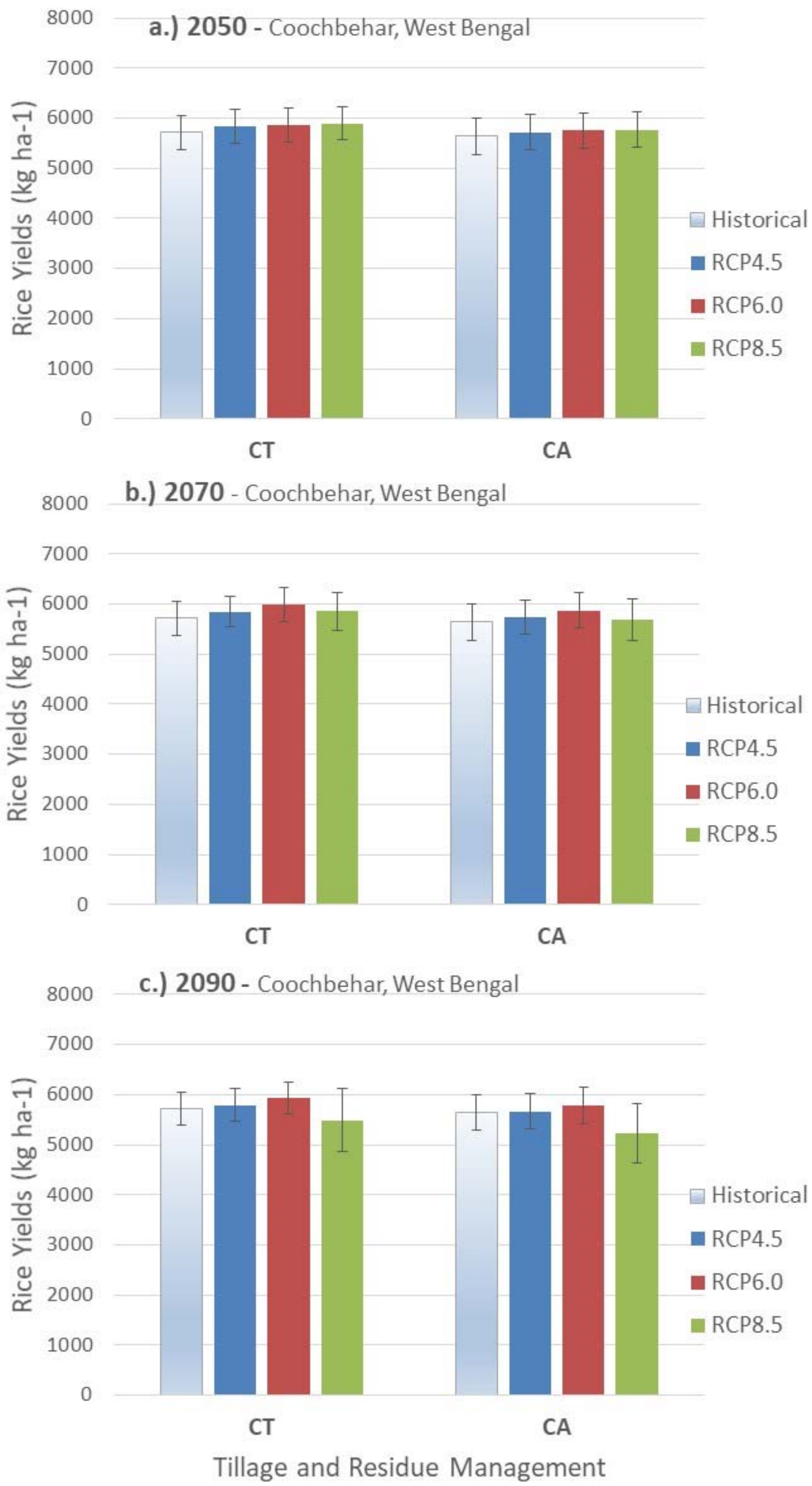

Figure A3.38. Simulated Kharif (wet-season) rice grain yields for Coochbehar, West Bengal, India, for a.) 2050; b.) 2070; and c.) 2090, comparing performance of CT vs CA under future climate scenarios RCP4.5 (blue), RCP6.0 (red), and RCP8.5 (green)

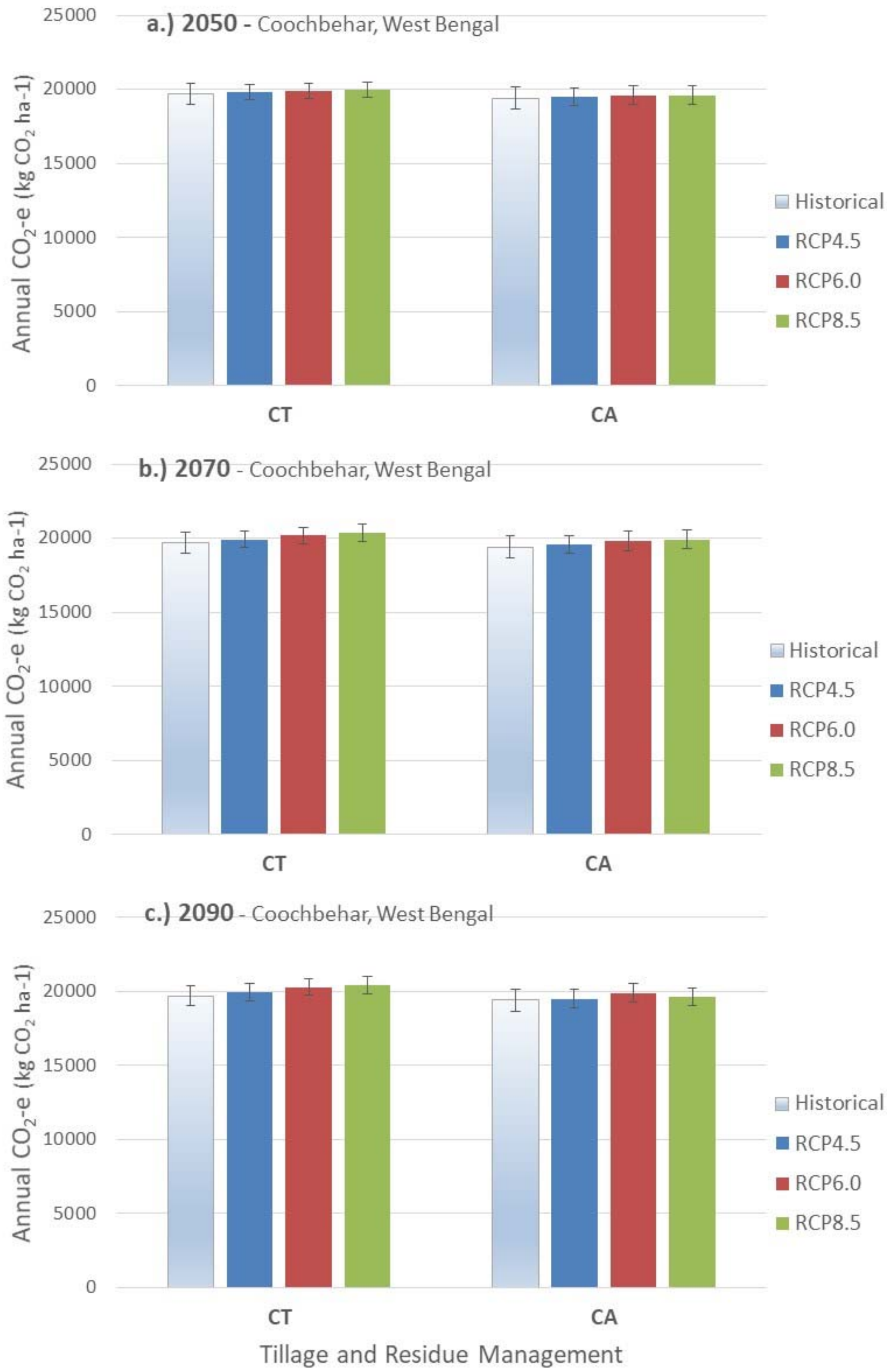

Figure A3.39. Simulated annual GROSS greenhouse gas (GHG) emissions (in CO_2-equivalents) in the rice-maize cropping system at Coochbehar, West Bengal, India, for a.) 2050; b.) 2070; and c.) 2090, comparing performance of CT vs CA under future climate scenarios RCP4.5 (blue), RCP6.0 (red), and RCP8.5 (green). Emissions are calculated from top 15cms soil, as per international protocols.

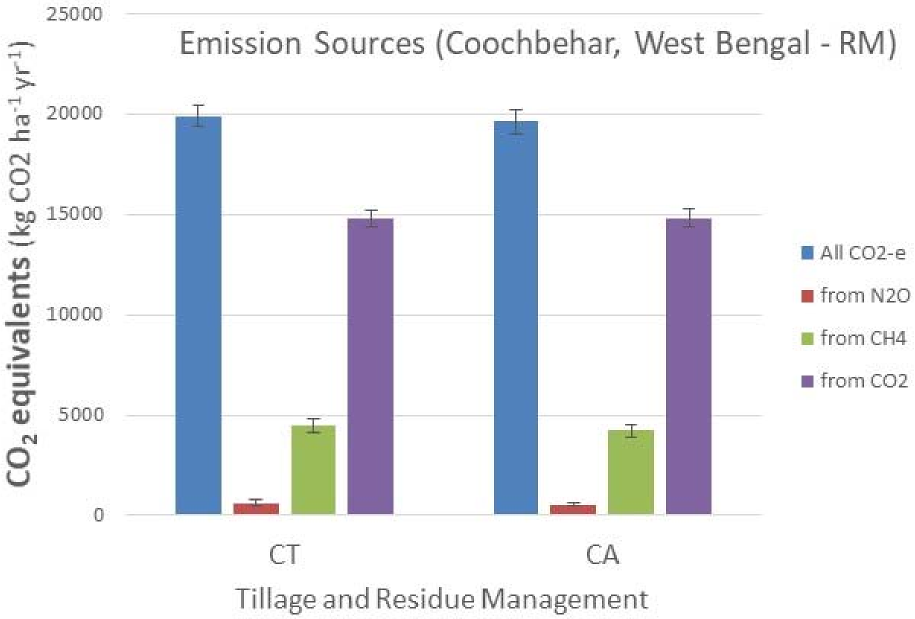

Figure A3.40. Simulated annual greenhouse gas (GHG) emissions (in CO_2-equivalents) in the rice-maize cropping system at Coochbehar, West Bengal, India, for 2050, RCP6.0, illustrating the relative contributions from CO_2, CH_4 and N_20.

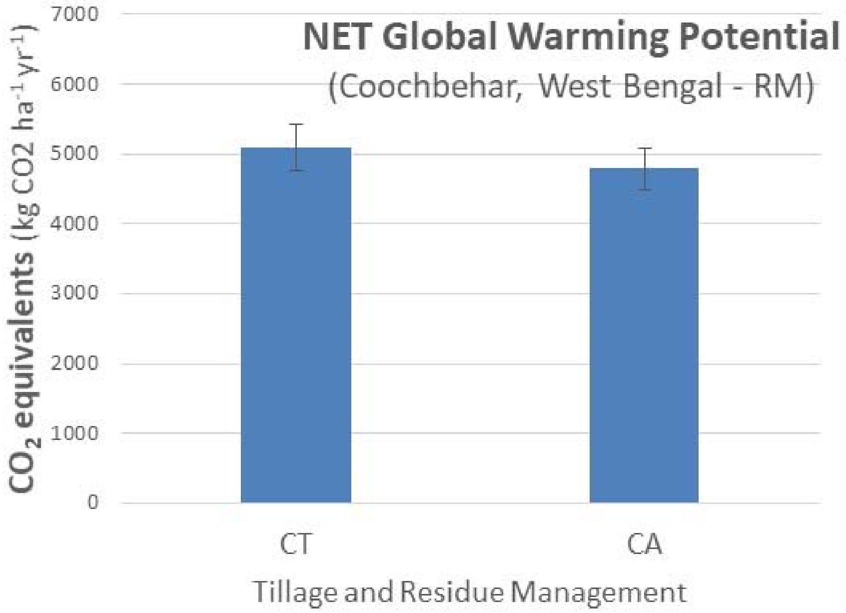

Figure A3.41. Simulated NET Global Warming Potential (GWP) (in CO_2-equivalents) in the rice-maize cropping system at Coochbehar, West Bengal, India, for 2050, RCP6.0, as defined by Lindquist et al., (2012) which considers only contributions from CH_4 + N_20. For net GWP calculations, it is considered that net CO_2 emissions represent < 1% of total GWP, as gross CO_2 emissions are closely matched by atmospheric CO_2 which the growing crops have fixed.

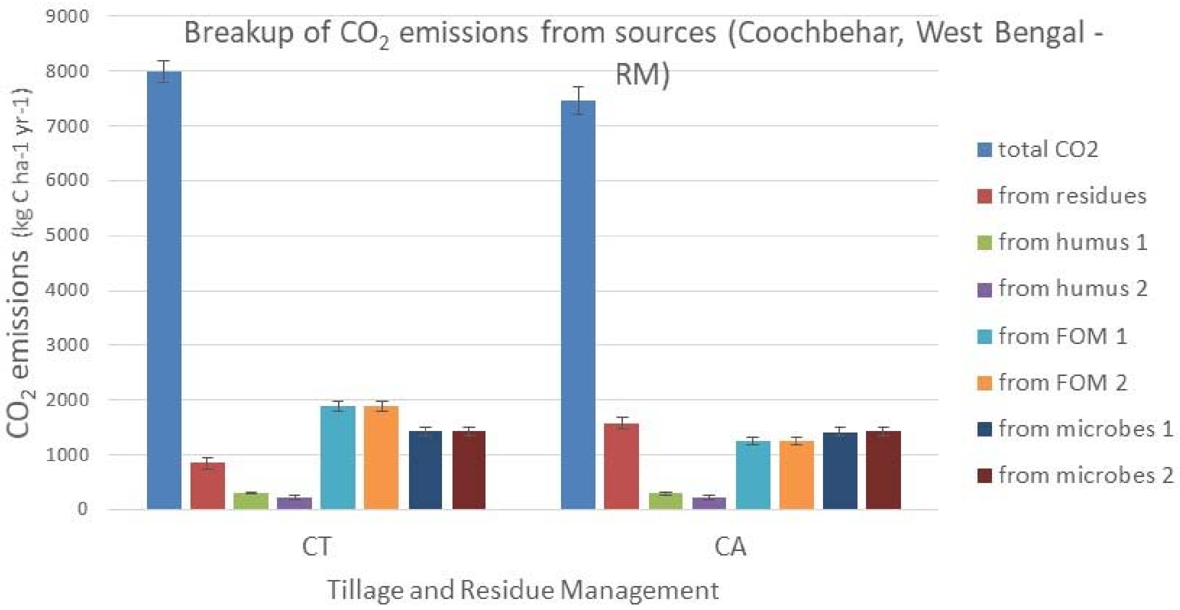

Figure A3.42. Simulated CO2 emissions (in kg C ha^{-1} yr^{-1}) between CT and CA managements in the rice-maize cropping system at Coochbehar, West Bengal, India, for 2050, RCP6.0, illustrating the relative contributions from breakdown/cycling of crop residues on the surface, soil fresh organic matter (FOM), soil humic materials (Humus) and soil microbiota (microbes). The "1" and "2" refer to soil layers 1 and 2 (0-15 and 15-30cms, respectively)

CONTACT US

t 1300 363 400
+61 3 9545 2176
e csiroenquiries@csiro.au
w www.csiro.au

AT CSIRO, WE DO THE EXTRAORDINARY EVERY DAY

We innovate for tomorrow and help improve today – for our customers, all Australians and the world.

Our innovations contribute billions of dollars to the Australian economy every year. As the largest patent holder in the nation, our vast wealth of intellectual property has led to more than 150 spin-off companies.

With more than 5,000 experts and a burning desire to get things done, we are Australia's catalyst for innovation.

CSIRO. WE IMAGINE. WE COLLABORATE. WE INNOVATE.

FOR FURTHER INFORMATION

Donald Gaydon
t +61 7 3214 2415
e Don.Gaydon@csiro.au

Alison Laing
t +61 7 3214 2431
e Alison.Laing@csiro.au